Multiplexed detection of SNPs using electrochemical melting curve analysis

Nassif Chahin

UNIVERSITAT ROVIRA i VIRGILI

Multiplexed detection of SNPs using electrochemical melting curve analysis

NASSIF CHAHIN

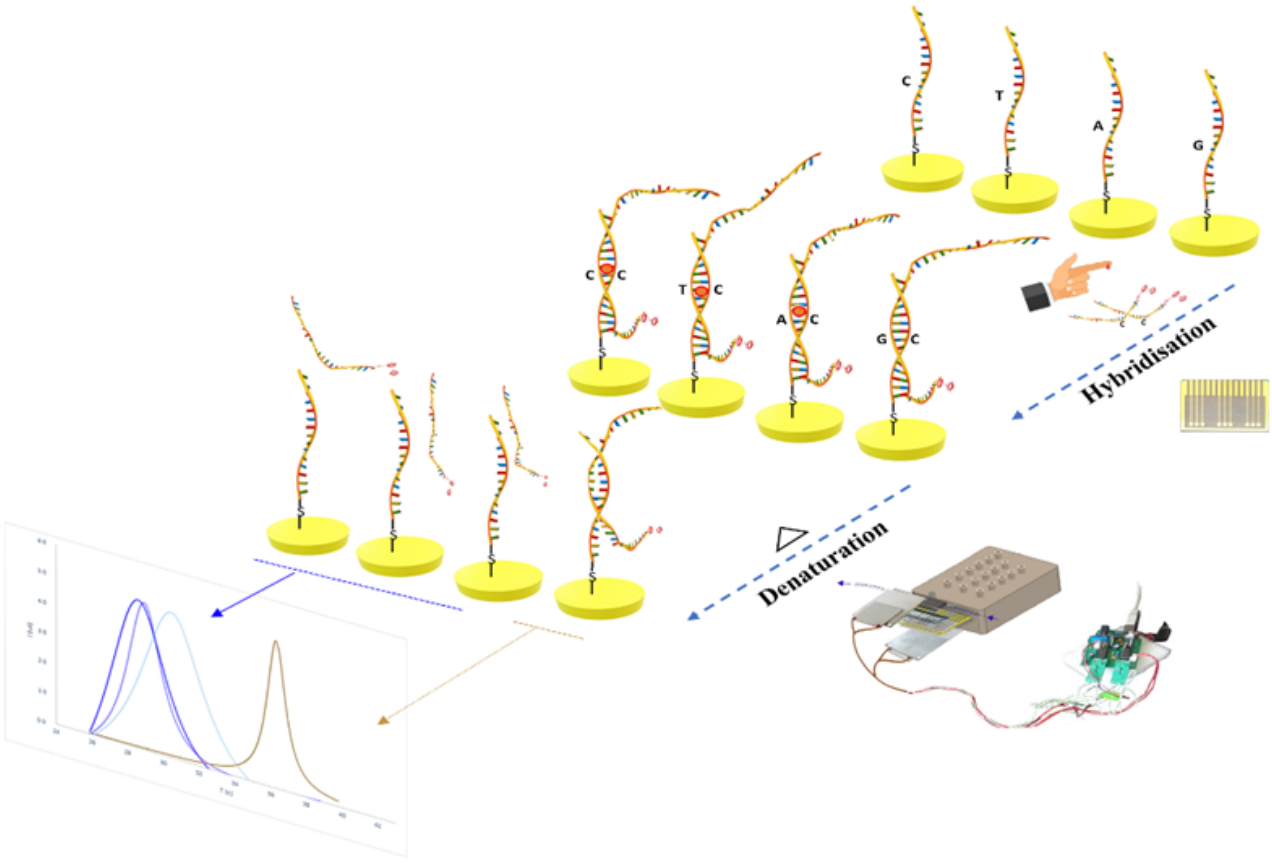

DOCTORAL THESIS
2020

Multiplexed detection of SNPs using electrochemical melting curve analysis

Nassif Chahin

DOCTORAL THESIS

Supervised by:
Prof. Ciara K. O´Sullivan
Dr. Mayreli Ortiz

Department of Chemical Engineering

UNIVERSITAT
ROVIRA i VIRGILI

Tarragona, 2020

UNIVERSITAT ROVIRA I VIRGILI
Multiplexed detection of SNPs using electrochemical melting curve analysis
Nassif Chahin

Department of Chemical Engineering

Universitat Rovira i Virgili

Av. Països Catalans 26

43007 Tarragona, Spain

Tel: 977 55 96 58

Fax: 977 55 96 67

Prof. Ciara K. O'Sullivan and Dr. Mayreli Ortiz

state that the present study, entitled "Multiplexed detection of SNPs using electrochemical melting curve analysis", presented by Nassif Chahin for the award of the degree of Doctor, has been carried out under my supervision at the Department Chemical Engineering of this university and that it fulfils all the requirements to be eligible for the International Doctorate Award.

Prof. Ciara K. O'Sullivan

Dr. Mayreli Ortiz

ACKNOWLEDGEMENT

First of all, all praises and thanks are due to God, for giving me the power, health and patience to finish my PhD thesis.

I would like to express my special appreciation and thanks to my advisors Prof. Ciara K. O'Sullivan and Dr. Mayreli Ortiz for the continuous support of my Ph.D. study and for their patience, and valuable guidance.

Besides my advisor, I would like to thank Eng. Phil Biggs for his guidance and hospitality during my research stay at Labman Automation (England, Stokesley).

A very special gratitude goes to all the Interfibio group members (and former members), and to Ms. Barbara Vastenavond, and Ms. Núria Juanpere Mitjana for their assistance in all the administrative works.

Last but not the least, I would like to thank my family: my parents and my sisters for their love and support.

Table of Contents

Chapter 1: Introduction

Chapter 2: Electrochemical primer extension based on polyoxometalate electroactive labels for multiplexed detection of single nucleotide polymorphisms

Chapter 3: Low cost platform for multiplexed electrochemical melting curve analysis

Chapter 4: Semi-automated electrochemical melting curve analysis device for the detection of an osteoporosis associated single nucleotide polymorphisms in a fingerprick blood sample

Chapter 5: Semi-automated electrochemical melting curve analysis platform for multiplexed detection of SNPs

Table of Contents in Supplementary information

Chapter 2:

List of abbreviations

AFM = atomic force microscopy

APEX = arrayed primer extension

AS-PE = allele specific primer extension

ASPEX = allele specific primer extension

CPE = common primer extension

ddNTP = dideoxy nucleotide triphosphate

DMSO-d_6 = deuterated dimethyl sulphoxide

dNTP = Deoxy Nucleotide Triphosphates

DPV = Differential Pulse Voltammetry

dsDNA = double stranded DeoxyriboNucleic Acid

DT1 = (10-(3,5-bis((6-mercaptohexyl)oxy)phenyl)-3,6,9-trioxadecanol

EDTA = ethylenediaminetetraacetic acid disodium salt dehydrate

éMCA= Electrochemical Melting Curve Analysis

Fc = Ferrocene

GCE = Glassy Carbon Electrode

GPES = General Purpose Electrochemical System

HapMap = Haplotype Mapping

HGP = Human Genome Project

HRP = Horse Radish Peroxidase

IUPAC = International Union of Applied Chemistry

LOD= Limit of Detection

MCH = Mercaptohexanol

M/Z = Mass-to-charge

NHE = Normal hydrogen electrode

O/C = Oxygen/carbon atomic ratio

PBS = Phosphate-buffered saline

PCB= Printed circuit board

PCR = Polymerase chain reaction

PEX = Primer extension

PGSTAT = potentiostat/galvanostat

PMMA = Polymethylmethacrylate

POM = polyoxometalate

RNA = Ribonucleic acid

RP = Reporter probe

RPA = Recombinase Polymerase Amplification

RuHex = Hexamine ruthenium (III) chloride ($[Ru(NH_3)_6]Cl_3$)

ssDNA = single stranded DeoxyriboNucleic Acid

SAM = Self-Assembled Monolayer

SEM = Scanning Electron Microscopy

SERS = Surface-Enhanced Raman Scattering

SBE = Single Base Extension

SNP = Single nucleotide polymorphism

S/N = Signal-to-noise

SPR = Surface plasmon resonance

SWV = Square wave voltammetry

TEA = Triethyl ammonium

TBS = Tris-buffered saline

TBA = Tetrabutyl ammonium

TCEP = Tris (2-carboxyethyl) phosphine

TMB = 3, 3', 5, 5'- tetramethyl benzidine

UHV = Ultra-high vacuum

UV = Ultraviolet

List of Tables **page**

List of Figures **page**

Summary

Shortly following the completion of the Human Genome Project and in the follow-up HapMap project, the presence of single nucleotide polymorphisms across both the coding and non-coding parts of the genome. Since then, through major advances in next generation sequencing (NGS) technologies and the fulfilment of subsequent and ongoing projects such as the 1000, 10,000 and 100,000 human genome projects. In parallel to the use of NGS for the identification of SNP sites, there has been a plethora of genotyping technologies that have been developed for the identification of the specific alleles present in a specific subset of SNPs, finding application in clinical prognostics and patient stratification, identification of antibiotic resistance, as well as in advanced forensics. However, there is still a defined and mature need for a robust platform for the rapid, cost-effective and reliable multiplexed detection of specific SNP alleles.

To address this need, the overall objective of my PhD thesis was thus to develop a low cost platform for the multiplexed electrochemical detection of SNPs. Primarily I focused on the detection of SNPS using solid phase primer extension and polyoxometalate labelled dideoxynucleotides (POM-ddNTPs), which was applied to the detection of a cardiomyopathy related SNP, used as a model system to demonstrate the feasibility of the approach. Whilst the approach did meet with the overall objective of the thesis for the multiplexed detection of SNPS, the synthesis of the POM-ddNTPS was not trivial and was relatively expensive, and we thus pursued a more straightforward, cost-effective solution, and turned our attention to detection of SNPs using electrochemical melting curve analysis, combining asymmetric amplification using ferrocene labelled primers, to generate labelled single stranded DNA for hybridization to target-specific oligonucleotides Immobilized on individual electrodes of an array. Following hybridization, the electrode array was exposed to a heating ramp, and denaturation of the ferrocene labelled amplicon from the surface-tethered probe was monitored using voltametric techniques. To move towards a semi-automated system for electrochemical melting curve analysis, I developed an “in-house” prototype peltier system, designed to integrate the electrode array, allowing heating of the array at a controlled rate, with concomitant continuous washing of the electrode array to remove any denatured labelled DNA, whilst simultaneously measuring the decreasing voltametric signal and storing the data for analysis. I designed and developed both the hardware and software required and used the set-up to demonstrate the proof of concept, we again used a model system for the detection of a SNP associated with cardiomyopathy. The optimum site for the position of the SNP site in the Immobilized probe was evaluated to determine which position could give the highest difference in melting temperature between the wild

type allele (i.e. present in the vast majority of the population) and the other three potential SNP alleles.

Using this set-up, I moved to an alternate model system, where I used the optimised SNP site in the surface-tethered oligonucleotide probe, now I applied the platform to the specific identification of the allele at the identified SNP site, this time applying to the detection of a SNP associated with increased risk of fracture in osteoporosis. In this approach, I used four probes, each Immobilized on individual electrodes (in triplicate), where each probe differed simply by the nucleotide at the SNP site (i.e. G, T, A, C), located in the middle of each of the Immobilized probes. Extending from my previous work I used asymmetric isothermal recombinase polymeras amplification to generate single stranded DNA for direct hybridization to the Immobilized probes, prior to executing the melting curve analysis. Once this had been demonstrated I applied the systems to detection of the SNP from a fingerprick blood sample, and a clear differentiation in melting temperature between the duplex fomed with the probe containing the complementary nucleotide to the allele at the SNP site as compared to ther other duplexes was observed, demonstrating an unequivocal identification of the allele present at the SNP site of the specific fingerprick blood sample interrogated, which was further confirmed using next generation sequencing.

During a research exchange visit to Labman Automation (Stokeley, United Kingdom), I worked together with the engineering team to develop a completely automated and integrated electrochemical melting curve analysis system, with addition of the ferrocene labelled asymmetric RPA amplicon onto an electrode array housed within the system, automated pump propulsement of washing buffer over the electrode array accompanied by controlled peltier ramping of the temperature applied to the electrode array, with concomitant data procurement of the voltammetric response as the temperature is decreased and the surface-tethered duplex denatures. Finally, this system was applied to the multiplexed detection of SNPs associated with osteoporosis.

This thesis is divided into 5 chapters: **Chapter 1** gives an introduction to single nucleotide polymorphisms (SNPs) and the methods used for SNP detection. It also provides a short outline of the detection of DNA sensors, focusing on the method of electrochemical melting curve analysis as a basis for the thesis work.

Chapter 2 describes the demonstration of the detection of SNPs based on electrochemical primer extension using dideoxynucleotides linked to Keggin and Dawson polyoxometalate electroactive

labels. The work successfully demonstrated the Therminator DNA polymerase-mediated single based extension of ssDNA probes tethered to the surface of gold electrodes. We termed this methodology, solid phase electrochemical primer extension (éPEX). In this reaction, an isothermal single-base extension reaction that takes advantage of Immobilized single stranded DNA probes designed to hybridize to a single stranded PCR target one base downstream from the SNP site to be interrogated, was exploited. Following hybridization, labelled ddNTPs, modified nucleotides that lack the 3'-hydroxyl groups were added. Using either ligation or elongation with a ligase or polymerase enzyme, the Immobilized probe is extended by a single labelled ddNTP, complementary to the SNP being addressed. Following incorporation of the electroactive labelled ddNTP, no further phosphodiester bonds can be formed due to the lack of the 3'-OH group, and therefore no elongation can take place after the addressed SNP site. The éPEX reaction with ddNTPs labelled with different electroactive markers including ferrocene, anthraquinone, phenothiazine and methylene blue was performed successfully, and the possibility of using POMs to label ddNTPs for use in éPEX were explored.

In **Chapter 3**, as an alternative, more facile and cost-effective approach for the detection of SNPs, we explored the use of a low cost and easy platform fabricated device with an integrated homemade Peltier to control the temperature, microfluidic, and electrochemical measurements to achieve electrochemical melting curve analysis (éMCA). The “in-house” fabricated Peltier consists of two aluminum blocks that can be heated in a controlled way using and Arduino UNO board at three different resolutions: 0.2, 0.5 and 1 °C/step. The heating system was characterized and the functionality of heating validated. Four different synthetic single stranded DNA sequences mimicking a cardiomyopathy model target, each one with the SNP under interrogation at a different position, designed to be located at the top, middle or bottom of the duplex formed following hybridization with the same capture probe tethered to the surface of individual gold electrodes of an array, were evaluated. Following hybridization, a controlled heating ramp was applied to the electrode array, and melting profiles were generated, the data analysed and the melting point for each duplex successfully determined. We observed that the maximum differentiation in melting temperature between the wild type (i.e. fully complementary duplex between Immobilized probe and synthetic target vs. single base mismatch) was achieved when the SNP to be interrogated was hybridized to the middle of the Immobilized probe.

In **Chapter 4**, I moved the system further towards the final goal of the project – to achieve multiplexed detection of SNPs from a real patient’s sample. In this part of the work, we focused on identifying

the allele present at the SNP site being interrogated. In order to achieve this, we designed four individual thiolated probes, each bearing a different oligonucleotide at the SNP site. Ferrocene labelled single stranded DNA containing the SNP site was produced using asymmetric isothermal recombinase polymerase amplification and a redox labelled primer, and the maximum yield was achieved using 15 minutes amplification and a labelled forward: unlabelled reverse primer ratio of 5:1. Following hybridization, a controlled heating ramp was applied and the melting profiles of the duplexes at each of the electrodes was simultaneously monitored and a clearly differentiable melting temperature between the electrode with fully complementary duplex and the three duplexes containing the single base mismatches was observed. In the second part of this work, I applied the system to detection of SNP in a real fingerprick blood sample. Following a rapid and clean extraction of genomic DNA from a 20 μL sample by heating at 95 °C for 30s, and the genomic DNA was directly used as a template in the asymmetric RPA using the ferrocene labelled primer, again followed by hybridization of the amplicon to each of the immobilized probes and finally simultaneous melting curve analysis was carried out, melting profiles generated and the melting temperature of each duplex was determined. The correct identification of the allele at the SNP site was confirmed using next generation sequencing.

In **Chapter 5**.to achieve the real multiplexed detection of the SNPs, there was a need to develop a new design for our éMCA setup. In this chapter, there is a description of the prototype instrument that was developed at Labman Automation (UK) during my research stay. Briefly, the heating system part was modified to allocate a new type of arrays with 64 working electrodes instead of the 9 electrode arrays usedin the former prototype. This prototype was tested by performing simultaneous detection of SNPs related to osteoporosis. Two sets of four probes were pre-immobilized on gold electrodes. Each set was complementary to one SNP carrying target and allocated a different base at SNP site, designed to be at the middle of that sequence. In previous work, the targets were amplified and labelled with ferrocene using asymmetric RPA and then left to hybridise with the probes for an hour. Finally, the éMCA were performed to determine the Tm.

Concluding remarks and an outlook for future work are described in **Chapter 6.**

Overall, this Ph.D. thesis focused on the development of methods for the electrochemical detection of single nucleotide polymorphisms. The initial focus was on the use of solid phase primer extension, which was successfully demonstrated but due to the complexity in obtaining purified labelled ddNTPs, an alternative approach of electrochemical melting curve analysis was pursued. An ‘in-

house' prototype for the housing of an electrode array within a heating device capable of heating at a highly controlled rate was designed and used for the detection of a cardiomyopathy associated SNP. Following demonstration of the proof-of-concept and optimisation of the SNP site within the surface-tethered probe, the system was then applied to detection of an osteoporosis associated SNP in a real fingerprick blood sample. Finally, a more automated thermal melting analysis prototype instrument was developed in collaboration with Labman Automation (UK), and this system was used for the multiplexed detection of two SNPs associated with osteoporosis. The potential of the approach has clearly been demonstrated and in future work, higher multiplexing capabailities will be pursued, specifically for the detection of 11 SNPs associated with rifampicin antibiotic resistance.

Chapter 1

Introduction

1.1. BIOSENSORS

Biosensors are analytical devices that convert a biological response into an electrical, thermal or optical signal providing analytical information, as defined by IUPAC. [1,2] The biosensor consists of a biocomponent (e.g. enzymes, antibodies, aptamers, tissues and whole cells), for the specific recognition of analytes, and a transducer that converts the bio-recognition event into a measurable signal that are usually proportional to the amount of analyte present. Biosensors may be classified either according to the biological specificity conferring mechanism or to the mode of signal transduction.[3,4]

Since the appearance of the first biosensor in the 1960s, which was developed for the detection of glucose, a plethora of affinity and catalytic biosensors have been developed, including DNA biosensors (also termed genosensors), immunosensors (exploiting antibody biocomponents), aptasensors (exploiting aptamers) and cell-based sensors, exploiting optical, electrochemical, magnetic, calorimetric and thermal transduction. Thse biosensors have been applied to many fields including clinical diagnostics, environmental monitoring, biodefense as well as control of food quality.[5]

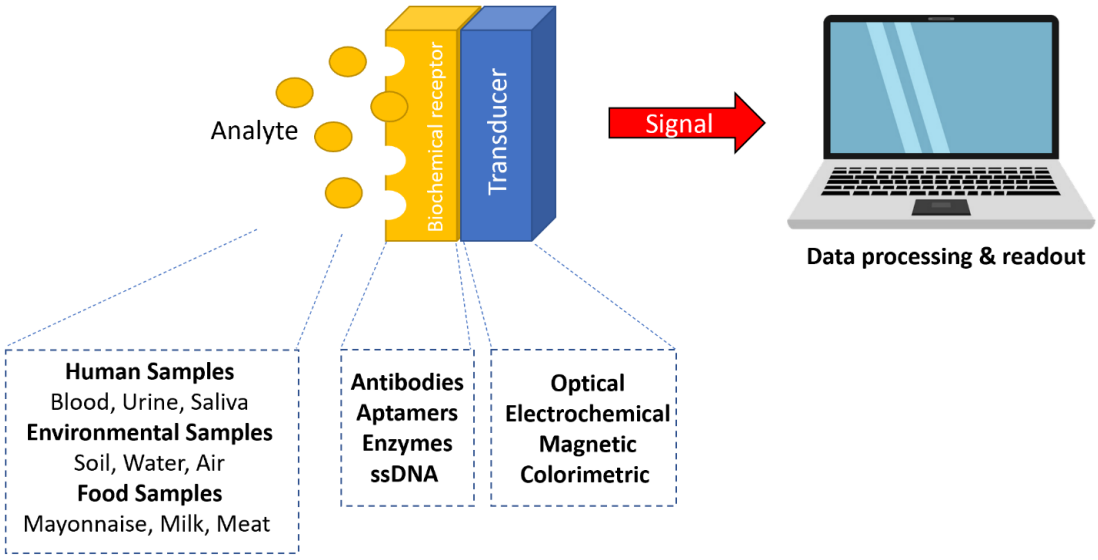

Figure 1.1. Biosensor components

1.2. Electrochemical biosensors:

Electrochemical techniques (including amperometry, voltammetry, capacitance, conductance, potentiometry and electrochemical impedance spectroscopy) are commonly used in biosensors due to their high sensitivity, ease-of-use, compatibility with microfabrication and relatively low cost as compared to other techniques.[6,7] Hybridization can be detected due to changes induced in electrochemical variables including capacitance and conductivity, or via the use of redox labels such as polyoxometalates (POMs), ferrocene, methylene blue (MB) or enzyme labels.[8] These techniques can be further classified into direct and indirect electrochemical detection strategies.

1.2.1. Amperometric biosensors

Amperometric biosensors monitor the current correlated with oxidation or reduction of an electroactive compound, with the current intensity depending on the concentration of the electroactive product, which is proportional to the target analyte.[9] Amperometric biosensors typically consist of three electrodes, a working electrode that acts as a transducer of the biochemical event, a reference electrode that maintains a known and stable potential on the working electrode and a counter electrode that allows the current to pass through the working electrode.

1.2.2. Potentiometric biosensors

In potentiometry, the charge potential at the working electrode surface compared to reference is measured when zero current flows between them in the electrochemical cell.[10,11]

Many potentiometric biosensors use ion-selective electrodes (ISE) as a sensor based on thin-film or selective membranes as a recognition element for detecting different ions such as Na^+, K^+, Ca^{2+}, H^+, NH_4^+.[12]

1.2.3. Conductimetric biosensors

Conductimetric biosensors measure the electrical conductivity in a solution produced by biochemical reactions, which generates or consumes ions at the transducer part using a fixed voltage.[13,14] Although the transducers can be produced through inexpensive thin-film standard technology without any reference electrode, the main drawback of these sensors is the low specificity.

1.2.4. Impedimetric biosensors

Impedimetric biosensors have mainly been designed to monitor a biological affinity based interaction at the surface of transducers [15] and these types of biosensors have been developed to detect a wide variety of biomolecules including nucleic acids, receptors, antibodies, antigens, enzymes, antibodies, cells, and microorganisms.[16,17] Impedimetric biosensors measure the changes in charge conductance and capacitance at the surface of the sensor where the selective binding of the target takes place. These measurements can be categorised in two main approaches, either by measuring the change in the charge transfer (Faradaic interface) or in the charge induction (non-Faradaic).

Non-Faradaic: If the target molecule is charged, as is the case for negatively charged DNA and the whole electrode assembly behaves as an insulator, capacitive measurement is performed since this additional charge interferes with the charge profile at the interface. **Faradaic:** if the target is not charged, a redox probe is usually added (such as ferricyanide), interaction of an Immobilized biocomponent with a target analyte hinders (impedes) the passage of the electrons to the electrode surface and the increase of the charge transfer resistance (RCT) is measured. [18] Electrochemical Impedance Spectroscopy (EIS) is one of the most complex techniques that can be used to detect DNA label free, by determining both the resistive and capacitive properties of materials.[19,20]

1.2.5. Voltammetric biosensors.

Cyclic Voltammetry (CV) is one of the most widely used in biosensors and useful voltammetric techniques that provides information about an analyte by measuring the obtained current after applying a variable potential. It is mostly used to study modofocations of the electrode surface in the preparation of biosensors.[21]

Other voltammetric techniques have been developed to increase the sensitivity of CV such as Square Wave (SWV), Differential Pulse (DPV) and many others.[22] Square wave voltammetry (SWV) is a pulsed technique, where the current response to the applied potential can yield 3 current potential plots: forward, reverse, and the difference between them (which is the most used). SWV doesn't introduce a large capacitive background current like in CV. Differential pulse voltammetry (DPV) has a stair waveform like SWV but with a small pulse potential that enhances the discrimination of electron transfer currents to the electrode surface, as well as improving the selectivity for monitoring different redox processes.[22] The DPV is widely exploited in biosensing and biomedical applications due to its high sensitivity in electrochemical transduction.[23]

1.3. Genosonsors:

A particular case of biosensors are the DNA biosensors, often referred to as genosensors, are biosensors that exploit nucleic acid recognition processes for the rapid, simple and low-cost testing of genetic and infectious diseases [24] via the detection of DNA interactions.[25] detection of nucleic acid sequences is achieved via hybridization with surface Immobilized oligonucleotide probes. These immobilized nucleic acid layers can be easily synthesized and regenerated for multiple use and can consist of DNA, RNA, PNA (peptide nucleic acid) or LNA (locked nucleic acid), functionalized to facilitate surface-tethering. These nucleic acid probes are designed to hybridize to a specific target to form a duplex that can be detected following the association of an appropriate hybridization indicator or through other changes resulting from the binding event.[26]

1.3.1. Probe immobilization

DNA probe immobilization on the transducer surface is a key factor for obtaining a high performance DNA biosensor, with optimal immobilization inferring a higher sensitivity and selectivity for DNA sensing by maximizing accessibility of the DNA under interrogation to the surface immobilized probe and the stability of the immobilized DNA probes, minimizing steric hindrance, whilst also minimizing non-specific adsorption. Many immobilization techniques have been developed in the past years, which are mainly based on three important mechanisms: physical adsorption, covalent bonding and affinity interactions.[27]

1.3.1.1. Probe Immobilization by physical adsorption

This is the simplest method of immobilization because there is no need for any nucleic acid modification and does not require any additional chemical reagents.[28] In one commonly used approach, immobilization can take advantage of ionic interactions between the positive charges covering the transduction surface e.g. activated surfaces, polymer-functionalized polymers, and the negatively charged DNA probe.[6] The stability of the probe through the electrostatic attraction between the positively charged surface and the negatively charged DNA could be enhanced by applying potential during the immobilization process. Simpler approaches, where DNA probes are simply adsorbed have also been reported, and the main drawbacks of the adsorption mechanism are random orientation and weak attachment of the DNA probes to the surface.[27]

1.3.1.2. Probe Immobilization by covalent attachment

Using covalent attachment, the two most commonly used methods are chemisorption and covalent crosslinking. Thiolated oligonucleotides have been widely used for ordered chemisorption into a variety of metallic surfaces, with highly stable and organised self-assembled monolayers (SAMs) formed, particularly in gold surfaces. Mixed SAMs are commonly used, exploiting a mixture of thiolated DNA with short chain alkanethiols, such as mercaptohexanol, which facilitates an optimal spacing of the probe, forcing a perpendicular orientation of the probes due to inter-probe electrostatic repulsion, thus maximizing accessibility, minimizing steric hindrance.[29] Additionally, thiols (−SH), sulfides (−S−) and disulfides (−S−S−), bearing functional groups (e.g. carboxyl, amine moieties) can be chemisorbed and then chemically cross-linked, for example using carbodimide chemistry, to oligonucleotides functionalized with either carboxyl or amine groups.[30]

The application of genosenores was favorably influenced by the Human Genome Project (HGP).

1.4. The Human Genome Project (HGP) and Single nucleotide polymorphism (SNP)

The Human Genome Project (HGP) was a multi-year, multi-partner project that aimed at understanding the role of each of the 3 billion bases in the human genome. Following sequencing the genome, the locations of the genes on the genome were identified and function assigned to the genes. The Human Genome Project was followed by huge advances in sequencing technologies, contributing to several further international projects such as the HapMap project, the 1000 and then 10000 genome projects. These projects involved deep sequencing and aimed at identifiying specific patterns in the genome that could be used for prediction of response to therapy and patient stratification in a type of individualised theranostic approach. The existence of single nucleotide polymorphisms was thus identified and the importance of these single base allelic changes are still being undercovered.

The human genome sequence reported some variations between individuals, related to; single nucleotide polymorphisms (SNPs), insertions & deletions (indels), microsatellites (MSs), as well as differences in the methylation status of important regions. Single nucleotide polymorphisms (SNPs) are the most common type of genetic variation among people (about 90%) and occurs in at least 1% of the total population [31] at a frequency of 1 in every 300-1000 bases.[32] Each SNP represents a change in one nucleotide in a defined sequence of DNA. Almost all SNPs are di allelic and fall into four classes, one transition (C↔T/G↔A) and three transversions (C↔A/G↔T, C↔G/G↔C and T↔A/A↔T).[29]

SNPs exist mostly in the non-coding region over the DNA. The SNPs present in coding regions that are responsible for synthesizing proteins may alter the structure and then the functionality of the encoded protein. These SNPs are considered biomarkers of genetic disorders. Many genetic diseases are associated with genetic variations including the inherited forms of cardiomyopathy, cystic fibrosis[33], thalassaemia[34], sickle cell anaemia[35] and retinitis pigmentosa[36].

1.5. SNP genotyping strategies

SNP genotyping is a great of importance for the early diagnosis and identification of genetic disorders. Most genotyping technologies require amplification of the desired region that contains the SNP by using the PCR to increase the number of molecules for detection following allelic discrimination.

Allele-discrimination can be achieved by, allele-specific hybridization[37,38], ligation [39], enzymatic cleavage.[40] or primer extension[41,42] Thereafter, products from various allele-discriminating reactions are analyzed for allelic differences. Most allele-detection methods include mass spectrometry[43], fluorescence[44] and chemiluminescence.[45]

1.5.1. Ligation.

In this approach, the specificity of ligase enzymes is employed to achieve allelic discrimination. When two oligonucleotides are adjacent to each other, they hybridize to single-stranded amplicon DNA with perfect complementarity, and ligase enzymes then join them to form a single oligonucleotide. Traditional ligation assays exploit 3 oligonucleotide probes, 2 of which are allele-specific and bind to the template at the SNP site. [39,46] The third probe is common and binds to the template adjacent to the SNP immediately next to the allele-specific probe. If the allele specific probe binds at the SNP site with full match, the DNA ligase joins it with the common probe. After ligation, the nucleotide at the SNP location could be identified by different techniques. Most ligation methods employ allele-specific probes with their 3'ends at the SNP sites because ligases are more sensitive to mismatches at the 3'end (Figure 1.2).

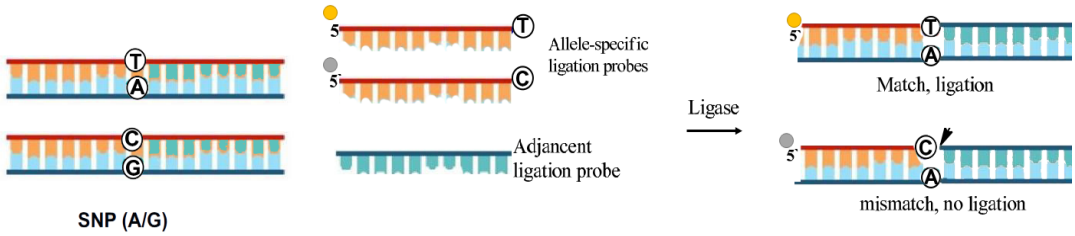

Figure 1.2. Schematic depiction of allele discrimination by ligation method

1.5.2. Enzymatic cleavage.

Enzymatic cleavage for allelic discrimination (Figure 1.3).uses a restriction enzyme to cleave DNA by recognition of specific sequences and structures. These enzymes can be used to discriminate between alleles when SNP sites have existed in an enzyme recognition sequence and allelic differences affect recognition. In the invader assay, two allele-specific probes that carry different reporter (R) and quencher (Q) dyes at either end and a common invader probe are used. The allele-specific probe and invader probe hybridize with target DNA to form a three-dimensional structure at the SNP site that is recognized by the cleavage enzyme. The enzyme cleaves the structure only when the allele-specific probe is a perfect match to the SNP and releases its reporter dye.[40,47]

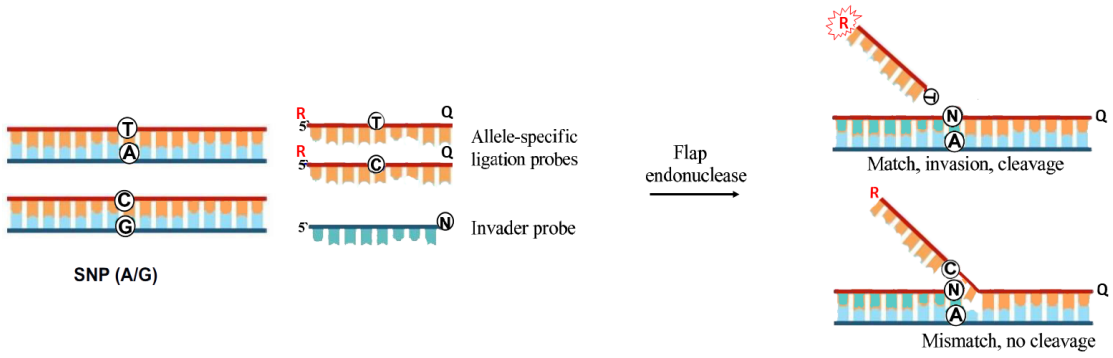

Figure 1.3. Allele-specific cleavage in an Invader reaction by flap endonucleases (FENs).

1.5.3. Differential Hybridization.

Differential hybridization uses the differences in the thermal stability of double-stranded DNA to distinguish between matched and mismatched target-probe pairs.[37] Allelic discrimination generally depends on the length of the probe, SNP position and the probe sequence, as well as hybridization conditions.[38]

1.5.4. Primer extension.

Primer extension has been used in many assays, including primer guided nucleotide incorporations, solid-phase minisequencing, allele specific primer extension (ASPEX), arrayed primer extension (APEX), genetic bit analysis (GBA), first nucleotide change (FNC), template-directed dye terminator incorporation (TDI) as well as the probe oligo base extension assay.[48] These approaches involve allele-specific incorporation of nucleotides in a primer extension reaction with a DNA amplicon template, by using the specificity of an enzyme for allelic discrimination. Primer extension typically uses either a common primer for detecting both alleles or specific primers for detecting each allele (ASPEX). In a common primer reaction, a primer is designed to anneal with its 3' end adjacent to a SNP site and extended with nucleotides by a polymerase enzyme.[49]

Alternative major detection methods for allelic differences are based on mass spectrometry, fluorescence and electrochemistry. Various reporters have been used in these methods as enzymatic probes[50,51], nanoparticles[52,53], binary probes[54], redox compounds[55,56] and fluorescent dyes [57]. Despite the sensitivity and specificity of these systems, they still suffer from drawbacks, such as the long processing steps, the need for expensive instruments (like fluorescence spectroscopy and mass spectrometer), and the tight control required over different conditions (temperature control).

Mass-based detection is based on a primer that anneals one base upstream of the SNP site followed by its extension with ddNTPs. Mass spectrometry detects the extension products and the difference between the mass of the extension products and the primers allowing the identification of the incorporated nucleotide(s) for the SNP genotyping. [58] Also, fluorescence spectroscopy can also be applied as detection method to the single-base extension and the 5'-nuclease assays.[59] However. it requires expensive instruments and is restricted to the lab work.Various fluorescent dyes have been used to modify oligonucleotide probes, as fluorescein, Texas-red, TAMRA, Cy3-dyes, HEX, JOE, Oregon green, rhodamine 6G, pyrene and coumarin,as well as the use of fluorescence quenching strategies, by using quencher molecules also covalently attached to the fluorescent oligonucleotides.

The (DABCYL) dimethyl-amino-phenyl-azo-benzoic acid has been widely used as a universal quencher. [60]

1.6. Electrochemical method for SNP detection

Electrochemistry has many advantages as compared to other methods for the detection of SNPs due to its relative low cost, ease-of-use, high sensitivity and compatibility with miniturisation and portability. These properties make electrochemical transduction very versatile and suitable for on-site analysis.[61] In general, the electrochemical biosensor detection depends on working electrodes, mainly gold, that can provide an electrochemical signal from the analyte in solutions or solid-phase surface by employing one of the electrochemical techniques such as EIS, CV, , SWV and DPV, described above. Several techniques for the electrochemical detection of SNPs have been developed.[59,62] For instance,

Wong. E. l. S. *et al*., (2006) described a very simple assay of electrochemical DNA biosensors with a detection limit of 1 pmol to detect single base mismatch on the electrode surface. Briefly, a capture probe immobilized in a gold electrode was left to hybridize to a complementary target sequence or other two targets each one containing a single base mismatch in the middle (C-A or G-A). The redox-active intercalator, anthraquinone monosulfonic acid was incubated with the DNA after the hybridization on the gold surface and the SWV measured for the three systems. The mismatched sequences were detected by the 73% signal decrease respect to the fully complementary. [62]

Ying Wang *et al*., (2018) reported a cost-effective electrochemical biosensor for SNP detection, using a 300-bp-long PCR product with a 19-nt-long sticky end, designed to hybridize to a gold electrode-tethered probe. Hybridization was monitored using cyclic voltammetry of the redox probe $[Fe(CN)_6]^{4-/3-}$ and DPV using RuHex. The strategy of this assay involves a PCR product of about 300 bp obtained using a rTaq polymerase, then it was degraded in the 3'→5' direction, using T4 polymerase and dGTP, to generate a 19-long sticky end of PCR product. A probe 1 with thiol at 3' end and a probe 2 can be hybridized with Target 1 (has SNP-33G at middle) or with target 2 (wildtype has SNP-33A at middle). In case of target 1 and the presence of HiFi Taq DNA ligase, the nick between probe 1 and probe 2 is closed, where the ligation reaction was triggered at 94 °C, then followed by denaturation at 94°C for 1 min, hybridization, and ligation at 55°C for 5 min, 30 cycles. Target 1 also recycled after the first round of ligation. In the case of target 2, A loci at the middle of target 2 didn't match to C loci at 5´end of probe1, and the ligation reaction couldn't happen. The ligated product (Probe 1 and 2 together) immobilized on the gold electrode through thiol group at the 3´end, and the sticky end of PCR product matched to 5´end of the ligated product.

Lastly, the electrode was immersed in RuHex buffer which bounds to the phosphate of the DNA, and a high redox signal could be obtained by DPV once the sticky end of PCR product was hybridized to the gold electrode surface.[63]

Ren *et al*., (2018) presented a simple and label-free electrochemical sensor for detecting SNPs in stem-loop nucleic acid secondary structures. The sensor consists of a) a gold electrode modified with a hairpin probe (HP) containing DNAzyme substrate sequence with ribonucleobase (rA) which can be cleaved by Mg upon binding to the Mg^{2+}-dependent DNAzyme in the loop region and G-rich sequence in the stem near the electrode surface. b) Two assistant strands (AS1, AS2) have two regions: complementary to the target SNP (HP) and the Mg^{2+}-dependent DNAzyme forming sequences. In presence of the SNP target (HP) with AS1, AS2, and HP on the sensor electrode, part of AS1 hybridizes with and opens the folded target SNP. Thereafter, AS2 further complements with the unfolded SNP part, which brings AS1 and AS2 into close position for partial hybridization to form stable complexes of the Mg^{2+}-dependent DNAzyme. The immobilized HP probe then can be cleavaged at the rA site with the existence of the Mg on the electrode to form ssDNA with many G-rich sequences. In the presence of K^+ and Hemin buffer, the Hemin substantially binds to G-quadruplex to form a complex, resulting in a high DPV response from electro-reduction of Hemin leading to sensitive detection of the SNP target sequences. Finally, the specificity of the sensor to recognize the SNP sequence was performed by measuring the current responses from a single base-mismatched DNA of Tau-C and Tau-A.[64] The peak current for the single base-mismatched sequences showed no signal like the blank test, whilst, additions of the same concentration of the SNP target (HP) resulted in a high increase in peak current**.**

An alternative approach has been reported for the electrochemical detection of a SNP in the p53 gene where a gold electrode immobilized PNA probe was hybridized to the SNP-containing DNA to form a PNA/ds-DNA triplex. The gold electrode is then immersed inside methylene blue (MB) for 5 minutes. The interaction between MB and oligonucleotides is measured by differential pulse voltammetry (DPV). The results show a significant increase in the reduction signal of MB of the probe with the fully complementary ds-DNA oligonucleotide as compared to that with a one-base mismatch.[65]

In the work we pursued two different approaches for the detection and identification of SNPs. In the first approach we exploited electrochemical detection of solid-phase primer extension using redox labelled ddNTPs, whilst in the second approach we explored the electrochemical detection of solid-phase melting curve analysis using redox labelled primers.

In primer extension, the ability of polymerases to incorporate nucleotides linked to an electroactive reporter or functional groups has been used for mini- sequencing.[66] It has been reported that the optimal site for nucleotide modification, which gives the best incorporation efficiency is via the 5-position of pyrimidines and the 7-position of purines.[67]

The flexibility and length of the modification linker can also affect nucleotide incorporation, with rigid linear linkers facilitating dNTP incorporation besides short linker arms (biotin-C_4-dUTP) are better substrates than longer linkers (biotin-C_{11}-dUTP). A bulky fluorescent nucleotide can be incorporated using the normal natural DNA polymerases but with slower kinetics due to a steric interference as compared to the natural substrates.[68] Therefore, the linker position and length, functional groups, the size of the label and the concentration of the dNTPs are important factors for successful incorporation. A few types of redox-active labels such as ferrocene and $Ru(bpy)_2$ conjugated dNTPs were also prepared, incorporated and used in biosensor and analytical applications. [69]

Diverse approaches that exploit electrochemical detection of primer extension have been reported, where the primer extension reaction takes place either in the solution phase and the products are then detected, or direct detection of solid-phase primer extension.

Brazill and Kuhr, described the first example of a SNP assay system that utilized a ferrocene-labelled chain terminator (ferrocene-acycloATP). [70] The primer extension reaction was carried out in solution followed by separating the reaction mixture by capillary gel electrophoresis. If the labelled chain terminator corresponded to the mutation site in the single-base extension reaction, the extension product showed an electroactive signal, which was detected at the separation anode with sinusoidal voltammetry detection. The incorporation of electroactive nucleoside triphosphates by polymerases or terminal transferases and their subsequent detection using HPLC-ECD has also been reported.[71]

Daniel *et al.,* (2004) described a single base extension (SBE) assays [69] that uses a various electroactive nucleoside triphosphates. For instance, the single primer extension (SBE) reactions were performed in solution with a mutant enzyme (exo- A488L Vent DNA polymerase) capable of incorporating both dNTPs and acyNTPs.[72] The polymerase was incubated with Vinyl-Fc-dUTP, oligonucleotide primer and template containing either an “A” (wildtype) or “C” (SNP) at the position directly downstream from the 3' primer terminus (Figure 1.4). SBE reaction products were purified by gel filtration chromatography and hybridized with electrode immobilized probes and square wave

voltammetry was applied to detect the unique electrochemical signals for incorporated Vinyl-Fc-dUTP.

Debela *et al*., (2016) also investigated the using of electrochemical primer extension termination assay to detect SNPs known to occur in the MYH7 gene by exploiting redox-labelled ddNTPs. The APEX reactions were performed after hybridization of the template followed by enzymatic incorporation of the label modified ddNTP which terminates the reaction. The electroactive molecules signals were detected electrochemically using differential pulse voltammetry and clear discrimination allowing reliable identification of the SNP was achieved . (Figure 1.4).[73]

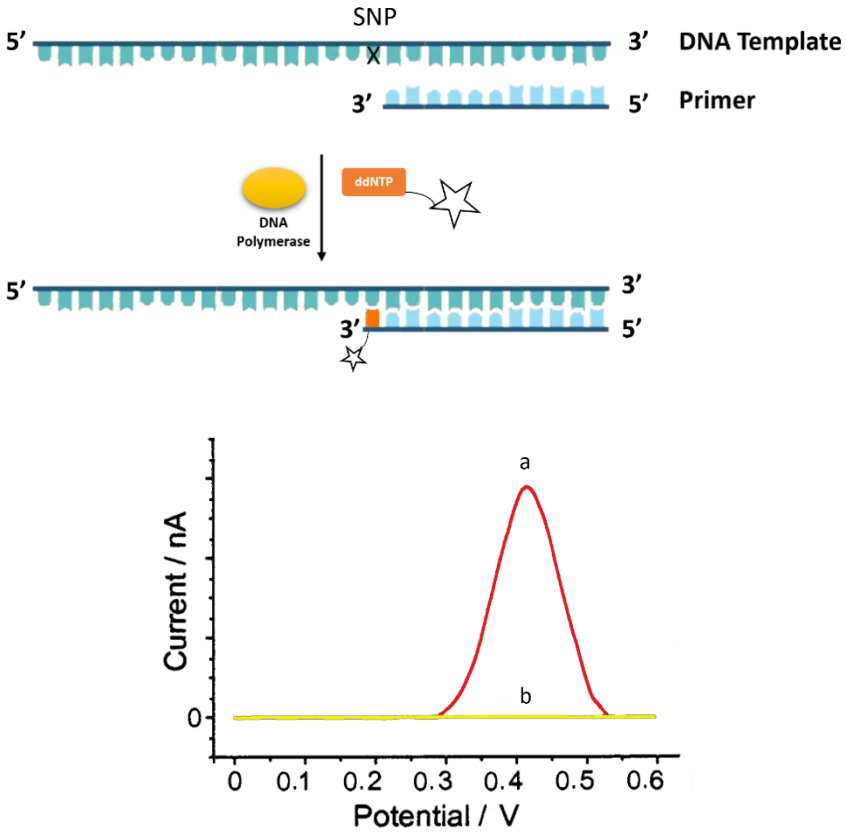

Figure 1.4. Top) Single base extension of a primer oligonucleotide with an labelled ddNTP. **Bottom)** electrochemical scan of DNA following extension by Fc-labelled-ddNTP (a) Correct SNP site, (b) Incorrect mismatched site in template.

In our work, we exploited traditional redox labels, including ferrocene, phenothiazine and antraquinone but we decided to explore an alternative label in the form of polyoxometalates (Figure 1.5 and Figure 1.6).. Polyoxometalates (POMs) are nano-meter-sized inorganic polyanions usually consisting of oxides of molybdenum or tungsten and, less frequently, vanadium, niobium and tantalum or a mixture of these elements in their highest (do, d1) oxidation state. The POM formula according to Pope, is [74] could be heteropolyanions $[X_xM_mO_y]^{q-}$ ($x \leq m$) or isopolyanions structure $[M_mO_y]^{q-}$. Each metal is located at the center of polyhedra, MOx, and the polyhedra are rarely faces together because of the bonding through their edges or the cornersr. For heteropolyanions, the polyhedra are constructed in symmetry around the central heteroatom X, that is usually a PO_4^{3-} or SiO_4^{4-} .Such as the Keggin POM which has tetrahedral symmetry of the phosphate ion or the silicate. Keggin anions has globular shape with a diameter around 1.2 nm and a formula as, α-$[XM_{12}O_{40}]^{n-}$ ($M = Mo^{VI}, W^{VI}$; heteroatom $X = Si^{IV}, Ge^{IV}, P^{V}, Fe^{III}$, etc.), Gathered by four $[M_3O_{13}]$ groups at the corners of a tetrahedron XO_4, including a large group of different shape molecules. Each group has a common oxygen atom which is shared with a central tetrahedron XO_4, and consisted of three octahedra sharing edges. Removal one or more MO groups will led to form the lacunary Keggin molecules. [74]

Dawson anion has the common formula of $[(X^{n+})_2M_{18}O_{62}]^{(16-2n)-}$, where the X^{n+} central heteroatom is P(**V**), S(**VI**), As(**V**) surrounded by addenda atoms each composed of MO_6 octahedral units. The phosphotungstic Dawson anion (reported by Kehrmann 1982 for the first time)[75] can be chemically modified removing MO groups to generate a lacunary anion by which has several unique properties distinct from their parent structures, such as reduced symmetry, higher charge density and increased reactivity.[74] The both of Keggin and Dawson lacunary anions can be loaded by different sorts of elements such as lanthanides, molybdenum, tin, vanadium..etc.

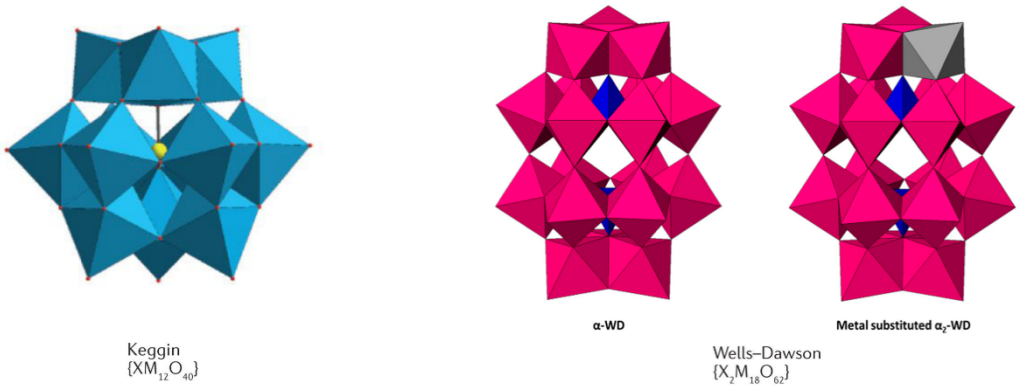

Figure 1.5. Illustrations of (**a**) Keggin $(XM_{12}O_{40})^{n-}$, (**b**) α-Wells–Dawson POM $[P_2W_{18}O_{62}]^{6-}$ (α-WD) and (**c**) the metal-substituted α_2-Wells–Dawson (WD) species with the substituted metal shown in grey, MO_6, in pink and XO_4 in blue. [Heterogeneous Photocatalysis, 63–107], [Materials, 12(13), 2175].

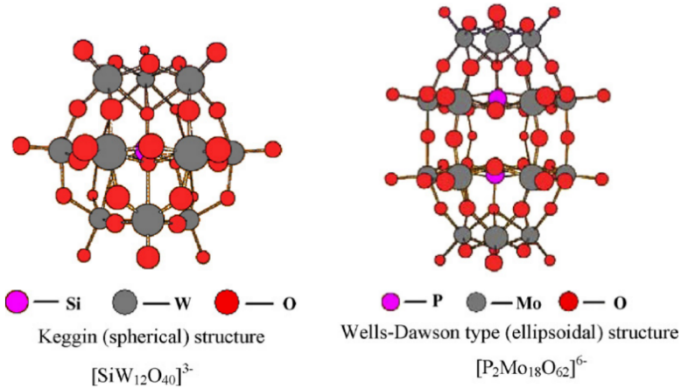

Figure 1.6. The structure of Keggin and Wells–Dawson anion [reported from, New progress of Keggin and Wells–Dawson type polyoxometalates catalyze acid and oxidative reactions, [Chemical 262 (2007) 67–76].

Organic POM derivatives (organic–inorganic POMs) have features of both inorganic polyanion and covalently bound organic molecules in one molecular structure. Additionally, they have chiral, magnetic and electrical properties [76,77] besides a catalytic properties. Organotin is a chemical compounds based on tin element bonded to carbon, and they are widely used in organic fuctionalisation providing a robust stable oxide clusters under physiological conditions. [78,79] Pope *et al.,* (1979) studied [80] the hydrolytic stability over a wide pH range, of the organotin derivatised Keggin and Dawson structures. He reported that the tin derivatised Keggin POMs were stable between pH 4 to 6, while, the tin derivatised Dawson POMs were stable over pH range from 2 to 8.

POMs have been widely used due to their unique properties.[80] POMs provide rich redox properties, with long stable redox states, stability at high temperatures (up to 350 °C), stability in air, solution and acidic conditions.[81] Moreover, these properties can be manipulated and controlled by organic functionalization of the hetero ions and addenda ions that are integrated into the structure.[82] The order of acidity and stability in the solution can be affected by changing the metal and the addenda atoms. For instance, the stability order of acidity and the oxidizing power can be related to the higher pH as shown in Dawson-Poms types, where the basicity increases with increasing Mo in the structure as $P_2W_{17}Mo$ higher than $P_2W_{16}Mo_2$ which is higher than $P_2W_{15}Mo_3$.[83,84]

With respect to their electrochemical behaviour, the heteropolyanions can exhibit rapid two-step one-electron reversible reduction processes producing the so-called "heteropoly blue", and further irreversible multielectron reductions associated with decomposition. Both Keggin ($XM_{12}O_{40}$) and Dawson ($X_2M_{18}O_{62}$) related structures form heteropoly blues where the reversible reduction occurs.[85]

The electrochemical behavior of these heteropolyanions presents different features because they differ in their redox potentials, pKa, and their stabilities. The redox potential depends on many factors, for example, for a given oxidation state, the redox potential increases with the size and decreasing electronegativity of X. The redox potential of Mn (III/II) increases with the size of X, where X = B < Zn < Si < Ge < P [$XM_{11}O_{39}M'^{n-}$ and $X_2M_{18}O_{61}M'^{n-}$)] .[86]

1.7. Melting curve analysis

In 1983 Kary Mullis developed the PCR (polymerase chain reaction) technique. It is a method that uses Taq polymerase and a thermocycler, and is used to rapidly amplify a specific part of DNA sample into billions of copies and has been widely used in molecular biology, clinical diagnostics and forensic analyses.[87] The polymerase chain reaction mechanism can be divided into three steps, the first one is called denaturation, which takes place at at 95 °C and separates the duplex DNA into two single strands. In the second step, called Annealing, the primers anneal (hybridize) to their complementary sequences in the formed single-stranded DNA at 58-65°C (dependent on the melting temperature of the primers). In the last step, elongation, complementary nucleotides are added via a thermophilic polymerase (Thermus aquatificus (Taq) polymerase), initiating from the 3' end of the primer, at 72°C, the optimal temperature of Taq. The product is two new double helices, each composed of one of the original strands hybridized to its newly assembled complement.

Thirty years after the invention of PCR [88], real-time PCR (rtPCR / qPCR) was developed for the quantitative measurement of nucleic acid templates via fluorescence detection. The most commonly used nethod in qPCR takes advantage of the intercalating dye, SYBR Green I. Following elongation at each cycle of PCR, SYBR green intercalates into the major and minor grooves of DNA and the fluorescence signal measured. When carrying out multiplexed amplification and detection, a technique known as melting curve analysis, is frequently employed to differentiate between different amplicons. In this technique, at the end of the qPCR reaction, the duplex DNA is melted completion of frequently a technique termed melting curve After PCR, the products are melted at a fixed rate (usually 0.1– 0.3°C/s) and the decrease in fluorescence is monitored as the DNA denatures and this melting temperature used to identify the specific amplicons.

Melting curve analysis (MCA) is a well-established technique for detection of mutations, detecting differences in complementarity between different strands and was initially based onUV-Vis detection of DNA at 260 nm, where increasing temperature results in duplex denaturation and increasing absorbance until all the duplex has been denatured. In order to improve the resolution and sensitivity of this technique, UV-Vis absorbance was replaced by fluorescence detection. In this approach, akin to that exploited in qPCR, a fluorescent dye binds to the DNA duplex via intercalation and a fluorescent signal measured. To generate the melting curve profile, the sample is subjected to a steady heating ramp, normally controlled by a Peltier, and as the T is increased, there is a concomitant decrease in fluorescence signal until all the duplexes have melted, with the melting temperature being defined as the point where 50% of the duplexes have denatured.[89] Further work introduced probe melting analysis as a convenient genotyping method, first with two labelled

oligonucleotides[90,91] and then with one[92], and finally with the development of saturating DNA dyes with unlabelled oligonucleotides. [93]

In 1997, rapid cycle PCR with real-time fluorescent monitoring and MCA were introduced, joined as lightcycler, a technology widely used in molecular biology. The first instruments developed for real-time PCR were the lightcycler (Roche, Indianapolis, IN) and the ABI 7700 (applied Biosystems, foster City, CA).[94] The LightCycler was introduced using SYBR Green I as a generic DNA dye whereas the ABI 7700 used hydrolysis probes (TaqMan). Hydrolysis probes are labelled with both a fluorescent reporter and a quencher, usually at opposite ends of the probe.[95] Using PCR, annealed probes are hydrolysed, separating the fluorophore from the quencher and increasing fluorescence.[96] As fluorescence results from probe hydrolysis, they are referred to as hydrolysis probes.[97] Initially, multiplexed amplification was carried out using SYBR Green and MCA,[98] but the Taqman approach takes advantage of different probes with diverse fluorescent labels. For example, a biallelic single base change can be genotyped with two hydrolysis probes, each complementary to one allele.[99] Multiplexing using MCA is possible due to the sequence-dependent difference in the stabilities of duplexes and associated different melting temperatures.[100]

Both the ABI 7700 and the Roche LightCycler platforms both evolved and ABI adopted SYBR Green I whilst hydrolysis probes became an option on the LightCycler. Melting curves on the LightCycler became known as dissociation curves on ABI instruments and these techniques have been used for the detection of a vast number of diagnostic targets.

High-resolution melting curve analysis expands the power of previous techniques and can be performed in just 1–2 min. When combined with rapid-cycle PCR [101], amplification and analysis can easily be performed in less than 30 min.[89] Idaho Technology developed the first high-resolution melting instrument and analysed samples that were amplified in LightCycler capillary tubes. The LightCycler 480 carries out amplification and high-resolution melting in a plate format. This high-resolution melting analysis has been widely used in cinical analysis, including the detection of the BRCA1/2 gene[102] cystic fibrosis,[103,104] hereditary hemorrhagic telangiectasia,[105] hemophilia, Charcot-Marie-Tooth disease as well as for the detection of tumours, [106] and to detect somatic changes in the exons of oncogenes such as EGFR, [107] KRAS, [108] PDGFRA, KIT, [109] BRAF, [110] and TP53. [111] High-resolution melting was employed by clinical laboratories due to its relatuive low cost and complexity for analysing whole genes with combined PCR amplification and probe-melting analysis. [112]

Modern high resolution melting curve instruments routinely utilize the SYBR GREEN I DNA binding dye. Whilst SYBR GREEN I is sensitive and suitable for PCR melting analysis, it does suffer from some drawbacks, the most important being the inhibition of PCR when the dye is presenta at high concentrations, but using too low a concentration of the dye can lead to rapis signal saturation due

to dye consumption.[113] New generation dyes, such as LC green I and LC green Plus are compatible with PCR over a wider range of concentrations[101,114] but are markedly more expensive. Alternatives include the SYTO dyes and Eva Green, which both perform better than SYBR Green in general as evidenced by a study where Eva-Green and the SYTO (13, 16, 80, and 82) dyes showed the sharpest peaks in MCA.[115]

Table.1.1 Reaction efficiency data (16S amplicon) [115]

Dye	Concentration	R2	Slope	Efficient
SYBR Green	0.32 × (0.64 µM)	0.985	-3.40	97%
SYBR Green	1× (2 µM)	0.395	-2.13	195%
EvaGreen	1×	0.995	-3.30	101%
EvaGreen	5×	0.999	-3.46	95%
SYTO 13	5 Mm	0.993	-3.42	96%
SYTO 13	10 Mm	0.993	-3.44	95%
SYTO 16	5 µM	0.983	-3.30	101%
SYTO 16	10 Mm	0.992	-3.43	96%
SYTO 80	10 Mm	0.992	-3.42	96%
SYTO 80	20 µM	0.986	-3.41	96%
SYTO 82	10 Mm	0.998	-3.41	96%
SYTO 82	20 µM	0.996	-3.37	98%

SYBR Green, Evergreen and four SYTO dyes were used in tests of reaction efficiency for the 16S target.

Miniaturized assays in a microarray format offer the possibility of low-cost, high-throughout SNP genotyping. One technique exploited in microarray detection is dynamic allele-specific hybridization (DASH), which uses dynamic heating while simultaneously monitoring DNA denaturation for accurate SNP discrimination.[116]

Russom introduced the possibility of analysing SNPs using DASH to perform melting curve analyses on monolayers of beads Immobilized on the surface of a microheater chip to detect three possible variants of SNP. The chip is heated from 20 - 85°C, with the fluorescence being monitored using a CCD camera. Subsequently, Russom[117] presented another rapid solid-phase melting curve analysis method for SNP genotyping based on (DASH) technology with a heating rate more than 20 times faster than conventional DASH, which significantly reduced the total analysis time to less than 1 min, enabling ultra-rapid SNP analysis.

Jasper *et al*.,(2008) described a robust genotyping assay, termed multi thermal array washing, based on a microfluidic device with eight relatively large, individually controlled heating zones for multi-stringency post-hybridization washing of microarrays printed on glass slides.[118]

Chen developed a thermal digital microfluidic (T-DMF) platform to perform a very fast DNA melting curve analysis in just 7 seconds. The T-DMF device was able to differentiate a Tm difference down to 1.6 °C with a variation of 0.3 °C in a droplet sample of 1.2 µL, which was 300 times faster and with 20 times less sample volume than used in a commercial qPCR machine (35 minutes, 25 µL).[119]

1.7.1. Multiplex solid-phase melting curve analysis

Arjang Hassibi *et al*., (2018) presented an efficient portable biosensor device for molecular diagnostics capable to perform a multiplex mutation detection. This sensor combines a nucleic acid amplification test (NAAT) platform housed in a microfluidic chamber for the multiplex asymmetric PCR amplification and the melting curve analysis method for the detection.HYDRA-1K biosensor array is composed of complementary metal oxide semiconductor CMOS-integrated sensor consisting of 32x32 pixels modified with various probes. Each one act as an electrode enabling target DNA sequence identification by optical detection. A dynamic range-photo-sensor and thermo-cycler are integrated into every pixel. To demonstrate the multiplexing and genotyping accuracy, a Mycobacterium tuberculosis sample was used to identify 54 SNPs related to the resistance torifampicin and isoniazid. The array was tethered by designed probes labelled fluorophore (FAM-TAM) to distinguish between wild (WT) and mutant (MT) type strains, that hybridized to ssDNA target labelled-quencher generated by asymmetric PCR using Q-dCTP. After performing a solid-phase MCA, the melting curve profile results showed the accuracy of identifying the WT with all SNPs even in those within the high rich G-C region with secondary structures.

The HYDRA-1k biosensor has many advantages as compared to other technologies such as the DNA arrays and sequencing with PCR, . In addition, the cost of the reader device (~$100) is very low compared with the cost ofa PCR instrument (~$25,000) and it can provide a rapid test in less than 1 hour with a price cost of (10$) for the test and up to 1000 different targets at the same time.[120]

In another report, Dana *et al*., (2019) presented a multiplexed solid-phase melting curve analysis test for detection of drug-resistance mutation (DRMs) in the HIV-1 RT gene. The platform is based on a microarray made of silicon slide immobilized with an 80-bp capture probe hybridized to a cyanine 3-labelled 80-bp HIV-1 target generated by asymmetric PCR and contained a 34-bp region complementary to each probe. After hybridization, the array is washed to remove unbound DNA and the MCA is performed in 20 minutes by elevating the temperature from 45 to 90 ºC, taking serial images every 10 s. Finally, the melting profiles obtained from plotting the fluorescent signal intensity versus the temperature

for each probe confirmed the distinction between each of the six codons at HIV-1 DRM reverse transcriptase position 103in both synthetic and plasma samples.[121]

1.7.2. Electrochemical based melting curve analysis

Solid-phase electrochemical based melting curve technique has been used to determine melting temperatre, where a probe is surface tethered and hybridized to the DNA sequence under interrogation, prior to measuring a change in electrochemical signal as the temperature applied to the electrode is arrayed. The probe should remain stably Immobilized on the surface as the temperature is increased and to address this a number of thermostable surface chemistries have been developed.

The formation of self-assembled monolayers (SAMs) is the most commonly used protocol for stably attaching thiolated DNA to an electrode surface. To enhance both lateral stability with SAMs and their coupling to substrates, and thus improving the thermal stability of the SAM, various approaches have been tested including lateral polymerisation [122], hydrogen bonding [123], multiple sulfur substrate coupling [124, 125] as well as the utilisation of more rigid aromatic SAMs.[125] An alternative approach is to graft the electrode surface with diazonium salts [126] for subsequent DNA attachment to amine/carboxy grafted electrodes through the generic carbodiimide coupling. The enhanced stability of the surface anchored DNA helps to improve reproducibility and reduce noise. [127]

Different approaches for the electrochemical determination of melting temperature, normally recording the thermogram (current versus temperature) of a redox label indicator on a dsDNA modified electrode as the duplex melts. Redox labels that have been used include anticancer agents such as echinomycin[128,129] and epirubicin[130], organic dyes such as methylene-blue, metal complexes such as cobalt phenanthroline[131,132], cobalt bipyridine[133,134] and ruthenium bipyridine[135], as well as enzymes and metal nanoparticles.

Alternatives include measurement of the decrease/increase in the oxidation/reduction peak current of redox labels that selectively bind to either dsDNA/ssDNA, the direct detection of the electroactive DNA bases guanine or adenine.

Prest proposed an approach using square wave voltammetry to measure the intercalating redox dey, methylene blue as the immbilised DNA duplex is denatured. Prest found that, in solution, addition of MB to the DNA induces a destabilization, resulting in a a decrease of Tm by >10°C, while the fixation of the DNA±MB complex on a support tends to stabilize the DNA, possibly to interactions in the DNA monolayer. The intensity of the square-wave voltammogram when MB was used as intercalator showed 12-fold higher as compared to that of $Ru(NH3)_6^{3+}$.This is because MB intercalates into the

DNA base backbone and participating in electron transfer mediated by the stacked bases. Defever reported a real-time PCR method based on the electrochemical monitoring of a $Os[(bpy)_2dppz]^{2+}$ DNA intercalator, a stable redox compound under PCR cycling conditions, that strongly and specifically binds to the amplified dsDNA without inhibiting PCR, and can be sensitively detected by square wave voltammetry during PCR cycling.[136]

Surkus and Flechsig introduced a fast and easy electrochemical melting curve biosensor that can distinguish between full match and mismatched targets. The assay used a gold electrode tethered by thiol- 20 bases capture probe hybridized to four different amplicon targets-labelled-Os (osmium-tetroxide-bipyridine, $[OsO_4(bipy)]$). The targets were one fully complementary to the probe and the others with one, two, and three mismatched bases. The melting curve performed by heating up the gold electrodes and applying alternating current voltammetry (ACV) to record the Os-label response at -0.32 V vs. Ag/AgCl reference. The generated melting profile results showed a 3 to 5 ºC decrease in melting point (Tm) for each per mismatch, and the first mismatch has the biggest effect.[137]

A new micro-platform device, fabricated using lithographic technology, integrated thermal control and a multi-electrode array, was designed by Shen to perform rapid electrochemical melting curve analyses on small-volume samples of 10µL.[138] By using a built-in peltier heater, rapid temperature ramping could be achieved and discrimination between full-match, single-mismatch and double-mismatches was demonstrated. It has advantage of producing multi-arrays associated microfluidics for high-throughput parallel measurements.

Nasef described a low cost method[139] based on labelless electrochemical melting curve analysis for the rapid detection of the cystic fibrosis associated DF508 mutant. A thiolated probe of 21-bases, complementary to specific region where the DF508 mutation exists was Immobilized on a Au electrode surface and hybridized to a single strand DNA generated using a PCR of mutant target (85 bases) or wild-type target of (82 bases). Methylene blue was used as electrochemical indicator to measure the levels of hybridization and the decrease in differential pulse voltametric signal was measured as the temperature was increased in a non-continuous format (i.e. increase temperature, stop, measure, further increase temperature, stop, measure etc.), a clear discrimination between mutant and wild-type target was observed. Nasef also developed an alternative approach based on an Immobilized probe hybridized to mutant amplicon labelled with ferrocene, again for the detection of these three-base deletion mutation.[140] Following hybridization of the sequence under interrogation to the Immobilized process, the entire array was subjected to temperature ramping and the dissociation of the ferrocene labelled DNA was monitored using differential pulse voltammetry. The Tm recorded for the fully complementary and for the mismatched duplex was 38 °C and 30 °C respectively, which provided a clearly discrimination between match and mismatch targets. The

equivalent Tm of the duplex in homogenous solution, measured using UV–Vis measurements (λ= 260 nm), was cdetermined to be 59 °C. This difference in melting behavior, with a significantly lower Tm observed for the surface-tethered duplex as compared with solution, could be attributable to the effect of the density of the Immobilized DNA probes on the charge density, due to the ionizability of the phosphate groups.

Luo X *et al*., (2009) reported a simple detection method for SNP analysis based on immobilization-free electrochemical method for real-time monitoring of the double strand DNA denaturation. The method used a ferrocene labelled peptide nucleic acid (PNA) and a fully-complementary or single-base-mismatched DNA on negatively charged electrode surface of indium tin oxide (ITO). [141] In general, the hybridization between PNA-labelled-Fc and the fully complementary DNA formed a negative hybrid on the negative ITO electrode resulting in a decrease in electrochemical signal due to a lower ferrocene diffusion to the surface by electrostatic repulsion.When the temperature is increased, the PNA-labelled-Fc is dissociated from the hybrid and the neutrally charged Fc-PNA easily diffuses to the electrode with a higher electrochemical signal. Therefore, the meting profiles could be generated by measuring the signal of the electroactive ferrocene versus the elevated temperature.

Miniaturized assays in a microarray format (DNA chip) offer the genotyping large numbers of SNPs at low cost [142]. One of these methods is called DASH (dynamic allele-specific hybridization) which enhanced by dynamic heating while monitoring the DNA denaturation simultaneously for accurate SNP discrimination.[116] Allen *et al*., (2014) presented a microE-DASH device with an electrochemical system for detection of SNPs that can perform melting-curve analysis in real-time, and discriminate accurately between homozygous and heterozygous mismatches of two SNPs in the E (ApoE) gene, by measuring a redox current as a factor of temperature. Even more, it can achieve multiplexed detection at multiple loci in one step. Basically, gold electrodes immobilized by redox labelled probes can be hybridized to a perfect match and a single mismatched targets. After performing the melting curve analysis, and measuring the redox signal of MB by alternating current voltammetry, the perfect match could be distinguished from the mismatched target based on its higher melting point.[113]

Whilst the possibility of electrochemically detecting and identifying SNPs has been demonstrated using melting curve analysis, all the platforms used have been crude laboratory set-ups, leading to problems in reproducibility and robustness. Furthermore, to date there are no examples of multiplexed solid-phase melting curve analysis.

Table. 1.2. Comparison of electrochemical biosensors for melting curve analysis determination.

Target	Detection strategiy	Lable	Detection	Method	Working electrode	Ref
Fc-PNA/DNA	Electrochemical MCA	Fc-PNA	DPV	Immobilization free	ITO	141
Amplify 283 BP hCMV DNA targeting DF508 mutation of CFTR gene	Electrochemical post PCR / MCA	$Os(BPy_2DPPz)_2$	SWV	Immobilization free	carbon	143
Synthetic tttt probe	Electrochemical MCA (direct measure)	MB -Intercalator $Ru(NH_3)_6$ - Intercalator	SWV	Immobilization free & Immobilized Probe	AU	144
Cyctic fibrosis model associated DF508 mutation		MB -Intercalator	DPV	Immobilized Probe	AU	139
Cystic fibrosis model associated DF508 mutation		FC-Probe	DPV	Immobilized Probe	AU	140
Designed Probe		MB-Probe	SWV	Immobilized Probe	AU	138
Analysis 2 Snp in APOE gene	Real time MCA	MB-Probe	ACV	Immobilized Probe	AU	113

1.8. Objective of the work

The overall objective of this PhD thesis was to explore different methodologies for the detection of SNPs, which could be exploited in semi-automated, multiplexed formats. We pursued two different avenues to achieve this goal. The first explored the use of the electrochemical detection of solid-phase primer extension with redox labelled dideoxynucleotide triphosphates. As an alternative to the traditional redox labels used, we also investigated the possibility of using polyoxometalate labels, as they showed great potential in terms of cost and stability. Whilst the platform was demonstrated to very effectively detect and identify a specif SNP associated with cardiomyopathy, the preparation and purification of the POM / redox-labelled ddNTPs was incredibly laborious and not of excellent yield and an alternative approach was thus subsequently pursued. In this second approach the use of electrochemical detection of solid-phase melting curve analysis was visited. In the first part of this work, an in-house melting curve analysis device was produced, integrating controlled heating of the electode array, with washing fo the electrode array surface and electrochemical measurement, facilitating continuous temperature ramping, washing to remove denatured labelled probes and voltametric measurement. The first objective of this part of the work was to demonstrate this semi-automated melting curve analysis, and using this device to optimise the position in the Immobilized probe to place the complementary to the SNP site under interrogation. The work then moved on to using the system for the detection and identification of a specific SNP, in this case related to osteoporosis, in a fingerprick blood sample. The aim of this part of the work was to optimise conditions for the asymmetric isothermal amplification of a specific DNA sequence from a fingerprick and to genotype the SNP present in the single stranded DNA amplicon. In the final part of the work, the objective was to manufacture an automated version of the melting curve analysis device and to apply it to the multiplxed detection of SNPs.

References

1. Cammann K. (1977). Bio-sensors based on ion-selective electrodes ‚Fresenius' Zeitschrift fur Analytische Chemie, 287(1), 1–9.
2. Thevenot D. R., Tóth K., Durst R. A., Wilson G. S. (1999). Electrochemical Biosensors: Recommended Definitions and Classification. Pure and Applied Chemistry, 71(12), 2333–2348.
3. Thévenot D. R., Toth K., Durst R. A., Wilson G. S. (2001). Recommended definitions and classification, Biosens. Bioelectron. Bioelectron, 16, 121–131.
4. Monošík D. R., Streďansky M., Šturdík E. (2012). Biosensors-classification, characterization and new trends. Acta Chim. Slovaca, 5, 109–120.
5. Mehrotra P. (2016). Biosensors and their applications – a review. Journal of Oral Biology and Craniofacial Research, 6(2), 153–159.
6. Rahman M., Li X. B., Lopa N., Ahn S., Lee, J. J. (2015). Electrochemical DNA Hybridization Sensors Based on Conducting Polymers. Mdpi Journal, 15(2), 3801–3829.
7. Yang C., Denno M. E., Pyakurel P., Venton B. J. (2015). Recent trends in carbon nanomaterial based electrochemical sensors for biomolecules: A review. Anal. Chim. Acta, 887, 17–37.
8. de Lumley T. Campbell C., Heller A. (1996). Electroanalytical Methods Of Biological Materials. J. Am. Chem. Soc, 118, 5504–5508. [Google Scholar]
9. Ahmed M. U., Saaem I., Wu P. C., Brown A. S. (2014). Personalized diagnostics and biosensors: A review of the biology and technology needed for personalized medicine . Crit. Rev. Biotechnol, 34, 180–196.
10. Wang J., Cai X., Rivas G., Shiraishi H. (1996). stripping potentiometric transduction of DNA hybridization process. Anal. Chim. Acta, 326, 141–147
11. Wang J. (1999). Amperometric biosensors for clinical and therapeutic drug monitoring : a review. Biomed. Anal, 47–53.
12. Gs S., Cv A., Mathew B.B. (2014). Biosensors : A Modern Day Achievement. J. Instru.Tech, 26–39.
13. Najeeb J., Ali J., Asim A. M., Farhan A. M., Raza A. (2017). Biosensors: Their Fundamentals, Designs, Types and Most Recent Impactful Applications. J.Biosens. Bioelectron, 081–9.
14. Ahmed N. (2018). Detecting food borne pathogens using electrochemical biosensors. J. Chem. Studies, 1031-1039.

15. Hleli S., Martelet C., Abdelghani A., Bessueille F., Errachid A., Samitier J. (2006). An immunosensor for haemoglobin based on impedimetric properties of a new mixed self-assembled monolayer. a. Mater Sci Eng C, 26, 322–327
16. Park J. Y., Park S. M. (2009). DNA Hybridization Sensors Based on Electrochemical Impedance Spectroscopy as a Detection Tool. Sensors, 9, 9513–9532.
17. Smiechowski M. F., Lvovich V. F., Roy S., Fleischman A., Fissell W. H., Riga A. T. (2006). Biosens. Bioelectron, 22, 670–677.
18. Daniels J. S., Pourmand N. (2007). Label-Free Impedance Biosensors: Opportunities and Challenges . Electroanalysis, 19(12), 1239–1257
19. Ye Y., Xie J., Ye Y., Cao X., Zheng H., Xu X., Zhang Q. (2018). A label-free electrochemical DNA biosensor based on thionine functionalized reduced graphene oxide N. Y. 129, 730–737.
20. Ribovski L., Zucolotto V., Janegitz B.C. (2017). A label-free electrochemical DNA sensor to identify breast cancer susceptibility . Microchem. J, 133, 37–42.
21. Grieshaber D., MacKenzie R., Vörös J., Reimhult E. (2008). Electrochemical Biosensors - Sensor Principles and Architectures. Sensors, 8(3), 1400–1458.
22. Scott K. (2016). Electrochemical principles and characterization of bioelectrochemical systems. Microbial Electrochemical and Fuel Cells, 29–66.
23. Dai Y., Molazemhosseini A., Liu C. C. (2017). A Single-Use, In Vitro Biosensor for the Detection of T-Tau Protein, A Biomarker of Neuro-Degenerative Disorders, in PBS and Human Serum Using Differential Pulse Voltammetry (DPV). Biosensors 7, 10
24. Zhai J., Cui H., Yang R. (1997). DNA based biosensors. Biotechnology Advances, 15(1), 43–58.
25. Paleček E., Fojta M., Tomschik M., Wang J. (1998). Electrochemical biosensors for DNA hybridization and DNA damage. Biosensors and Bioelectronics, 13(6), 621–628.
26. Manzanares-Palenzuela C. L., Martín F. B., Sánchez P. L. M., López R. B. (2015). Electrochemical genosensors as innovative tools for detection of genetically modified organisms. Anal. Chem, 66 19–31.
27. Nimse S., Song K., Sonawane M., Sayyed D., Kim, T. (2014). Immobilization Techniques for Microarray: Challenges and Applications. Sensors, 14(12), 22208–22229.
28. Rashid J. I. A., Yusof N. A. (2017). The strategies of DNA immobilization and hybridization detection mechanism in the construction of electrochemical DNA sensor: A review, Sens. Bio-Sensing Res, 16 19–31.

29. Elsholz B., Worl R., Blohm L., Albers J., Feucht H., Grunwald T., Jurgen B., Schweder T., Hintsche R. (2006). Automated detection and quantitation of bacterial RNA by using electrical microarrays. Chem, 78, 4794–4802.
30. Wittmann C., Marquette C. (2012). DNA Immobilization. Encyclopedia of Analytical Chemistry, 15(3).
31. Brookes A. J. (1999). The essence of SNPs. Gene, 234 (2), 177–186.
32. Venter J. C., Adams M. D., Myers E. W., Li P. W., Mural R. J., Sutton G. G., Holt R. A. (2001). The sequence of the human genome. Science, 291(5507), 1304–1351.
33. Drumm M. L., Konstan, M. W., Schluchter, M. D., Handler, A., Pace, R., Zou, F., Knowles, M. R. (2005). Genetic Modifiers of Lung Disease in Cystic Fibrosis. New England Journal of Medicine, 353(14), 1443–1453.
34. Muniz M. G., Lavinha J., Pacheco P.,(2000). Allele Increases the Genetic Diversity at the HBB Locus in the Caribbean .Am. J. Hemathology, 64, 7-14.
35. Wu D. Y., Ugozzoli, L., Pal, B. K., & Wallace, R. B. (1989). Allele-specific enzymatic amplification of betaglobin genomic DNA for diagnosis of sickle cell anemia. Proceedings of the National Academy of Sciences, 86(8), 2757–2760.
36. Neveling K., Collin R. W. J., Gilissen C., van Huet R. A. C., Visser L., Kwint M. P., Scheffer H. (2012). Next-Generation Genetic Testing for Retinitis Pigmentosa. Human Mutation, 33(6), 963–972.
37. Howell W. M., Jobs M., Gyllensten U., Brookes A. J., (1999). A new method for scoring single nucleotide polymorphisms . Nat. Biotechnol, 17, 87–88.
38. Whitcombe J. T., Guy S. P. (1999). Detection of PCR products using self probing amplicons and fluorescence . Nat Biotechnol, 17, 804–7.
39. Huh Y. S., Lowe A. J., Strickland A. D., Batt C. A., Erickson D. (2009). Surface-Enhanced Raman Scattering Based Ligase Detection Reaction. J. Am. Chem. Soc, 131, 2208.
40. Lyamichev V., Mast A. L., Hall J. G., Prudent J. R., Kaiser M. W. (1999). Polymorphism identification and quantitative detection of genomic DNA by invasive cleavage of oligonucleotide probes. Biotechnol, 17, 292–296.
41. Di Giusto D., King G. C. (2003). Nuc. Single base extension with proofreading polymerases and phosphorothioate primers. Ac. Res. 31, e7
42. Di Giusto D., Wlassoff W. A., Giesebrecht S., Gooding J. J., King G. C. (2004). Multipotential Electrochemical Detection of Primer Extension Reactions on DNA Self-Assembled Monolayers. J. Am. Chem. Soc. 126, 4120–4121.

43. Meyer K., Ueland M. P. (2011). Use of Matrix assisted laser desorption ionization time of flight mass spectrometry for multiplex genotyping. Advances in Clinical Chemistry, 53, 1-29
44. Duan X., Liu L., Wang S. (2009). Homogeneous and one step fluorescent allele specific PCR for SNP genotyping assay using conjugated polyelectrolytes. Biosens. Bioelectro, 24, 2095–2099.
45. Ding C., Wang Z., Zhong H., Zhang S. (2010). Ultrasensitive chemiluminescence quantification of single-nucleotide polymorphisms by using monobase-modified Au and CuS nanoparticles . Biosensors and Bioelectronics, 25, 1082-1087
46. Li Y., Wark W. A., Lee H. J., Corn R. M. (2006). Single-nucleotide polymorphism genotyping by nanoparticle-enhanced surface plasmon resonance imaging measurements of surface ligation reactions. Anal Chem, 78, 3158.
47. Olivier M. (2005). The Invader assay for SNP genotyping. Mutat Res, 573, 103–110
48. Syvanen A. C. (1999). From gels to chips: “Minisequencing” primer extension for analysis of point mutations and single nucleotide polymorphisms. Human mutation, 13, 1-10
49. Sokolov P. (1990). Primer extension technique for the detection of single nucleotide in genomic DNA. Nuclic Acids Res, 18, 671.
50. Livak K. J., Marmaro J., Todd J. A. (1995). Towards fully automated genome-wide polymorphism screening. Genet, 9, 341–342.
51. Patolsky., Lichtenstein A., Willner I. (2001). Detection of single-base DNA mutations by enzyme-amplified electronic transduction. Nat. Biotechnol, 19, 253–257
52. Liu G., Lee T. M. H., Wang J., (2005). Nanocrystal-based bioelectronic coding of single nucleotide polymorphisms. Am. Chem. Soc, 127, 38–39
53. Liu G., Lin Y. (2007). Electrochemical Quantification of Single-Nucleotide Polymorphisms Using Nanoparticle Probes. J. Am. Chem. Soc, 129, 10394–10401.
54. Kolpashchikov M. D. (2010). Binary Probes for Nucleic Acid Analysis. Chem. Rev, 110, 4709–4723
55. Zhang Y. L., Huang Y., Jiang J. H., Shen G. L., Yu R. Q. (2007). Electrochemical aptasensor based on proximity-dependent surface hybridization assay for single-step, reusable, sensitive protein detection. J. Am. Chem. Soc, 129, 15448–15449
56. Abi A., Ferapontova E. E. (2013). Electroanalysis of single-nucleotide polymorphism by hairpin DNA architectures. Anal Bioanal Chem, 405, 3693-3703
57. Rösler J. S., Briggs J., Cuss S., Horsey I., Kenrick M., Kingsmore S., Kent L., Pickering J., Knott T., Shipstone E., Scozzafava G. (2001). ROLLING CIRCLE AMPLIFICATION FOR

SCORING SINGLE NUCLEOTIDE POLYMORPHISMS. Nucleosides Nucleotides Nucleic Acids, 20, 893– 894

58. Meyer K., Ueland M. P. (2011). Use of matrix-assisted laser desorption/ionization time-of-flight mass spectrometry for multiplex genotyping .Advances in Clinical Chemistry, 53, 1-29
59. Hsu T. M., Chen X., Duan S., Miller R. D. & Kwok P. Y. (2001). Universal SNP genotyping assay with fluorescence polarization detection. BioTechniques, 31(3), 560–570
60. Anderson J. P., Angerer B., Loeb L. A. (2005). Incorporation of reporter-labeled nucleotides by DNA polymerases. Biotechniques, 38, 257-64
61. Wang J. (2006). Electrochemical biosensors: towards point-of-care cancer diagnostics. Biosens Bioelectron 21, 1887-1892.
62. Wong E. L. S., Gooding J. J. (2006). Charge Transfer through DNA: A Selective Electrochemical DNA Biosensor. Analytical Chemistry, 78(7), 2138–2144
63. Ying W., Binxiao L., Jing L., Hong Z. (2018). Electrochemical monitoring of single nucleotide polymorphisms of rice varieties related to blast resistance based on PCR product and T4 DNA polymerase. Sensors and Actuators, 273, 649-655.
64. Ronghui R., Jianmei Y., Ruo Y., and Yun X. (2018). Label-Free and Amplified Electrochemical Detection of Single Nucleotide Polymorphism in Folded Nucleic Acid Secondary Structures. Electrochemical Society, 16, B880-B884
65. Ezat H. A., Jahan B. R., Reza O., Seyed M. G., Mohammad S. H. (2013). A new peptide acid biosensor for electrochemical detection of SNP in duplex DNA via triplex structure formation. Iranian Chemical Society. 10, 1075–1083.
66. Syvanen A. C. (1999). From gels to chips: Minisequencing primer extension for analysis of point mutations and single nucleotide polymorphisms. Human Mutation, 13(1), 1–10.
67. Barone A. D., Chen C., McGall G. H., Rafii K., Buzby P. R., Dimeo, J. J. (2001). Novel nucleoside triphosphate analogs for the enzymatic labeling of nucleic acids. Nucleic Acids, 20(4-7), 1141–1145.
68. Zhu Z., Waggoner A. S. (1997). Molecular mechanism controlling the incorporation of fluorescent nucleotides into DNA by PCR. Cytometry, 28, 206-211
69. Hocek M., Fojta M. (2011). Nucleobase modification as redox DNA labelling for electrochemical detection. Chem. Soc. Rev, 40, 5802–5814
70. Brazill S. A., Kuhr W. G. (2002). A Single Base Extension Technique for the Analysis of Known Mutations Utilizing Capillary Gel Electrophoresis with Electrochemical Detection. Anal. Chem, 74, 3421-3428

71. Wlassoff W. A., King G. C. (2002). Ferrocene conjugates of dUTP for enzymatic redox labelling of DNA. Nucleic Acids Res, 30, e58
72. Gardner A. F., Jack W. E. (2002). Acyclic and dideoxy terminator preferences denote divergent sugar recognition by archaeon and Taq DNA polymerases. Nucleic Acids Res, 30, 605-613
73. Debela A. M., Thorimbert S., Hasenknopf B., O'Sullivan C. K., Ortiz M. (2016). Electrochemical primer extension for the detection of single nucleotide polymorphisms in the cardiomyopathy associated myh7 gene. Chemical Communications, 52(4), 757–759
74. Mizuno N., Misono M. (1994). Heteropolyanions in catalysis. Journal of Molecular Catalysis, 86(1-3), 319–342.
75. Kehrmann F., Anorg z. (1892). Chem. 1, 432
76. Coronado E., Curreli S., Giménez-Saiz C., Gómez-García C. J., Roth J. (2005). A new BEDT-TTF salt and polypyrrole films containing the chiral polyoxometalate [H4Co2Mo10O38]6−. Synth. Met, 154, 241– 244
77. Coronado E., Giménez C., Gómez-García C. J. (2005). Recent advances in polyoxometalate-containing molecular conductors. Chem. Rev, 249, 1776– 1796
78. Sazani G., Pope M. T., (2004). Organotin and organogermanium linkers for simple, direct functionalization of polyoxotungstates. Dalton Transactions, 1989-1994
79. Zonnevijlle., Pope M. T. (1979). Attachment of organic groups to heteropoly oxometalate anions. J. Am. Chem. Soc, 101, 2731– 2732
80. Hill C. L. (1998). Introduction: Polyoxometalates Multicomponent Molecular Vehicles To Probe Fundamental Issues and Practical Problems. Chemical Reviews, 98(1), 1–390.
81. Long D. L., Burkholder E., Cronin L. (2007). Polyoxometalate clusters, nanostructures and materials: from SAM to designer materials and devices. Chem. Soc. Rev,36, 105–121
82. Neumann R. (2010). Activation of Molecular Oxygen, Polyoxometalates, and Liquid-Phase Catalytic Oxidation Inorg. Chem, 49, 3594–3601
83. Tommasino B., Contant R., Michaut J.P., Roncin J. (1998). Electrochemical characterization of a series of substituted Dawson type tungstophosphates α[P2W18−xMozVyO62]n− (x = y + z; n = 6 + y). Polyhedron. Polyhedron,17,357-366
84. Okuhara T., Misuno N., Misono M. (1997). Catalysis by Heteropoly Compounds. J. Catal, 96, 107.
85. Vilà-Nadal L., Romo S., López X., & Poblet J. M. (2012). Structural and Electronic Features of Wells-Dawson Polyoxometalates. Complexity in Chemistry and Beyond: Interplay Theory and Experiment, 171–183.

86. Flynn C. M., & Pope M. T. (1973). Tungstovanadate heteropoly complexes. IV. Vanadium(IV) complexes. Inorganic Chemistry, 12 (7), 1626–1634.
87. Zhang Y., Ozdemir P. (2009). Microfluidic DNA amplification A review Analytica Chimica Acta, 115–125.
88. Egbuna O. I., Brown E. M. (2008). Hypercalcaemic and hypocalcaemic conditions due to calcium sensing receptor mutations.Clin Rheumatol, 22, 129-148
89. Reed G. H., Kent J. O., Wittwer C. T. (2007). High-resolution DNA melting analysis for simple and efficient molecular diagnostics Pharmacogenomics, 8(6), 597-608.
90. Lay M. J. and Wittwer C. T., (1997). Real-time fluorescence genotyping of factor V Leiden during rapid-cycle PCR. Clin. Chem. 43, 2262 – 2267.
91. Bernard P. S., Ajioka R. S., Kushner J. P., and Wittwer C. T. (1998). Homogenous multiplex genotyping of hemochromatosis mutations with fluorescent hybridization probes. Am. J. Pathol. 153, 1055 – 1061.
92. Crockett A. O. and Wittwer C. T. (2001). Fluorescein-labeled oligonucleotides for real-time pcr: using the inherent quenching of deoxyguanosine nucleotides . Anal. Biochem, 290, 89 – 97.
93. Zhou L., Myers A. N., Vandersteen J. G., Wang L., and Wittwer, C. T. (2004). Closed-tube genotyping with unlabeled oligonucleotide probes and a saturating DNA dye . Clin. Chem, 50, 1296 – 1298.
94. Lyon E., Wittwer C. T. (2009). LightCycler technology in molecular diagnostics. J Mol Diagnostics, 11(2), 93-101
95. Livak K. J., Flood S. J., Marmaro J., Giusti W., Deetz K. (1995).oligonucleotides with fluorescent dyes at opposite ends provide a quenched probe system useful for detecting PCR product and nucleic acid hybridization. Methods Appl, 4, 357 – 362
96. Heid C. A., Stevens J., Livak K. J., Williams P. M. (1996). Real time quantitative PCR. Genome Res, 6, 986–994
97. Bustin S., Garson J., Hellemans J., Huggett J., Kubista M., Mueller R., Nolan T., Pfaffl M., Shipley G., Vandesompele J., Wittwer C. (2009). MIQE guidelines:minimum infor for publication of quantitative real time PCR. Clin Chem 55,4 611–622
98. Ririe K. M., Rasmussen R. P., Wittwer CT. (1997). Product Differentiation by Analysis of DNA Melting Curves during the Polymerase Chain Reaction. Anal Biochem, 245, 154 – 160
99. Livak K. J. (1999). Allelic discrimination using fluorogenic probes and the 5' nuclease assay. Genet Anal, 14, 143–149
100. Lay M. J., Wittwer CT. (1997). Real-Time Multiplex PCR Assays . Chem, 43, 2262–2267

101. Wojdacz T. K., Dobrovic A. (2007). a new approach for sensitive and high-throughput assessment of methylation. Nucleic Acids Res, 35, 41
102. De Juan I., Esteban E., Palanca S., Barragán E., Bolufer P. (2009). High resolution melting analysis for rapid screening of and spanich mutations. Breast Cancer Res Treat, 115(2), 405-414
103. Montgomery J., Wittwer C. T., Kent J. O., Zhou L. (2007). Scanning the cystic fibrosis transmembrane conductance regulator gene using high-resolution DNA melting analysis. Clin Chem, 53, 1891 – 1898.
104. 104. Audrezet M. P., Dabricot A., Le Marechal C., Ferec C. (2008). Detection of Non-Amplified Genomic DNA. J Mol Diagn, 10, 424 – 434
105. Vandersteen J. G., Bayrak-Toydemir P., Palais R. A., Wittwer C. T. (2007). Identifying common genetic variants by high-resolution melting. Clin Chem, 53, 1191-1198.
106. Farrar J. S., Wittwer C. T. (2017). High-Resolution Melting Curve Analysis for Molecular Diagnostics. Molecular Diagnostics, 79–102.
107. Takano T., Ohe Y., Tsuta K., Fukui T., Sakamoto H., Yoshida T., Tateishi U., Nokihara H, Yamamoto N., Sekine I., Kunitoh H., Matsuno Y., Furuta K., Tamura T. (2007). Epidermal growth factor receptor mutation detection using high-resolution melting analysis predicts outcomes in patients with advanced nonsmall cell lung cancer treated with gefitinib. Clin Cancer Res, 13, 5385 – 5390.
108. Simi L., Pratesi N., Vignoli M., Sestini R., Cianchi F., Valanzano R., Nobili S., Mini E., Pazzagli M., Orlando C. (2008). High-resolution melting analysis for rapid detection of KRAS, BRAF, and PIK3CA gene mutations in colorectal cancer. Am J Clin Pathol, 130, 247-253.
109. Willmore C., Holden J. A., Zhou L., Tripp S., Wittwer C. T., Layfield L. J. (2004). Detection of c-kit-activating mutations in gastrointestinal stromal tumors by high-resolution amplicon melting analysis. Am J Clin Pathol, 122, 206 – 216.
110. Willmore-Payne C., Holden J. A., Tripp S., Layfield L. J. (2005). Human malignant melanoma: detection of BRAF- and c-kit-activating mutations by high-resolution amplicon melting analysis. Hum Pathol, 36, 486-493.
111. Bastien R., Lewis TB., Hawkes J. E., Quackenbush J. F., Robbins T.C., Palazzo J., Perou C. M., Bernard P. S. (2008). High-throughput amplicon scanning of the TP53 gene in breast cancer using high-resolution fluorescent melting curve analyses and automatic mutation calling. Hum Mutat, 29, 757- 764.

112. Zhou L., Wang L., Palais R., Pryor R., Wittwer C. T. (2005). High-resolution DNA melting analysis for simultaneous mutation scanning and genotyping in solution. Clin Chem, 51, 1770-1777
113. Allen H. J., Hsieh K., Patterson A. S., Ferguson B. S., Eisenstein M., Plaxco K. W. & Soh H. T. (2014). Accurate Zygote-Specific Discrimination of Single-Nucleotide Polymorphisms Using Microfluidic Electrochemical DNA Melting Curves. Angewandte Chemie, 126(12), 3227–3231
114. Krypuy M., Newnham G. M., Thomas D. M., Conron M., Dobrovic A. (2006). High resolution melting analysis for the rapid and sensitive detection of mutations in clinical samples. BMC Cancer, 12, 1-12.
115. Eischeid A. C. (2011). SYTO dyes and EvaGreen outperform SYBR Green in real-time PCR. BMC Res Notes, 4(1), 263.
116. Russom A., Haasl S., Ohlander A. (2004). Genotyping by dynamic heating of monolayered beads on a micro heated surface. Electrophoresis, 25(21-22), 3712-3719.
117. Russom A., Haasl S., Brookes A. J., Andersson H. (2006). Rapid melting curve analysis on monolayered beads for high-throughput genotyping of single-nucleotide polymorphisms. Analytical Chemistry, 78(7), 2220-2225.
118. Petersen J., Poulsen L., Petronis S., Birgens H., Dufva M. (2008). Use of a multi-thermal washer for DNA microarrays simplifies probe design and gives robust genotyping assays. Nucleic Acids Res, 36(2).
119. Chen T., Jia Y., Dong C., Gao J., Mak PI., Martins RP. (2016). Sub-7-second genotyping of single-nucleotide polymorphism by high-resolution melting curve analysis on a thermal digital microfluidic device. Lab Chip, 16(4), 743-752
120. Hassibi A., Manickam A., Singh R., Bolouki S., Sinha R., Jirage K. B., … Schoolnik G. (2018). Multiplexed identification, quantification and genotyping of infectious agents using a semiconductor biochip. Nature Biotechnology, 36 (8), 738-745.
121. Clutter D. S., Mazarei G., Sinha R., Manasa J., Nouhin J., LaPrade E., Shafer R. W. (2019). Multiplex Solid-Phase Melt Curve Analysis for the Point-of-Care Detection of HIV-1 Drug Resistance. The Journal of Molecular Diagnostics, 21 (4), 580-592.
122. 122. Clegg R. S., Reed S. M., and Hutchison J. E. (1998). Self-assembled monolayers stabilized by three-dimensional networks of hydrogen bonds. Am. Chem. Soc , 120 2486–2487

123. 123. Lee H. J., Jamison A. C., Yuan Y., Li C. H., Rittikulsittichai S., Rusakova I., Lee T. R. (2013). Robust Carboxylic Acid-Terminated Organic Thin Films and Nanoparticle Protectants Generated from Bidentate Alkanethiols. Langmuir, 29 , 10432–10439.

124. Shon Y. S., Lee T. R. (2000). Desorption and exchange of self-assembled monolayers (SAMs) on gold generated from chelating alkanedithiols. J. Phys. Chem. B, 104 , 8192–8200

125. Sabatani E., Cohen Boulakia J., Bruening M., Rubinstein I. (1993). Thioaromatic monolayers on gold: a new family of self-assembling monolayers. Langmuir, 9 , 2974–2981

126. 126. Hansen N. M., Farjami E., Kristiansen M., Clima L., Pedersen U. S., Daasbjerg K., Ferapontova E. E., Gothelf K.V. (2010). Synthesis and Application of a Triazene−Ferrocene Modifier for Immobilization and Characterization of Oligonucleotides at Electrodes. J. Org. Chem, 75, 2474–2481.

127. Tyler J. P., Caleb E. W., and Aric O. (2014). Influence of Attachment Strategy on the Thermal Stability of Hybridized DNA on Gold Surfaces. Langmuir, 30 (50), 15277-15284..

128. Hason S., Dvorak J., Jelen F. and Vetterl V. (2002). Electrochemical impedance spectroscopy of polynucleotide adsorption. Talanta, 56,905-13

129. Jelen F., Erdem A. and Palecek E. (2002). Cyclic voltammetry of echinomycin and its interaction with double-stranded and single-stranded DNA adsorbed at the electrode. Bioelectrochemistry, 55, 165-7.

130. Erdem A. and Ozsoz M. (2001). Interaction of the anticancer drug epirubicin with DNA.Anal. Chim, 437, 107-14.

131. Erdem A., Kerman K., Meric B., Akarca U. S. and Ozsoz M. (1999). Electrochemical biosensor for the detection of short DNA sequences related to the hepatitis B virus. Electroanalysis, 11, 586-7.

132. Erdem A., Meric B., Kerman K., Dalbasti T. and Ozsoz M. (1999).Detection of interaction between metal complex indicator and DNA by using electrochemical biosensor. Electroanalysis, 11, 1372-6.

133. Millan K. M., Saraullo S. and Mikkelsen S R. (1994).Voltammetric DNA biosensor for cyctic fibrosis based on a modified carbon paste electrode. Anal. Chem, 66, 2943-8.

134. Millan K. M. and Mikkelsen S R. (1993). Sequence-selective biosensor for DNA based on electroactive hybridization indicators. Anal. Chem, 65, 2317-23.

135. Napier M E., Loomis C R., Sistare M F., Kim J., Eckhardt A E and Thorp H H. (1997). Probing biomolecule recognition with electron transfer: electro- chemical sensors for DNA hybridization. Chem, 8, 906-13

136. Meunier-Prest R. (2003). Direct measurement of the melting temperature of supported DNA by electrochemical method. Nucleic Acids Research, 31(23), 150e–150.
137. Surkus A. E., & Flechsig G. U. (2009). Electrochemical Detection of DNA Melting Curves by Means of Heated Biosensors. Electroanalysis, 21(10), 1119–1123.
138. Shen Z., Sintim HO., Semancik S. (2015). Rapid nucleic acid melting analyses using a microfabricated electrochemical platform. Anal Chim Acta, 853(1), 265-270
139. Nasef H., Beni V., O'Sullivan CK. (2010). Labelless electrochemical melting curve analysis for rapid mutation detection. Anal Methods, 2(10),1461-1466
140. Nasef H., Beni V., O'Sullivan CK. (2010). Electrochemical melting-curve analysis. Electrochem commun, 12(8),1030-1033
141. Luo X., Hsing I.M. (2009). Real time electrochemical monitoring of DNA/PNA dissociation by melting curve analysis. Electroanalysis. 21(14), 1557-1561.
142. Hacia J. G. (1999) Resequencing and mutational analysis using oligonucleotide microarrays . Nat. Genet , 21, 42–47.
143. Deféver T., Druet M., Evrard D., Marchal D., Limoges B. (2011). Real-time electrochemical PCR with a DNA intercalating redox probe . Anal Chem, 83(5),1815-1821

Chapter 2

Chapter 2

Electrochemical primer extension based on polyoxometalate electroactive labels for multiplexed detection of single nucleotide polymorphisms

Electrochemical primer extension based on polyoxometalate electroactive labels for multiplexed detection of single nucleotide polymorphisms

Nassif Chahin[a,1], Laura A. Uribe[a,1], Ahmed M. Debela[b], Serge Thorimbert[b], Bernold Hasenknopf[b], Mayreli Ortiz[a,*], Ioannis Katakis[a], Ciara K. O'Sullivan[a,c,*]

[a] Interfibio Research Group, Department of Chemical Engineering, Universitat Rovira i Virgili, Avinguda Països Catalans 26, 43007 Tarragona
[b] Sorbonne Université, Institut Parisien de Chimie Moléculaire, UMR CNRS 8232, 4 place Jussieu, 75005 Paris, France
[c] ICREA, Passeig Lluís Companys 23, 08010 Barcelona, Spain

Abstract

Polyoxymetalates (POMs) ($[SiW_{11}O_{39}\{Sn(CH_2)_2CO)\}]^{4-}$ and $[P_2W_{17}O_{61}\{Sn(CH_2)_2CO)\}]^{6-}$) were used to modify dideoxynucleotides (ddNTPs) through amide bond formation, and applied to the multiplexed detection of single nucleotide polymorphisms (SNPs) in an electrochemical primer extension reaction. Each gold electrode of an array was functionalised with a short single stranded thiolated DNA probe, specifically designed to extend with the POM-ddNTP at the SNP site to be interrogated. The system was applied to the simultaneous detection of 4 SNPs within a single stranded 103-mer model target generated using asymmetric PCR, highlighting the potential of POM-ddNTPs for targeted, multiplexed SNP detection. The four DNA bases were successfully labelled with both ($[SiW_{11}O_{39}\{Sn(CH_2)_2CO)\}]^{4-}$ and $[P_2W_{17}O_{61}\{Sn(CH_2)_2CO)\}]^{6-}$), and $[SiW_{11}O_{39}\{Sn(CH_2)_2CO)\}]^{4-}$ demonstrated to be the more suitable due to its single oxidation peak, which provides an unequivocal signal. The POM-ddNTP enzymatically incorporated to the DNA anchored to the surface was visualised by AFM using gold coated mica. The developed assay has been demonstrated to be highly reproducible, simple to carry out and with very low non-specific background signals. Future work will focus on applying the developed platform to the detection of SNPs associated with rifampicin resistance in real samples from patients suffering from tuberculosis.

Keywords: SNP detection, Polyoxometalate-labelled ddNTPs, Electrochemical primer extension reaction (éPEX), Multiplexed electrochemical detection.

2.1. Introduction

Polyoxometalates (POMs) are anionic metal oxygen clusters with remarkable properties including tuneable redox properties, magnetism and biocompatibility. [1,2] POMs are formed from early transition metals (such as W, Mo or V), oxygen, and can also bear a heteroatom (e.g. Si, P, Ge). Recently the successful bioconjugation of polyoxotungstates $[SiW_{11}O_{39}\{Sn(CH_2)_2CO)\}]^{4-}$ (SiW_{11}Sn-Keggin) and $[P_2W_{17}O_{61}\{Sn(CH_2)_2CO)\}]^{6-}$ (P_2W_{17}Sn-Dawson) with DNA primers [3], and deoxynucleotide triphosphates [17] and the incorporation of these POM-primers and POM-dNTPs in PCR has been described. In both cases, the electroactive properties of POM allowed rapid and sensitive electrochemical detection of a DNA target. In the work reported here, we wish to expand the extraordinary possibilities of POMs in electrochemical genotyping, by their application in SNP detection through an electrochemical primer extension (éPEX) reaction (Figure 2.1).

A SNP is a DNA sequence variation occurring when a single nucleotide in the genome differs between members of a species or paired chromosomes and occur in at least 1% of the total population.[18,19] By unravelling the human genome, and in subsequent international efforts such as the HapMap project, the presence of around 15 million SNPs has been identified to date. SNP genotyping can be used to facilitate patient stratification, to detect predisposition to certain diseases[28] , to perform evolutionary studies[9], as well as providing information on drug metabolism.[7] Furthermore, SNP genotyping shows great promise for forensics, where SNPs can be used to obtain a genetic fingerprint even in degraded DNA samples and can also be used for prediction of phenotypic characteristics. Whilst next generation sequencing has been extensively used for the identification and detection of SNPs, there is a defined need for the targeted detection of a specific subset of SNPs, rather than a genome wide SNP map. The discrimination of a single point mismatch in DNA analysis is a challenge that needs to be addressed, with multiplexed detection of SNPs finding increasing application in diagnostics, theranostics, as well as in advanced forensics. The combination of fluorescence and nanostructured composites have been demonstrated to be a highly promising strategy for the solution-based detection of SNPs. [21,22,25,6] However, this approach suffers great difficulties in the simultaneous multiplexed detection of SNPs and to address this shortfall, array-based primer extension (APEX) using fluorescent detection has been successfully employed. However, fluorescence APEX is inherently expensive and laboratory based due to the optics and instrumentation required. In the APEX reaction, an isothermal reaction that takes advantage of immobilized single stranded DNA (ssDNA) probes designed to hybridize to a single stranded PCR amplicon one base downstream from the SNP site being interrogated. Following hybridization, labelled ddNTPs, modified nucleotides that lack the 2' and 3'-hydroxyl groups, are added.[23] Using

either ligation or elongation with a ligase or polymerase enzyme, respectively, the immobilized probe is extended by a single labelled ddNTP, complementary to the SNP being addressed [20] (Figure 2.1b). Following incorporation of the ddNTP, no further phosphodiester bonds can be formed due to the lack of the 2'/3'-hydroxyl group, and thus further elongation cannot take place. [20]

Electrochemical techniques for screening of SNPs offer cost-effective and facile detection platforms as an alternative to colorietry [27], fluorescence [20] or radioactive detection. [13] A broad spectrum of electro active markers such as intercalators [24], ferrocene modified probes [26] and nanoparticle probes [14] and nanocrystal labelled nucleotides [14] have been reported for the electrochemical detection of SNPs. Solid phase éPEX is a variant of APEX using an electroactive label. In this context, we recently demonstrated the feasibility of performing éPEX reaction with ddNTPs labelled with different electroactive markers: ferrocene, anthraquinone, phenothiazine and methylene blue. [4] Whilst the concept of éPEX was successfully demonstrated, a small level of nonspecific background signal was observed due to the electrostatic interaction with methylene blue, and to this end, an alternative redox label was pursued. Consequently, we explored the possibility of using POMs to label ddNTPs for use in éPEX. POMs are robust molecules at neutralacid pH, inexpensive and easy to prepare and functionalise, and offer a potential window compatible with biomolecules. Furthermore, we expanded on our previous proof-of-concept work, extending to simultaneous, multiplexed detection of SNPs using an electrode array housed within a microfluidic set-up.

2.2. Materials

2.2.1. Reagents

All reagents were of analytical grade and used as received. Potassium dihydrogen phosphate (KH_2PO_4), sodium chloride (NaCl), potassium chloride (KCl), were purchased from Fluka, while sodium perchlorate ($NaClO_4$) was received from Acros Organics. Sodium hydroxide, sulphuric acid (95–97%), Tris-HCl and boric acid were purchased from Scharlau, Barcelona, Spain and hydrochloric acid (35% v/ v) from Panreac. Phosphate-buffered saline (PBS), trisodium citrate, acetone, dimethyl sulfoxide (DMSO), perchloric acid (70% v/v), triethylamine, glacial acetic acid, phenothiazine, anthraquinone carboxylic acid, ferrocene carboxylic acid, N-(3-dimethylaminopropyl N´-ethylcarbodiimide hydrochloride and N-hydroxy succinimide were all purchased from Sigma Aldrich, Spain. The propargyl amino modified ddNTPs were purchased from Jena Bioscience and the 10-(3,5-bis((6mercaptohexyl)oxy)phenyl)-3,6,9-trioxadecanol (DT1) was purchased from Senso Path

Technologies (Bozeman, MT). Unless otherwise stated, all reactions were carried out under argon atmosphere with magnetic stirring. The organic solvents were redistilled before use. Thermo sequenase polymerase was purchased from GE Healthcare Life Technology (GE Healthcare Europe GmbH, Spain) and Therminator™ DNA Polymerase from New England BioLabs. Inc, UK. GelRed nucleic acid stain was acquired from Biotium, KAPA2G Robust polymerase from KAPABIOSYSTEMS (distributed by Sigma Aldrich, Spain) and Lambda exonuclease, agarose and DNA Gel Loading Dye (6×) from ThermoFisher Scientific, Spain. DNA Clean &Concentrator and Oligo Clean &Concentrator Kits were purchased from Zymo Research, USA. A model target sequence was designed based on SNPs previously identified within the MYH7 gene present in a group of patients known to suffer from Laing cardiomyopathy [15], where several SNP sites were included in a single PCR amplicon, thus mimicking the SNP sites found in genomic DNA. However, in human genomic DNA these SNP sites are located in different parts of the MYH7 gene and would require multiple amplifications, whereas in our "model" system we have four different SNP sites located in a 103-mer amplicon that is amplified in a single amplification. The sequences were selected using specific oligonucleotide selection and design programs (http://bioinfo.ebc.ee/apex2/). The sequences were designed in such a way to detect the SNPs using four different labels corresponding to the four bases. The HPLC purified oligonucleotides were purchased from Biomers.net, Germany and used as received. The sequences used (from 5`to 3`) are listed below IN Table 2.1:

Table. 2.1. Sequences of oligonucleotides used in this work

Primers and ssDNA template used for PCR amplification:		
Forward primer (FW-P)		5'-CGAAGTGTGAACTAGTCCCAC-3'
Phosphorylated Reverse primer (Rv-P)		5'-PO3GGGGACTAGGGGACTGAAGAA-3'
The 103-mer oligonucleotide DNA target/template (a synthetic sequence containing four "SNPs")		5`CGAAG TGTGAACTAGTCCCACCACCTTAAT TTCACTGTGTGTTAACACTTGTAAAGA ACCTGCATAATGTGTGTATCTTAAC TTCTTCAGTCCCCTAGTCCCC -3
The surface-tethered thiolated probes and the short ssDNA sequences containing SNPs used in the electrochemical detection of SNPs are detailed below:		
SNP	Surface-tethered thiolated probes	Short ssDNA sequences containing SNPs:
A	thioctic acid-C5AGATACACACATTATGCAGGT	AAG**A** ACCTGCATAATGTGTGTATCT
C	thioctic acid-C5TACAAGTGTTAACACACAGTGAA	TAA**C** TTCTTCAGTCCCCTAGTCCCC
G	thioctic acid-C5AGGTGGTGGGACTAGTTCACA	CGAA**G** TGTGAACTAGTCCCACCACCT
T	thioctic acid-C5GGGGACTAGGGGACTGAAGAA	TAA**T** TTCACTGTGTGTTAACACTTGT

2.3. Methods

2.3.2. Electrochemical measurements

All electrochemical measurements were carried out using an Autolab model PGSTAT 12 potentiostat/galvanostat controlled with the General Purpose Electrochemical System (GPES) software (Eco Chemie B.V., The Netherlands). All Optimization studies were carried out with individual 1.6 mm gold electrodes (BAS model MF-2014, 1.6 mm diameter), platinum counter electrode (BAS model MW-1032) and a pseudo-reference electrode of Ag/AgCl (CH Instruments., model CHI111) and the electrochemical measurements were performed in a 1cm3 cell. For the multiplexed detection of SNPs, electrode arrays of 36 individual 1mm2 square gold working electrodes (150 nm in thick) with a common gold counter electrode andAg silverreferenceelectrode were used. Figure. SI2.3). The electrodes were fabricated at Fraunhofer ICT-IMM, Germany using a photolithographic process as previously reported. [8,14,16] (See SI for more details). Differential Pulse Voltammetry (DPV) was used to detect the incorporation of the labelled ddNTPs. The measurements were performed at room temperature in 10 mM Tris buffer containing 0.5 M NaCl, pH 7. For the three electrodes configuration (Optimization studies), the measurements were recorded in a 1mL electrochemical cell and for the electrode array (multiplexed studies) in 20 µL of volume. DPVs were recorded at various potential windows depending on the redox potential of the labels (vs Ag/AgCl), using a pulse amplitude of 0.1 V, a step potential of 10 mV, a pulse width of 100 ms and a pulse period of 5 ms. For specificity studies and multiplex detection of SNP, the potential window used was from – 0.8 to 0.8 V vs Ag/AgCl, including all the potentials corresponding to the redox labels used in the work reported.

2.3.3. Atomic force microscopy characterisation

The enzymatic incorporation of P_2W_{17}-ddCTP after 103-mer ssDNA hybridized on thiol surface tethered capture probe on 10nm thick gold coated mica was studied by atomic force microscopy (AFM). Prior to measurement, the surface was incubated with a 25mM water solution of $MgCl_2$ to extend the DNA from the surface by minimising the repulsion forces from the gold surface, DNA and polyoxometalate [10,11], and dried with nitrogen. The details of surface preparation and reaction are explained in detail in SI. The AFM images were recorded in a 5420at. Force Microscope (AFM) from Agilent Technologies (USA) and processed using WSxM 5.0 Develop 9.2. [11] The surface was scanned in tapping mode at 0.25 ln/min using a SHR-150 kHz frequency tip from NanoAndMore GMBH, Germany. The SHR-150 probe has a single hydrophobic diamond-like carbon extra tip at the apex of a gold coated silicon etched probe. The tip diameter is ca. 1 nm.

2.4. Results and discussion

Activated polyoxotungstates $[SiW_{11}O_{39}\{Sn(CH_2)_2CO)\}]^{4-}$ (SiW_{11}SnKeggin) and $[P_2W_{17}O_{61}\{Sn(CH_2)_2CO)\}]^{6-}$ (P_2W_{17}Sn-Dawson) were coupled with propargyl amino derivatised dideoxynucleotides at position 7 of the purine and 5 of the pyrimidine bases through amide bond formation (Figure 2.1) following our established protocol[1,2,4,17] with small variations. A 1.6mm gold electrode was functionalised with a mixture of thioctic acid ssDNA probe and a bipodal alkanethiol at a ratio of 1:100 (see SI for details). The optimum buffer for the éPEX reaction and differential pulse voltammetry (DPV) detection was elucidated by evaluating assay performance in Tris-HCl, or phosphate buffered saline (PBS) at pH of 3, 7 and 8. The sharpest and highest DPV peaks was obtained using Tris-HCl at pH7.Furthermore theuseofthetwo polymerases, Therminator® and Thermosequenase®, both known to be compatible with modified nucleotide incorporation, were compared. Higher DPV signals were obtained using the Therminator® enzyme, which is also relatively less expensive than the Thermosequenase®. Whilst the optimal temperature for Therminator activity is 75°C, the use of milder temperatures (24, 42 and 50°C) were also evaluated. Equivalent performance was observed at 42 and 50°C, whilst a lower DPV signal intensity was observed at 75°C, which can be attributed to the thermal cleavage of the thiol-Au bond, resulting in release of the immobilized probe from the electrode surface. No ddNTP incorporation was observed at 24°C. Figure 2.1b shows the DPV of ddUTPs labelled with SiW_{11}Sn-Keggin and P_2W_{17}Sn-Dawson POMs at SNP A position, using a short (24–mer) synthetic ssDNA target. POMs have different oxidation states as indicated by oxidation peaks at different potentials. Following the éPEX reaction, the main signal is observed at −0.3V vs Ag/AgCl for both SiW_{11}Sn-Keggin and P_2W_{17}Sn-Dawson ddNTPs. Once the incorporation of the POM–ddNTP was demonstrated for a short oligonucleotide target sequence, the possibility of carrying out the éPEX reaction using a longer synthetic target sequence was then tested. To demonstrate multiplexing, a 103-mer DNA target containing 4 different "SNP sites" (5`CGA-AGT-GTG-AAC-TAG-TCC-CAC-CAC-CTT-AAT-TTC-ACT-GTGTGT-TAA-CAC-TTG-TAA-AGA-ACC-TGC-ATA-ATG-TGT-GTA-TCTTAA-CTT-CTT-CAG-TCC-CCT-AGT-CCC-C-3), was amplified using asymmetric PCR followed by exonuclease digestion to generate ssDNA for hybridization to the surface immobilized probe (Figures SI 2.1 and 2.2).

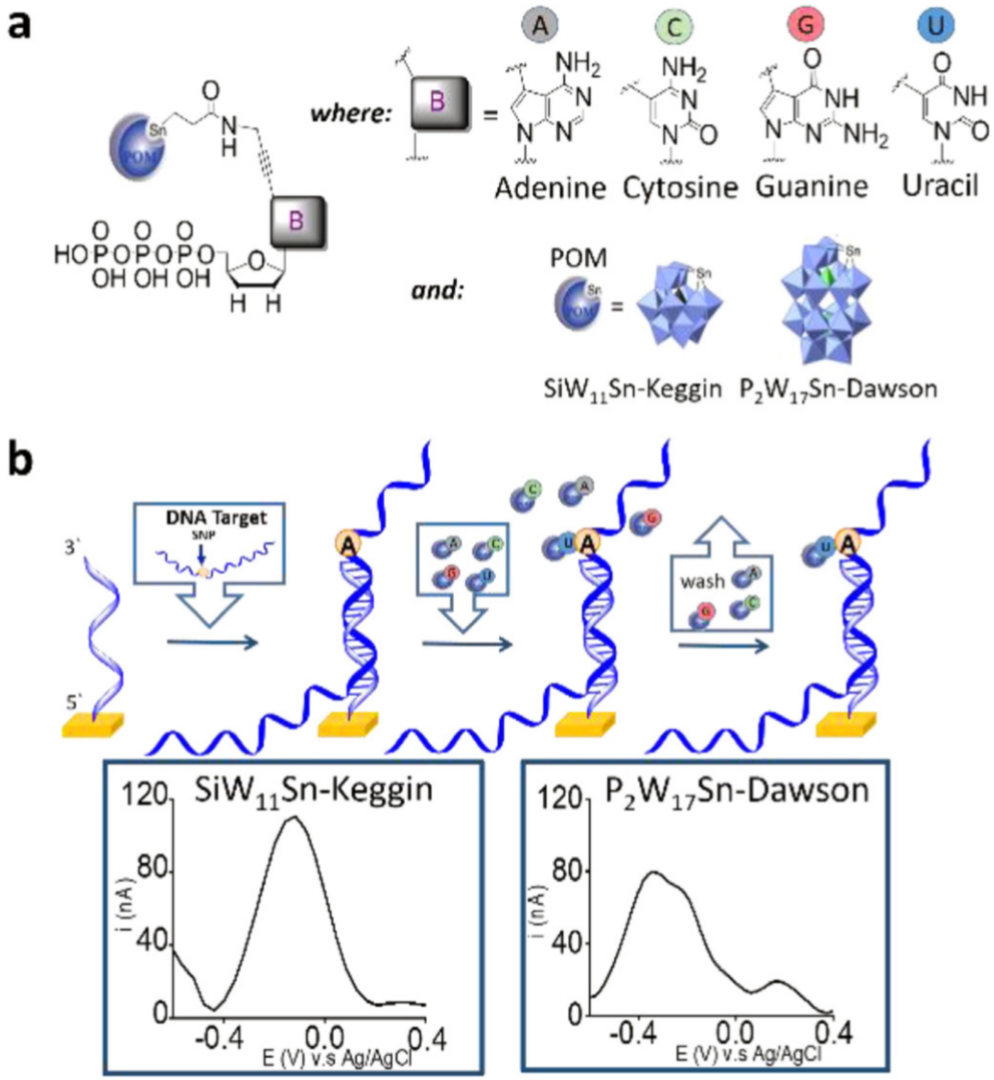

Figure 2.1. Schematic representation of a) POM-modified-ddNTPs and b) the application of POM-modified-ddNTPs in éPEX (Insets: Differential Pulse Voltammograms (DPV) of $SiW_{11}Sn$-ddUTP and $P_2W_{17}Sn$-ddUTP incorporated at 3'-end of primers. DPV were recorded in 10 mM Tris + 0.5 NaCl, pH 7).

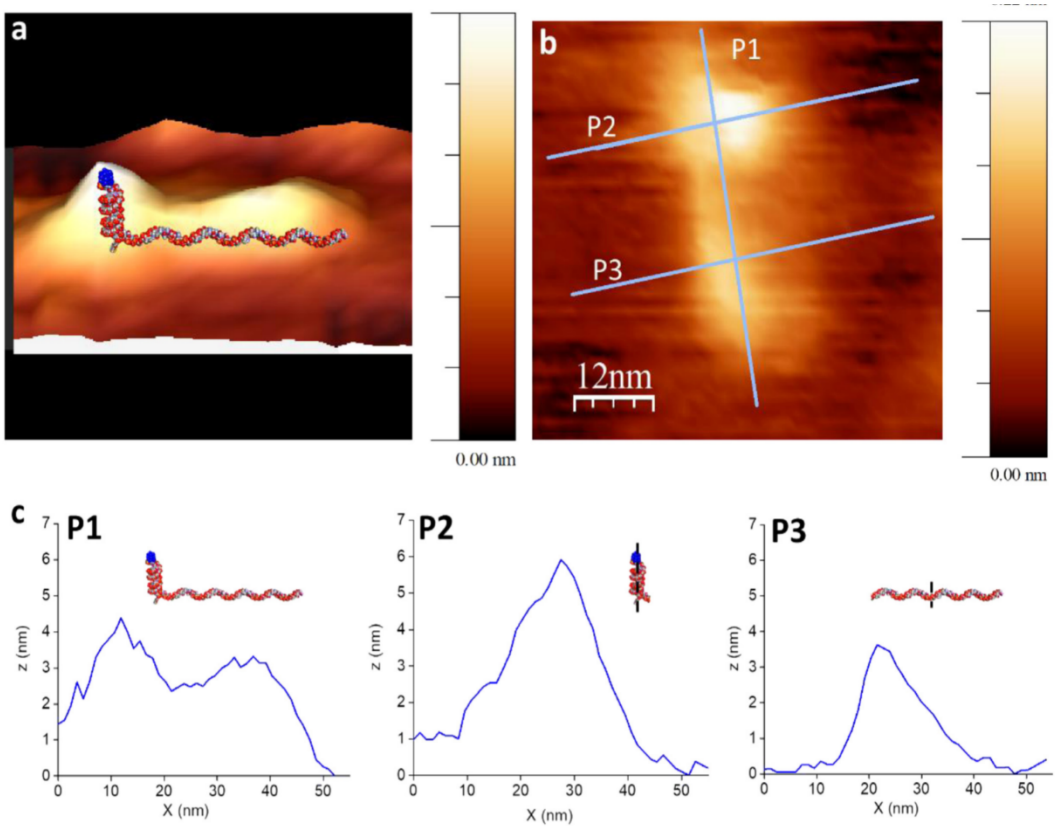

Figure 2.2. Topographic AFM images in ambient conditions of the enzymatic incorporation of P_2W_{17}-ddCTP. The 21-mer thiotic acid capture probe was first self-assembled on a 10nm thick gold coated mica surface followed by hybridization of a 103-mer ssDNA target before POM incorporation. a) 3D image, b) 2D image including profile lines, c) x-z profiles obtained along the P1, P2 and P3 lines shown in b).

The enzymatic incorporation of POM in the DNA system was visualised by Atomic Force Microscopy (AFM). As observed in Figure 2.2, the topographic AFM images obtained using a 1 nm diameter ultra sharp tip show an elongated feature of about 50 nm long and 3–6 nm height, compatible with the size of a 103-mer target hybridized to an immobilized and in situ POM-modified 21-mer probe, in ambient conditions of humidity [5]. The multiplexed detection of SNPs was carried out using DPV. Following incorporation of the POM-labelled ddNTP, the duplex was chemically denatured using glycine-HCl (pH 3), facilitating increased flexibility and elasticity of the surface tethered POM-DNA, allowing the POM label to move closer to the electrode surface, thus enhancing electron transfer and addressing higher DPV signal (Figure 2.3a and SI2.4). This denaturation step also served to wash away unincorporated labelled ddNTPs and the low pH used can also contribute to the stability of the POM cluster during washing steps. As can be seen in Figure 2.3b, the incorporation of either the Keggin or Dawson labelled ddNTPs e.g. SNP A only shows incorporation of POM-ddUTP and no signal is observed with either AQ-ddATP, PTZ-ddCTP or Fc-ddGTP. The difference in responses for different SNPs can be attributed to different degrees of elasticity of the POM-tethered surface bound

DNA, and the dissimilar shapes ofthe Keggin andDawson labels. As the signal for $SiW_{11}Sn$-Keggin was consistently higher than the $P_2W_{17}Sn$-Dawson for all ddNTPs, they were used as labels for the simultaneous and multiplexed detection of SNPs. Here, an array of 36 electrodes [8,14,16] was used (Figure SI 2.3), with each electrode functionalised with a mixture of 1:100 thioctic acid-DNA probe and a bipodal alkanethiol, with six electrodes per SNP, and the remaining twelve electrodes were used as negative controls. A patterned double-sided adhesive gasket was used to create microfluidic channels, and the fluidic housing was completed with PMMA creating a channel with an inlet and outlet for reagent addition (Figure SI 2.3). Figure 2.4a shows the electrochemical signals for the multiplexed detection of the four SNPs using a mixture of SiW_{11}SndUTP (SNP A), Fc-ddGTP (SNP C), PTZ-ddCTP (SNP G) and AQ-ddATP (SNP T), (Schematic representation shown in Figure SI 2.5) and Figure 2.4b shows the highly distinguishable specific signal of $SiW_{11}Sn$-dUTP (SNP A) from the other non-specific redox labelled ddNTPs. Moreover, the possibility of also using SiW_{11}-Keggin-ddATP, SiW_{11}Keggin-ddCTP and SiW_{11}-Keggin-ddGTP for multiplex detection of SNP in combination with other redox labelled bases was also successfully carried out and is reported in Figure SI 6.

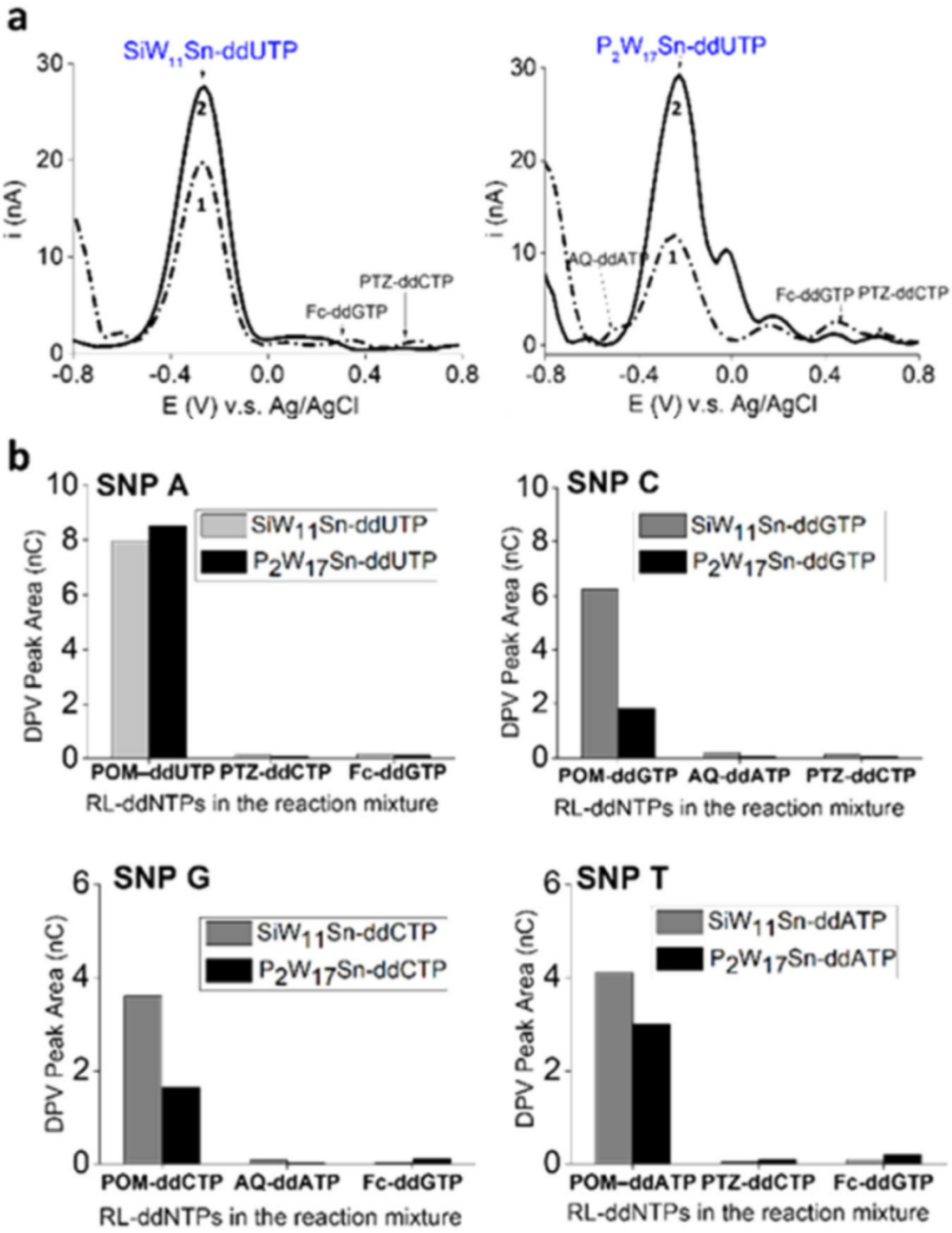

Figure 2.3. (a) Comparison of the DPV after the incorporation of SiW_{11}-ddUTP (left) and P_2W_{17}Sn-ddUTP (right) at the SNP A position before (1) and after (2) duplex denaturation; (b) DPV peak area values of the redox-labelled bases (RL-ddNTPs) present in the reaction mixture for detecting each SNP in a synthetic 103-mer ssDNA. The residual signal coming from the non-specific bases (AQ-ddATP, PTZ-ddCTP and Fc-ddGTP) is also plotted (Average of three electrodes RSD less than 5%).

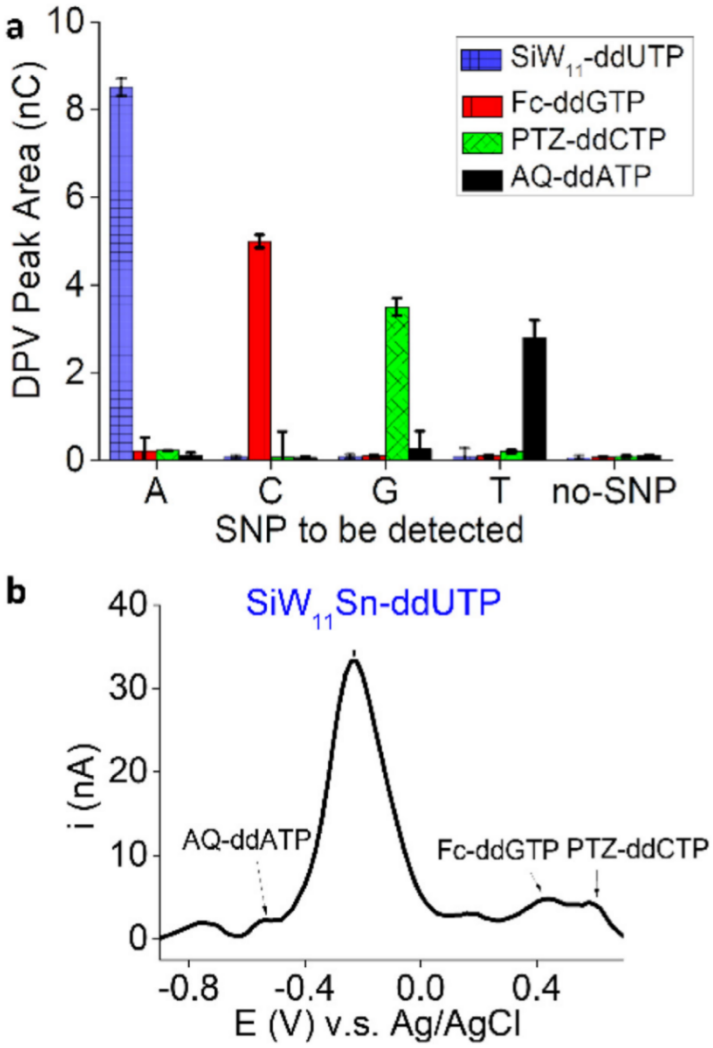

Figure 2.4. (a) Averaged integrated areas (nC) of the specific and non-specific DPV signals per SNP interrogated (A for SNP A, C for SNP C, G for SNP G, T for SNP T. Each column represents the value of the DPV signal of each electrochemically active bases (SiW_{11}-ddUTP, PTZ-ddCTP, Fc-ddGTP and AQ-ddATP) measured on the same electrode (Average of six electrodes, RSD less than 5%). (b) DPV registered for detecting SNP A by the incorporation of the complementary SiW_{11}Sn-dUTP in 10mM Tris-HCl containing 0.5 NaCl, pH 7 (after denaturation at pH 3).

2.5. Conclusions

In summary, we have demonstrated the exploitation of ddNTPs labelled with $SiW_{11}Sn$-Keggin and $P_2W_{17}Sn$-Dawson POMs for solid phase primer extension, and the electrochemical detection of SNPs. The use of the relatively inexpensive Therminator® polymerase was demonstrated to successfully and accurately incorporate the POM-labelled ddNTPs. A post-incorporation denaturation step was observed to increase the DPV signal due to enhanced flexibility and elasticity of the POM-tethered surface bound ssDNA as compared to the rigid duplex. This denaturation step also assisted in the removal of any residual nonspecific ddNTPs. $SiW_{11}Sn$-Keggin ddNTPs gave consistently higher signals as compared to the $P_2W_{17}Sn$-Dawson ddNTPs and were thus used for the simultaneous and multiplexed detection of SNPs using an electrode array housed within a microfluidic set-up. Four different “SNP sites” were successfully interrogated with negligible background signals.

Acknowledgements

This project has received partial funding from the European Union's Horizon 2020 research and innovation program under grant agreement No 767325 and under the Marie Sklodowska-Curie grant agreement No. 659211. We want to thank to Fraunhofer ICT-IMM for provision of gold electrode arrays and the Microscopy and Nanometric Techniques Area of the SRCiT, Universitat Rovira I Virgili, especially to Dr. M. Stefanova Stankova and Dr. L. Vojkuvka for their valuable help in the AFM measurements and surface preparation.

References

1. Boglio C., Micoine K., Derat E., Thouvenot R., Hasenknopf B., Thorimbert S., Lacôte E., Malacria M. (2008). Regioselective Activation of Oxo Ligands in Functionalized Dawson Polyoxotungstates. J. Am. Chem. Soc, 130, 4553–4561.
2. Debela A. M., Ortiz M., O'Sullivan C. K., Thorimbert S., Hasenknopf B. (2014). Postfunctionalization of keggin silicotungstates by general coupling procedures, Polyhedron, 68, 131–137.
3. Debela A. M., Ortiz M., Beni V., Thorimbert S., Lesage D., Cole R. B., O'Sullivan C. K., Hasenknopf B. (2015). Biofunctionalization of polyoxometalates with dna primers, their use in the polymerase chain reaction (pcr) and electrochemical detection of pcr products. Chem. Eur, 21, 17721–17727.
4. Debela A. M., Thorimbert S., Hasenknopf B., O'Sullivan C. K., Ortiz M. (2016). Electrochemical primer extension for the detection of single nucleotide polymorphisms in the cardiomyopathy associated myh7 gene. Chem. Commun, 52, 757–759.
5. DiSanto G., Tobenas S., Adamcik J., Dietler G. (2009). ImagingMicrosc. ⟨https://www.imaging-git.com⟩.
6. Duan X., Liu L., Wang S. (2009). Conjugated polyelectrolyte-DNA complexes for multi-color and one-tube SNP genotyping assays. Biosens. Bioelectron, 24, 2095–2099.
7. Evans W. E., Relling M. W. (1999). Pharmacogenomics: Translating Functional Genomics into Rational Therapeutics. Science, 286, 487–491.
8. Fragoso A., Latta D., Laboria N., Germar F. V., Hansen-Hagge T. E., Kemmner W., Gartner C., Klemm R., Drese K. S., O'Sullivan C. K. (2011). Integrated microfluidic platform for the electrochemical detection of breast cancer markers in patient serum samples. Lab Chip, 11, 625–631.
9. Hacia J. G., Fan J. B., Ryder O., Jin L., Edgemon K., Ghandour G., Mayer R. A., Sun B., Hsie L., Robbins C. M., Brody L. C., Wang D., Lander E. S., Lipshutz R., Fodor S. P., Collins F.S. (1999). Determination of ancestral alleles for human single-nucleotide polymorphisms using high-density oligonucleotide arrays. Nat. Genet, 22, 164–167.
10. Hansma H. G., Bezanilla M., Zenhausern F., Adrian M., Sinsheimer R. L. (1993). Atomic force microscopy of DNA in aqueous solutions. Nucleic Acids Res, 21, 505–512.
11. Horcas I., Fernández R., Gómez-Rodríguez J. M., Colchero J., Gómez-Herrero J., Baro A.M. (2007). WSXM: A software for scanning probe microscopy and a tool for nanotechnology. Rev. Sci. Instrum. Nanotec Electron. WSxM Free, 78, 013705.

12. Joda H., Beni V., Alakulppi N., Partanen J., Lind K., Strömbom L., Latta D., Höth J., Katakis I., O'Sullivan C. K. (2014). Medium-high resolution electrochemical genotyping of HLA-DQ2/DQ8 for detection of predisposition to coeliac disease. Anal. Bioanal. Chem, 406, 2757–2769.
13. Krjutskov K., Andreson R., Magi R., Nikopensius T., Khrunin A., Mihailov E., Tammekivi V., Sork H., Remm M., Metspalu A. (2008). Development of a single tube 640-plex genotyping method for detection of nucleic acid variations on microarrays. Nucleic Acids Res, 36, e75.
14. Liu G., Lee M.H., Wang J. (2005). Nanocrystal-based bioelectronic coding of single nucleotide polymorphisms. Am. Chem. Soc, 127, 38–39
15. Muelas M., Hackman P., Luque H., Suominen T., Espinós C., Garcés-Sánchez M., Sevilla T., Azorín I., Millán J. M., Udd B., Vílchez J. J. (2012). Spanish MYH7 founder mutation of Italian ancestry causing a large cluster of Laing myopathy patients. Clin. Genet, 81, 491–494.
16. Ortiz M., Joda H., Hoth J., Beni V., Katakis I., Klemm R., Lind K., O'Sullivan C. K., Fragoso A. (2015). Bleed-to-read disposable microsystems for the genetic and serological analysis of celiac disease markers with amperometric detection. Electrophoresis , 36, 1920–1926.
17. Ortiz M., Debela A. M., Svobodova M., Thorimbert S., Lesage D., Cole R. B., Hasenknopf B., O'Sullivan C. K. (2017). PCR Incorporation of Polyoxometalate Modified Deoxynucleotide Triphosphates and Their Application in Molecular Electrochemical Sensing of Yersinia pestis. Chem. Eur, 23, 10597–10603
18. Pastinen T., Kurg A., Metspalu A., Peltonen L., Syvanen A. (1997). Minisequencing: a specific tool for DNA analysis and diagnostics on oligonucleotide arrays. Genome Res, 7, 606–614.
19. Sachidanandam R., Weissman D., Schmidt S.C. (2001). A map of human genome sequence variation containing 1.42 million single nucleotide polymorphisms. Nature, 409, 928–933
20. Sanger F., Nicklen S., Coulson A.R. (1977). DNA sequencing with chain-terminating inhibitors. Proc. Natl. Acad. Sci. USA 74, 5463–5467.
21. Tian J., Liu Q., Shi J., Hu J., Asiri A. M., Sun X., & He Y. (2015). Rapid, sensitive, and selective fluorescent DNA detection using iron-based metalorganic framework nanorods: Synergies of the metal center and organic linker. Biosensors and Bioelectronics, 71, 1–6.
22. Tian J., Cheng N., Liu Q., Xing W., Sun X. (2015). Cobalt phosphide nanowires: efficient nanostructures for fluorescence sensing of biomolecules and photocatalytic evolution of dihydrogen from water under visible light. Angew. Chem. Int. Ed, 54, 5493–5497.

23. Tonisson N., Oitmaa E., Krjutskov K., Pullat J., Lind I., Leego M., Kurg A., Metspalu A. (2010). Molecular Diagnostics. Second edition. Elsevier Ltd, 267–284.
24. Wakai J., Takagi A., Nakayama M., Miya T., Miyahara T., Iwanaga T., Takenaka S., Ikeda Y., Amano M. (2004). A novel method of identifying genetic mutations using an electrochemical DNA array. Nucleic Acids Res, 32, e141.
25. Yang L., Liu D., Hao Sh., Qu F., Ge R., Ma Y., Du G., Asiri A. M., Chen L., Sun X. (2017). Topotactic Conversion of α-Fe2O3 Nanowires into FeP as a Superior Fluorosensor for Nucleic Acid Detection: Insights from Experiment and Theory. Anal. Chem, 89, 2191–2195.
26. Yu C. J., Wan Y. J., Yowanto H., Li J., Tao C. L., James M. D., Tan C. L., Blackburn G. F., Meade T. J. (2001). Electronic detection of single-base mismatches in DNA with ferrocene-modified probes. Am. Chem. Soc, 123, 11155–11161.
27. Zhang H., Liu X., Liu M., Gao T., Huang Y., Liu Y., Zeng W. (2018). Gene detection: An essential process to precision medicine. Biosens. Bioelectron, 99, 625–636.
28. Durbin R. (2001). A map of human genome variation from population-scale sequencing. Nature, 467, 1061-1073.

2.6. Supporting information

2.6.1. Preparation of polyoxometalate-ddNTP conjugates

Activated POMs $[SiW_{11}O_{39}\{Sn(CH_2)_2CO)\}]^{4-}$ (SiW_{11}Sn-Keggin) and $[P_2W_{17}O_{61}\{Sn(CH_2)_2CO)\}]^{6-}$ (P_2W_{17}Sn-Dawson) were prepared following previously described procedures. [1,2] Briefly, the first step was to introduce the $Sn(CH_2)_2COOH$ moiety into lacunary POM, activation of the carboxylic acid in the second step, and finally link it to the ddNTP in the third step of the process.

Redox labelled ddNTPs were prepared by adapting previous procedures. [1,2,17]

Step 1: 0.4 mmol of the lacunary POM, were added to an acetonitrile solution of trichlostannyl propionic acid (0.6 mmol) and TBABr (4.0 mmol). After 1 h at room temperature under argon and with stirring conditions, the remaining solid was filtered off. A pale yellow oily solid was obtained after the evaporation of the solvent. Finally, a white solid was obtained after precipitation with acetone/ethanol/diethyl ether (1/1/excess).

Step 2: The POM-$Sn(CH_2)_2COOH$ was dissolved in distilled acetonitrile and 2.2 equivalents of triethylamine and 1.2 equivalents of isobutyl chloroformate were added to the mixture and left to react overnight under argon atmosphere at room temperature. The cation exchange resin (Amberlyst 15, 16–50 mesh, TBA^+ form) was then added followed by addition of 10 mL acetone and stirred for 1 h. Then, the resin was filtered off and the filtrate concentrated under vacuum. An oil was obtained, dissolved in acetone and precipitated as a white solid, by the addition of ethanol and diethyl ether. Finally, the solid was centrifuged and dried under vacuum.

Step 3: The activated POM dissolved in 20 μL of DMSO was added to an equimolar amount of the propargylamine modified ddNTP (400 nmol) dissolved in 1 mL of double distilled water containing triethylamine (~1 mL). After sealing the tube under Argon, the reaction was kept shaking at 45 ^oC for 24 h. The reaction mixture was kept in the freezer overnight followed by freeze drying. The labelled ddNTPs were purified by using preparative TLC using $CHCl_3/CH_3OH$: 85/15. The products were freeze dried again and re-dissolved in water, aliquoted and defrosted immediately before use.

2.6.2. PCR amplification of DNA 103-mer target for further SNP detection in the ePEX reaction

Optimisation of the PCR reaction

For the amplification of the 103-mer target sequence, 150 µL of master mix containing 1 X KAPA2G Robust PCR buffer, 1 X KAPA2G Robust PCR buffer enhancer, 200 µM regular dNTPs, 200 nM forward primer, 200 nM phosphorylated reverse primer and 1.5 units of KAPA2G Robust enzyme was prepared.

This master mix was divided in 6 portions to perform a PCR optimisation. 1.5 µL of 1 nM DNA target (final concentration of 60 pM) was added to the three of the master mix samples, to be amplified for a different number of cycles (5, 10 and 15 cycles) and the remaining three samples were used as negative controls without any addition of DNA target. Amplification was performed in an iCycler Thermal Cycler (Biorad). The PCR program used was one cycle of denaturation at 95°C for 2 min, followed by annealing at 58°C for 30 s and then 72°C elongation for 30 s, for 5, 10 or 15 cycles, followed by a final extension step performed at 72°C for 5 min. At the end of the program, the tubes were held at 4 °C. The PCR products were analysed using gel electrophoresis in 2.4 % w/v agarose gel in Tris-Borate-EDTA buffer (pH 8) (Figure. SI 2.1). 10 cycle-PCR was selected as the optimum for further studies.

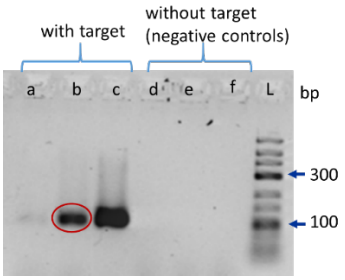

Figure SI 2.1. 2.4 % w/v agarose gel after electrophoresis of PCR products obtained by applying different number of PCR cycles: 5 cycles (a, with DNA target and d, without DNA target as negative control), 10 cycles (b, with DNA target and e, without DNA target as negative control) and 15 cycles (c, with DNA target and f, without DNA target as negative control). The band obtained with 10-cycle PCR is circled.

For the generation of the single stranded DNA (ssDNA) from the PCR product, a combination of asymmetric PCR and exonuclease digestion was used.

10 µL of PCR product was added to a master mix (final volume 100 µL) containing 1 X KAPA2G Robust PCR buffer enhancer, 200 µM of regular dNTPs, 400 nM forward primer (5'-CGAAGTGTGAACTAGTCCCAC-3') and 1 unit of the KAPA2G Robust enzyme. In this case, only an excess of forward primer was needed and no reverse primer was used to favor the generation of single stranded DNA. The PCR program used was 12 cycles, with denaturation at 95°C for two minutes, annealing at 58°C for 30 seconds and elongation at 72°C for 2 min and a final extension step at 72°C for 5 min. The PCR products were analysed using gel electrophoresis in 2.4 % w/v agarose gel Tris-Borate-EDTA buffer (pH 8), to confirm the generation of the single stranded target DNA.

Following asymmetric PCR, the amplicon, phosphorylated at the 5'- terminus was subjected to lambda exonuclease digestion via addition of 10 units (10 unit/µL) of lambda exonuclease enzyme and 10 µL of exonuclease buffer followed by incubation at 37°C for 2 h and a final denaturation of the enzyme at 80°C for 10 minutes. An Oligo Clean & Concentrator™ kit was used to purify the products and gel electrophoresis was then performed in 2.4 % w/v agarose gel Tris-Borate-EDTA buffer, to confirm the generation of single stranded DNA.

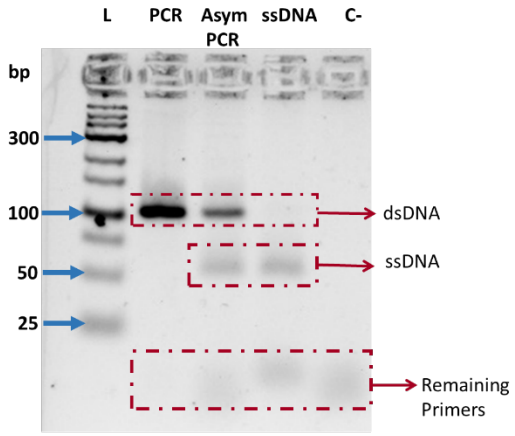

Figure SI 2.2. 2.4 % w/v agarose gel after electrophoresis of PCR products obtained after: PCR, asymmetric PCR, and lambda exonuclease digestion, while (C-) is the negative control of the PCR.

2.6.3. Electrochemical measurement (details of electrode preparation and fluidic setup)

Single gold electrodes (for optimisation studies) were polished consecutively with 0.3 and 0.05 µm alumina powder for 5 min each, followed by sonication in pure ethanol and then MilliQ water for 5 min. Finally, the electrodes were washed thoroughly with MilliQ water and dried under nitrogen. Electrochemical cleaning was then performed by sweeping for 40 cycles between -0.4 and 1.7 V vs. Ag/AgCl reference electrode in 0.5 M H_2SO_4. Electrode cleanliness was checked by performing cyclic voltammograms in 1 mM $K_3[Fe(CN)_3]$ + 0.5 NaCl in a potential range of 0.1-0.7 V v.s. Ag/AgCl and, the electrodes were considered clean if the peak separation between the oxidation and reduction peaks in the cyclic voltammograms was ΔE =70 mV. Twenty microlitres of 1 M KH_2PO_4 containing 5 µM of 5'-thioctic acid modified ssDNA, and 100 µM solution of the DT1 (10-(3,5-bis((6-mercaptohexyl)oxy)phenyl)-3,6,9-trioxadecanol) was drop-casted onto the clean gold electrodes and after incubation for 3 h at 22°C the electrodes were washed under stirring in 10 mM Tris buffer containing 0.5 M NaCl (pH 7) and dried with a nitrogen stream. Twenty microlitres of 1 µM DNA target in 10 mM Tris buffer containing 0.5 M NaCl (pH 7) was drop-casted onto the electrode and incubated in a humidity chamber for 1 h at 37°C. The electrodes were rinsed in 10 mM Tris buffer containing 0.5 M NaCl (pH 7) to remove any non-hybridized DNA and then dried with nitrogen.

For the multiplexed detection of SNPs, electrode arrays of 36 individual 1 mm^2 square gold working electrodes (150 nm in thick) with a common gold counter electrode and Ag silver reference electrode were used. Figure. SI 2.3). The electrodes were fabricated at Fraunhofer ICT-IMM, Germany using a photolithographic process as previously reported [8,14,16] . Briefly, the lithographic process employed to fabricate the electrode arrays was achieved as follows: a circular borofloat glass wafer (ϕ = 12 cm) was fully covered with 5 mm of LOR5214 lift-off resist, then UV patterned to reveal the reference electrode areas and corresponding connections. Ten nanometres of titanium, used as a glass/metal adhesion promoter, were sputtered followed by a 150 nm thick silver layer. The patterned substrate was fully coated a second time with the same lift-off resist and UV patterned to reveal working and counter electrode areas and their corresponding connections, and finally coated with a 10 nm thick titanium layer followed by a 150 nm thick gold layer. The remaining photoresist was finally removed with acetone, revealing the planar gold and silver patterns. Since the connection lines between the electrodes and their connection points have to cross the fluidic channels, an insulation of the chip was required. Thus,

an SU8 negative photoresist was applied to the whole surface of the chip and was only partially removed at the electrode and connection areas. This ensured that only electrode would be later exposed to the sample fluids. In order to extend storage lifetime by reducing contamination of the electrode surfaces, the patterned wafers were coated with a 5 mm protection layer of AZ6632, which can be easily removed by rinsing the arrays with acetone, isopropanol and water immediately prior to use.

The electrode arrays were sonicated in acetone, isopropanol and finally in MilliQ water for 5 min each. Electrochemical cleaning was performed by sweeping for 25 cycles between -0.2 and 1.5 V vs. Ag/AgCl (external reference electrode) in 0.5 M H_2SO_4. After cleaning, the electrodes were washed with MilliQ water and dried under nitrogen. Electrode cleanliness was checked by performing cyclic voltammograms in 1 mM $K_3[Fe(CN)_3]$ + 0.5 NaCl in a potential range of 0.1-0.7 V v.s. Ag/AgCl and, the electrodes were considered clean if the peak separation between the oxidation and reduction peaks in the cyclic voltammograms was ΔE = 100 mV.

One microlitre of 1 M KH_2PO_4 containing 5 µM of 5'-thioctic acid modified ssDNA, and 100 µM solution of the DT1 (10-(3,5-bis((6-mercaptohexyl)oxy)phenyl)-3,6,9-trioxadecanol) was spotted onto each electrode of the array and incubated for 3 h in a humidity chamber to prevent evaporation. Each probe was added to six electrodes of the array and a non-specific probe was added to six electrodes and just DT1 to the final six electrodes of the array. Following washing, a double-sided adhesive gasket was attached to the array with the now functionalised electrodes, followed by a PMMA block, with integrated inlet and outlet holes to address the microfluidic channels formed by the patterned adhesive gasket (Figure. SI 2.3a.) The electrodes were hydrated with 10 mM Tris buffer containing 0.5 M NaCl, pH 7 and then single stranded PCR amplicon (20 µL) was injected in each channel and incubated for 1 h at 37°C in a humidity chamber, and washed thoroughly by injecting 3 x 100 mL 10 mM Tris buffer containing 0.5 M NaCl to remove any non-hybridized DNA.

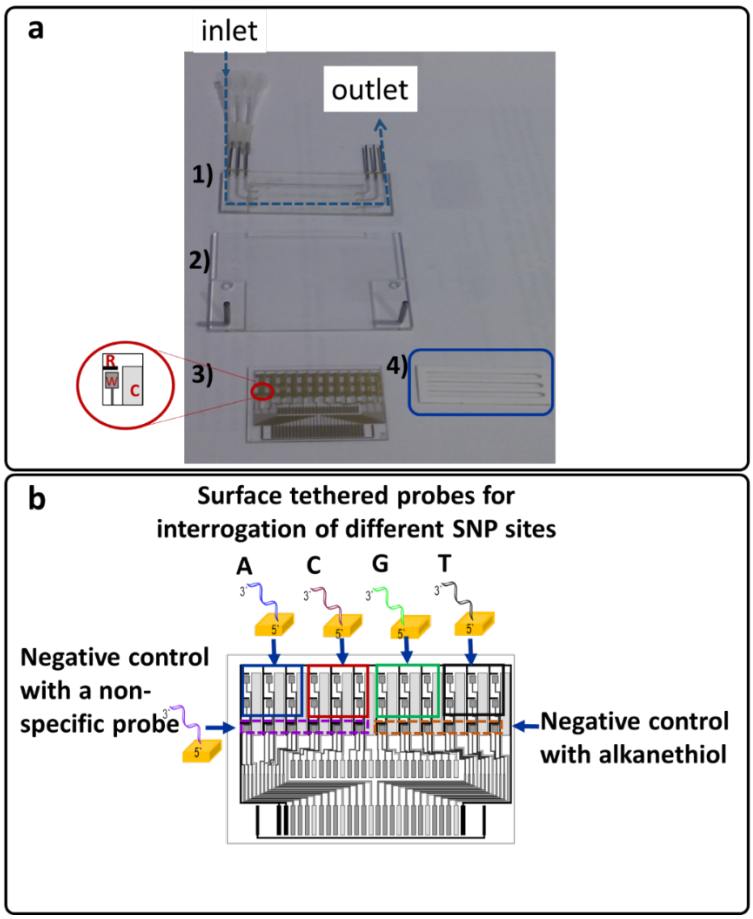

Figure SI 2.3. (a) Microfluidic setup: 1) Top and 2) bottom parts of PMMA microfluidic platform, 3) 36-gold electrode arrays and 4) the double-sided adhesive gasket. (b) Position in the 36-gold electrode arrays of surface tethered probes for interrogation of different SNP sites and the negative controls.

2.6.4. éPEX optimisation experiments

4.1. Selection of polymerase: Both Therminator and Thermosequenase were compared in terms of efficiency of incorporation of ddNTPs at 42ºC. Individual electrodes with surface tethered probes hybridized with their complementary short target sequences were incubated in a solution containing 1 µM of a single redox labelled ddNTP (AQ-ddATP, PTZ-ddCTP, Fc-ddGTP and SiW11-ddUTP) and a) 0.5 µL of Thermosequenase® DNA polymerase in 20 ml of reaction buffer (1X 50% v/v glycerol, 0.1 mM EDTA, 0.5% v/v Tween, 0.5% v/v nonidet-P40, 1 mM DTT, 100 mM KCl, 65 mM $MgCl_2$), or b) 0.5 µL Therminator™ enzyme in 20 µL of reaction buffer (1X ThermoPol® reaction buffer containing 20 mM Tris-HCl, 10 mM $(NH_4)_2SO_4$, 10 mM KCl, 2 mM $MgSO_4$, 0.1% v/v Triton® X-100). The electrodes were sealed with parafilm, incubated at 42°C for 30 min, subsequently washed with 10 mM Tris buffer (pH 7) + 0.5 M NaCl, and finally Differential Pulse Voltammetry (DPV) was carried out.

Similar results were obtained for both polymerases. Due to the lower price of Therminator polymerase, it was selected for further studies.

4.2 pH optimisation: The éPEX reaction was tested in Tris buffers at acid (pH 3), neutral (pH 7) and slightly basic (pH 8), prepared by adjusting the pH of the commercial buffer (pH 8.8) (10X ThermoPol® reaction buffer containing 20 mM Tris-HCl, 10 mM $(NH_4)_2SO_4$, 10 mM KCl, 2 mM $MgSO_4$, 0.1% v/v Triton® X-100, pH 8) using 1 M HCl. Phosphate buffers (PBS) at same pH (3, 7 and 8) were also tested as reaction buffers, by diluting the original 10X buffer to 1X in PBS.

Individual electrodes with surface tethered probes hybridized with their complementary short target sequences were incubated in a solution containing 1 µM of a single redox ddNTP (AQ-ddATP, PTZ-ddCTP, Fc-ddGTP and SiW_{11}-ddUTP) and 0.5 µL Therminator™ enzyme in 20 µL of the different reaction buffers at different pH. The electrodes were sealed with parafilm, incubated at 42 °C for 30 min, subsequently washed with 10 mM Tris buffer (pH 7) + 0.5 M NaCl, and finally Differential Pulse Voltammetry (DPV) was carried out.

It was found that PEX reactions carried out at pH 7 in Tris buffer produced the narrowest and clearest DPV peaks for POM-ddNTP incorporation. Tris buffer seems to be more appropriate than phosphate buffers. Additionally, POMs degrade at basic pH and acid conditions denature

the duplex of the DNA on the surface. In conclusion, Tris buffer pH 7 was used to perform the following PEX experiments in order to prevent any condition that could alter POM stability.

4.3 Selection of reaction temperature: The optimum temperature for the incorporation of electrochemically labelled ddNTPs using the Therminator polymerase was tested at four different temperatures: 75 °C (which is the proposed working temperature for the enzyme), 50, 42 and 24 °C. Briefly, individual electrodes with surface tethered probes hybridized to their complementary short target sequences were incubated in a solution containing 1 µM of a single redox labelled ddNTP (AQ-ddATP, PTZ-ddCTP, Fc-ddGTP and SiW_{11}-ddUTP) and 0.5 µL Therminator™ enzyme in 20 µL of 1X ThermoPol® reaction buffer (at pH 7) containing 20 mM Tris-HCl, 10 mM $(NH_4)_2SO_4$, 10 mM KCl, 2 mM $MgSO_4$, 0.1% v/v Triton® X-100. The electrodes were sealed with parafilm, incubated at the four different temperatures (75, 50, 42 and 24 °C) for 30 min, subsequently washed with 10 mM Tris buffer (pH 7) + 0.5 M NaCl, and finally Differential Pulse Voltammetry (DPV) was carried out. It was found PEX reactions carried out at 42 °C in Tris buffer pH 7, produced the narrowest and clearest DPV peaks for POM-ddNTP incorporation.

Equivalent performance was observed at 42 and 50 °C temperatures, a lower DPV signal intensity at 75 °C (probably because of damage in the surface chemistry (thiol-Au)) and no ddNTP incorporation observed at 24 °C.

The optimised methodology for the ddNTP-POM éPEX reaction was the use of 0.5 µL of Therminator® polymerase enzyme, 1 µM redox labelled ddNTP and 1 X ThermoPol® reaction buffer (pH 7, adjusted by adding 1 M HCl) (total volume of 20 µL), for 30 min at 42°C.

2.6.5. ddNTP-POM specificity studies

ddNTPs (ddATP, ddGTP, ddTTP, ddCTP) labelled with SiW_{11}Sn-Keggin POM and P_2W_{17}Sn-Dawson POM were mixed with ddNTPs labelled with ferrocene, anthraquinone or phenothiazine (AQ-ddATP, Fc-ddGTP, PTZ-ddCTP). A total set of eight éPEX reactions was performed by mixing 1 µM SiW_{11}Sn-ddNTP or P_2W_{17}Sn-ddNTP with two other redox labelled ddNTPs (1 µM each), in the presence of 0.5 µL of Therminator® polymerase enzyme, and 20 µL ThermoPol® reaction buffer. The electrodes were incubated at 42 °C for 30 min, and then washed under stirring conditions, firstly in 10 mM Tris buffer (pH 7) and then in the denaturation buffer glycine-

HCl (pH 3) for 15 min, followed by a final wash with 10 mM Tris pH 7 and the electrode was then dried under nitrogen and the DPV measurements were carried out from -0.8 to 0.8 V vs. Ag/AgCl in 10 mM Tris containing 0.5 NaCl.

Figure SI 2.4 shows a comparison between the integrated areas of the DPV peaks following this "one-pot" reaction (the specific POM-ddNTP + other non-specific redox-labelled ddNTPs). Two protocols for removing the non-specific bases were tested: protocol **1** based on washing under stirring the electrode in 10 mM Tris buffer, pH 7 for 15 min and protocol **2** based on washing under stirring the electrode in glycine buffer pH 3 for 15 min (Figure. SI 2.4a) in order to denature the DNA duplex and also preserve the integrity of POM. Finally, all electrodes were washed with 10 mM Tris buffer + 0.5 NaCl and the electrochemical measurements (DPV) were carried out in the latter buffer.

As observed in Figure SI 2.4b for SiW_{11}-ddNTP and in Figure. SI 2.4c for P_2W_{17}-ddNTP, for both protocols, the higher signals correspond to the specific POM-ddNTP and the lower signals to the non-specific AQ-ddATP, Fc-ddGTP, PTZ-ddCTP bases. Moreover, higher specific and lower non-specific signals were observed when the electrodes were washed in pH 3 solutions for 15 min before measurements.

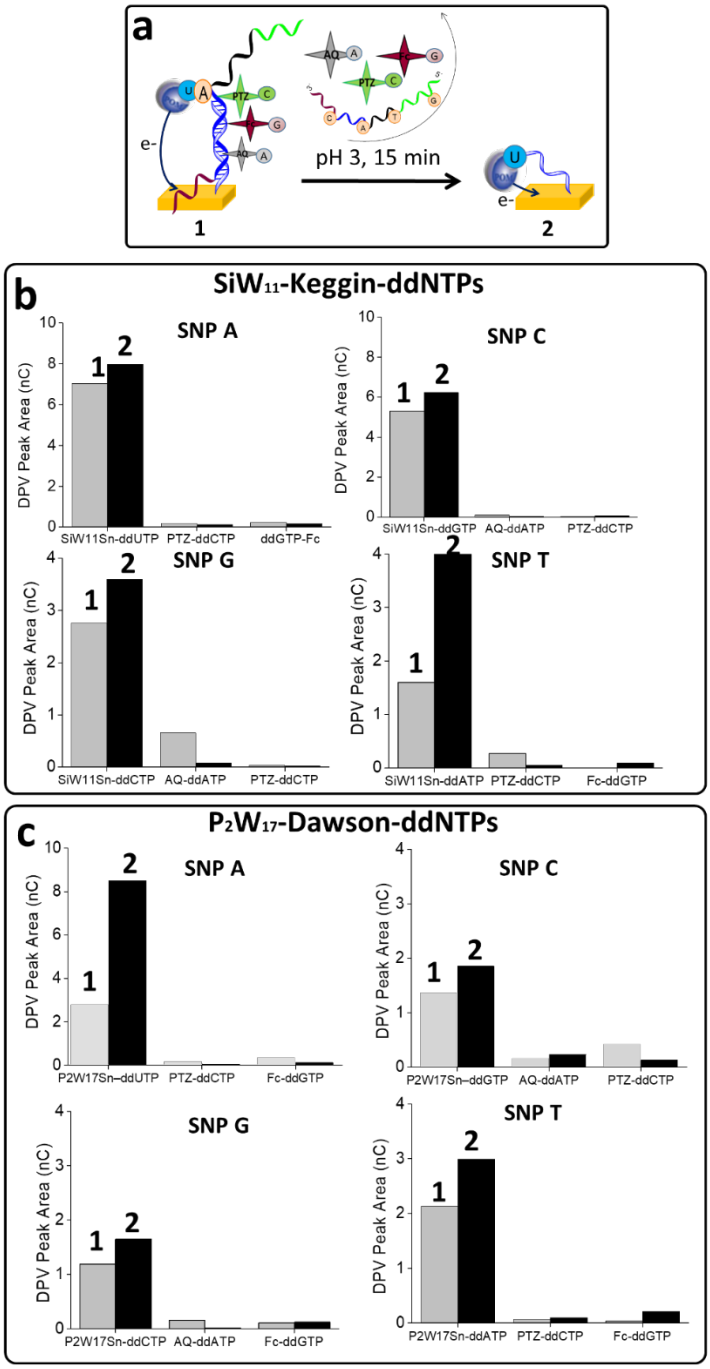

Figure SI 2.4. a) dsDNA denaturation and removal of non-specific bases. b,c) Comparison between the integrated areas of the DPV peaks of electrodes washed under stirring conditions for 15 min in: 10 mM Tris buffer (pH 7) (gray columns) and in glycine-HCl buffer (pH 3) (black columns). In each graph, the first columns (higher signals) correspond to the specific POM-ddNTP and the following (lower signals) to the non-specific AQ-ddATP, PTZ-ddCTP and Fc-ddGTP bases.

2.6.6. Multiplexed SNP detection using POM-ddNTPs

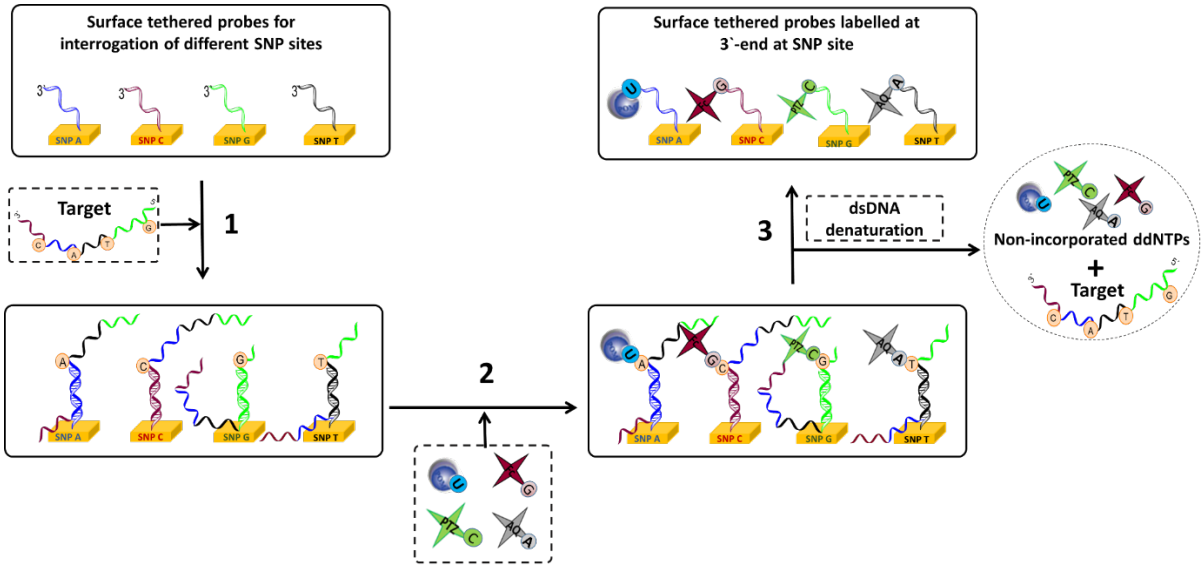

Figure SI 2.5. Representation of the process of the simultaneous multiplex detection of SNPs in a microfluidic platform. 1) Addition of ssDNA target to the platform containing the probes for interrogation of different SNP sites and the subsequent hybridization of the different regions of target to the corresponding complementary surface tethered probe. 2) Addition of the mixture of redox labelled ddNTP ($SiW_{11}Sn$-ddUTP, PTZ-ddCTP, Fc-ddGTP and AQ-ddATP) and the enzyme and the subsequent incorporation at the 3`-end position. 3) Denaturation of the duplex by washing the electrode under stirring at pH 3 during 15 min. The target and non-incorporated ddNTPs are washed away leaving the 3'-end electrochemically labelled surface tethered probes ready for electrochemical interrogation.

The possibility of using SiW_{11}-ddGTP, SiW_{11}-ddCTP, SiW_{11}-ddATP, for multiplex detection of SNP in combination with other redox labelled based was also carried out and the results are reported in Figure SI 2.6.

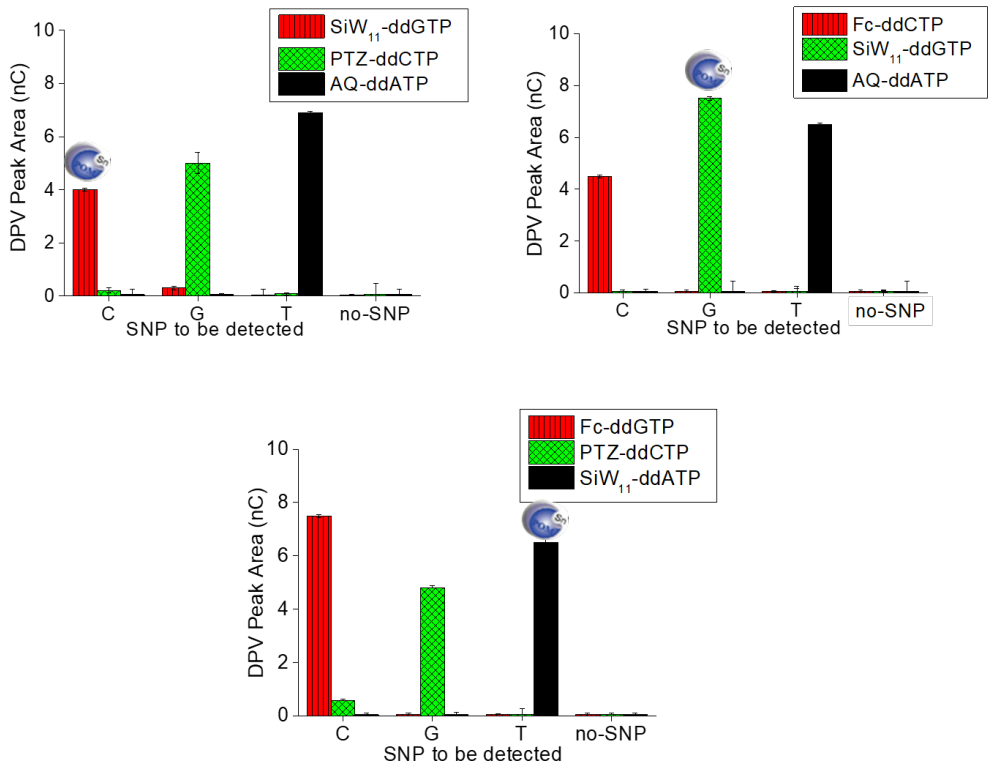

Figure SI 2.6. Averaged integrated areas (nC) of the specific and non-specific DPV signals per each electrode containing thiol tethered probes hybridized to a 103-mer ssDNA in their complementary region containing a SNP (C for SNP C, G for SNP G, T for SNP T). Each column corresponds to the value of the DPV signal of each electrochemical labelled base measured at the same electrode to evaluate the specific and non/specific signal.

2.6.7. Atomic Force Microscopy (AFM) study.

Preparation of gold substrate: Using a Quorum Q150R-S sputtering coater, 10 nm thick gold coated mica was prepared by sputtering gold on recently cleaved mica fixed with adhesive tape on a magnetic support. The sputtering conditions were: Applied current: 30 mA; Deposition rate: 8-9 nm/min; Target to sample spacing: 30mm; and using Argon at 0.1 mbar.

DNA anchoring to the surface, hybridization and enzymatic incorporation of P_2W_{17}Sn-Dawson-ddCTP: 1 µM solution in 1 M K_2HPO_4 of the thiolated capture probe (thioctic acid-C5-AGGTGGTGGGACTAGTTCACA) was anchored to the surface by drop-casting on the substrate immediately following gold deposition, and left to react for 2 h in a humidity chamber at 22 ºC.

The substrates were then gently washed with nuclease-free, autoclaved and 0.2 μm filtered water (Fisher Scientific, Spain).

Subsequently, 200 nM purified ssDNA generated from a PCR product, was drop-casted on the surface and left to hybridize with the immobilized probe for 1 h at 22ºC in a humidity chamber (5`CGAA***G***TGTGAACTAGTCCCACCACCTTAATTTCACTGTGTGTTAACACTTGTAAAGAAC CTGCATAATGTGTGTATCTTAACTTCTTCAGTCCCCTAGTCCCC-3). After washing with the same nuclease-free water, the enzymatic incorporation of POM-ddCTP was carried out as described before. Finally, the modified surface was again washed, incubated for 10 min with 25 mM $MgCl_2$ water solution, to extend the DNA on the surface and facilitate the subsequent AFM study, and following a final thorough washing with water, the surface was prepared for AFM analysis.

The AFM images were recorded in a 5420 Atomic Force Microscope (AFM) from Agilent Technologies (USA) and processed using WSxM 5.0 Develop 9.2 (Horcas, 2007). The surface was scanned in tapping mode at 0.25 ln/min using a SHR-150 KHz frequency tip from NanoAndMore GMBH, Germany. The SHR-150 probe has a single hydrophobic diamond-like carbon extra tip at the apex of gold-coated silicon etched probe. The tip diameter is around 1 nm. The images were processed using WSxM 5.0 Develop 9.2 [11]

Chapter 3

Chapter 3

Low cost platform for multiplexed electrochemical melting curve analysis

Low cost platform for multiplexed electrochemical melting curve analysis

Nassif Chahin[a], Santiago Escobar-Nassar,[a,b] Johann Osma[b], Mayreli Ortiz[a]*, Ciara K. O'Sullivan[a,c]*

[a] Interfibio Research Group, Department of Chemical Engineering, Universitat Rovira i Virgili, Avinguda Països Catalans 26, 43007 Tarragona
[b] Faculty of Engineering, Universidad de los Andes, Colombia
[c] ICREA, Passeig Lluís Companys 23, 08010 Barcelona, Spain

Abstract

The detection and identification of single nucleotide polymorphisms (SNPs) has garnered increasing interest in the last decade, finding potential application in detection of antibiotic resistance, advanced forensic science as well as clinical diagnostics and prognostics, moving towards the realisation of personalised medicine. Many different techniques have been developed for genotyping SNPs and ideally these techniques should be rapid, easy-to-use, cost-effective, flexible, scalable, easily automated and requiring minimal end-user intervention. Whilst high-resolution melting curve analysis has been widely used for the detection of SNPs, fluorescence detection does not meet many of the desired requirements and electrochemical detection is an attractive alternative due to its high sensitivity, simplicity, cost-effectiveness and compatibility with microfabrication. Herein, we describe the multiplexed electrochemical melting curve analysis of duplexes surface tethered to electrodes of an array. In this approach, thiolated probes designed to hybridize to a DNA sequence containing the SNP to be interrogated are immobilized on gold electrodes. Asymmetric PCR using a ferrocene labelled forward primer is used to generate this single-stranded redox labelled PCR amplicon. Following hybridization with the probe immobilized on the electrode surface, the electrode array is exposed to a controlled ramping of temperature, with concomitant constant washing of the electrode array surface whilst simultaneously carrying out voltammetric measurements. The optimum position of the complementary to the SNP site in the immobilized probe to achieve maximum differentiation in melting temperature between wild type and single base mismatch, thus facilitating allelic discrimination, was determined, and applied to the detection of a cardiomyopathy associated SNP.

3.1. Introduction

Human genomes are 99.9% identical[1]. Even though, a person hosts millions of variations in their gene coding regions and the most common variations are due to single nucleotide polymorphisms (SNPs). These are single nucleotide variations in a defined genetic location and occur at a frequency of between 1 in 100 to 1 in 300 bases[2]. The understanding of the importance and application of SNPs is an emerging field, and it is widely believed that SNPs will have a critical role in pharmacogenetics, disease genetics and advanced forensics[3]. As an increasing number of SNPS are identified using next generation sequencing technologies[4] a battery of genotyping technologies for the detection of SNPs, including primer extension, ligation, enzymatic cleavage, mass spectroscopy, conformational analysis, amongst others, have emerged. [5,6] However, many of these approaches are expensive, labour-intensive and often requiring considerable infrastructure and instrumentation.

Hybridization approaches for the identification of SNPs exploit the differences in the thermal stability of double stranded DNA between perfectly matched and mismatched target-probe pairs to achieve allelic discrimination (Kim & Misra, 2007).[7] This methodology is referred to as melting curve analysis a PCR amplified duplex is placed in a cuvette and the melting temperature is determined by measuring the UV-Vis absorbance at 260nm as the temperature is ramped using a peltier. To improve the sensitivity of the technique, fluorescent intercalating dyes such as SBYR Green or Eva Green were employed and the decrease in fluorescence with increasing temperature was measured. High resolution melting curve analysis using highly controlled heating ramps and fluorescence detection facilitated single base mismatch differentiation. However, the technique is limited as it cannot achieve high levels of multiplexing due to limited availability of fluorescent intercalating with non-overlapping emission spectra.[8] Recently, a platform capable of multiplexed melting curve analysis was developed, where >1000 parallelised melts can be detected on a CMOS array. The platform, termed the Hydra 1K, uses cyanine labelled primers and asymmetric PCR to generate single stranded labelled amplicons, which are captured vis hybridization to probes immobilized on the CMOS array, which is then exposed to a controlled temperature ramp. The platform has been applied to the multiplexed fluorescence detection of 54 drug-resistance-associated mutations that are present in six genes of Mycobacterium tuberculosis.[9,10]

Electrochemistry is an attractive alternative to fluorescence due to its ease-of-use, high sensitivity, low cost, facile and cost-effective fabrication of electrode arrays and compatibility with multiplexed detection with multi-channel potentiostats. Indeed, different approaches of electrochemical melting curve analysis have been reported, using a variety of labels such as methylene blue (MB), cobalt phenanthroline[11,12], cobalt bipyridine,[13,14] ruthenium bipyridine,[15] echinomycin[16,17] and epirubicin.[18]

Prest *et al.*, developed a method using methylene blue as an intercalating redox molecule, and measuring the change in the square wave voltammetry response to calculate the melting temperature.[19] Defever *et al*. reported a real-time PCR and melting curve analysis method based on the use of a osmium bipyridyl complex ($[Os(bpy)_2dppz]^{2+}$) intercalating redox molecule, again measuring the change in the square wave voltammetry response as the temperature was increased, and then generating the positive first-derivative analyses (*di/dT*) of the melt.[20] A microfluidic device integrating thermal control and a multi-electrode array was designed by Shento *et al.* who performed a rapid electrochemical melting curve analyses on small-volume samples of 10 µL. In this case an immobilized probe was hybridized to target labelled with methylene blue and the dissociation of the labelled target measured using square wave voltammetry.[21] In a similar approach, dsDNA denaturation between a ferrocene-labelled-PNA and a fully-complementary or single-base-mismatched DNA on the negatively charged electrode surface of indium tin oxide (ITO) was monitored electrochemically.[22]

Nasef *et al*, described a method based on labelless electrochemical melting curve analysis for the detection of the cystic fibrosis associated DF508 mutant, which a 3-base deletion mutation. A 21-base thiolated probe was immobilized on a gold electrode and hybridized to a ssDNA PCR amplicons of mutant target (85 bases) or wild type target of 82 bases. Methylene blue was used as an electrochemical indicator of hybridization, and differential pulse voltammograms were recorded during a discontinuous ramping of the temperature, and a clear discrimination between the melting temperature of the mutant and wild-type target was observed. Nasef *et al.* went on to report an alterntive approach, using ferrocene labelled target, and in this approach two different electrodes of an array were functionalised with probe complementary to the mutant and and probe complementary to the wild type, and both were hybridized with the ferrocene modified mutant sequence. The entire sensor array was subjected to discontinuous temperature ramping and the dissociation of the ferrocene labelled DNA from immobilized probes was monitored using DPV. The T_m recorded for the fully complementary and for the mismatched duplex was 38°C and 30°C, respectively which provided a clear discrimination between match and mismatch targets.[23]

The work reported herein aims to improve on these last two works, which were carried out in our group. These previous works were very laborious, where the electrodes were placed in a cuvette The work carried out by Nasef *et al*., was carried out in our group, and whilst the use of electrochemical melting curve analysis for the detection of the DF508 was clearly demonstrated, the methodology was very laborious, requiring extensive hands-on time. In these previous works, the electrode was placed in a cuvette, which was housed in a peltier device, and the temperature was

increased in steps of 1 or 5 ºC, and after each step, the electrode was removed from the cuvette, washed and then electrochemical measurement was carried out in an electrochemical cell, and then the electrode was returned to the cuvette for the next increase in temperature. In the work reported herein, we wanted to move towards a more automated set-up, where the electrode array was housed in a microfluidic chamber, integrated within a peltier heating device which could be programmed to ramp the temperature as desired. During the temperature ramp, the electrode array was continuously washed to remove and denatured DNA, and the electrochemical signal measured throughout.

The objective of this work was thus to develop a Peltier heating device using a computer-controlled heating block, consisting of a pair of aluminum blocks that can be heated in a controlled way using a pulse width modulation protocol implemented on an Arduino UNO. Using this "in-house" semi-automated peltier heating set-up, we wanted to demonstrate that it could be used for carrying out multiplexed electrochemical melting curve analysis (éMCA) for the detection of a SNP associated with cardiomyopathy as a model system. To carry out a demonstration of a proof-of-concept of the éMCA, individual gold electrodes of an array were functionalised with thiolated 21-mer probes, which were designed to hybridize to a ferrocene labelled complementary 21-mer oligo and subjected to a temperature ramp (Figure 3.1). We wanted to explore if the position of the complementary to the SNP site on the immobilized probe had an effect on increasing the difference in melting temperature between fully complementary and mismatch, we design the probes to be fully complementary, or to have a mismatch at the top, bottom or middle of the probe. Single stranded ferrocene labelled PCR 124-mer amplicons were also hybridized to the four different probes, as well as four different probes hybridized to the same 124-mer amplicon and subjected to éMCA, and finally the results were confirmed using fluorescent melting curve analysis.

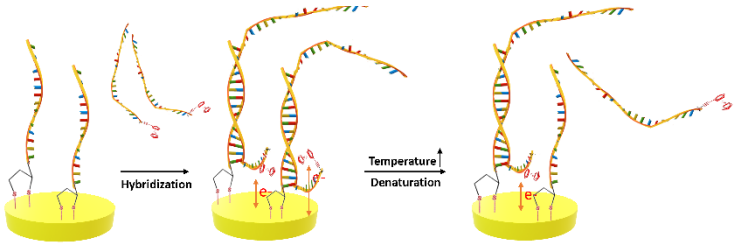

Figure 3.1. Conceptual schematic representation of the electrochemical melting curve analysis approach; (a) Immobilization of dithiolated probe on the gold electrode surface; (b) Hybridization with single stranded DNA PCR amplicon containing the SNP to be interrogated; (c) Temperature ramping and denaturation of the surface-tethered duplex and concomitant decrease in the electrochemical signal

3.2. Materials

3.2.1. Chemicals and Materials Solutions were prepared using a Milli-Q water purifier system (Milipore, Madrid, Spain) with a resistance level of 18.2 MΩ cm. All chemicals and reagents were of analytical grade and used without further purification. Potassium dihydrogen phosphate (KH_2PO_4), acetone and isopropanol were purchased from Scharlau, Spain. Potassium hydroxide (KOH), hydrogen peroxide (H_2O_2 30% (v/v)), potassium ferricyanide ($K_3[Fe(CN)_6]$), and Tris buffer at pH 7.4 were provided by Sigma Aldrich, Spain. The surface spacer dithiol 16-(3,5-bis((6-mercaptohexyl)oxy)phenyl)-3,6,9,12,15-pentaoxahexa-decane) (DT1)[29] was obtained from SensoPath Technologies (Bozeman, MT, USA) . Three millimeter thick polymethylmethacrylate (PMMA) was purchased from La Industria de la Goma (Tarragona, Spain) and the double-sided adhesive foil ARsealTM 90880 was purchased from Adhesive Research, Ireland. Oligonucleotide capture probes and targets were purchased as lyophilised powder from Biomers.net, Ulm, Germany), reconstituted in nuclease free water (ThermoFisher Scientific, Spain) and used without further purification. Table SI 3.1 shows the oligonucleotides sequences used in this study. Eva Green dye was purchased from Applied Biosystems (Spain), GelRed Nucleic Acid Gel Stain from Biotium (Barcelona, Spain) and the certified molecular biology agarose gel powder from ThermoFisher Scientific (Spain).

3.2.2. Melting curve analysis device components The Arduino UNO, IRF520, the resistances, condensers, type K thermocouples, connectors, BI BPC10 resistors, AD595, breadboard, and the 2.5 W/mK thermally conductive tapes were all purchased from Farnell (Madrid, Spain). For the temperature reference system, a type K thermocouple connected to the precision thermometer Hi 93531 (Hanna instruments, Bilbao, Spain) was used. The variable DC power supply PeakTech 6006D (Telonic instruments LTD, Berkshire, UK) was used to supply the temperature reading system at 5.1 V**.**

Figure 3.2a shows a schematic of an integrated system for the detection of SNPs, based on performing electrochemical melting curve analysis using a homemade Peltier device. A gold electrode array functionalised with DNA is set between two aluminum plates of a homemade Peltier device providing a robust control and ramping of temperature in three fixed rates (0.2, 0.5, or 1^{o} C / Step). The Peltier consists of an Arduino Uno board using the free Arduino software for data visualization. The gold electrode array is covered by a (PMMA) Poly (methyl methacrylate) microfluidic that allows liquid buffer to continuously wash the electrode array surface while heating.

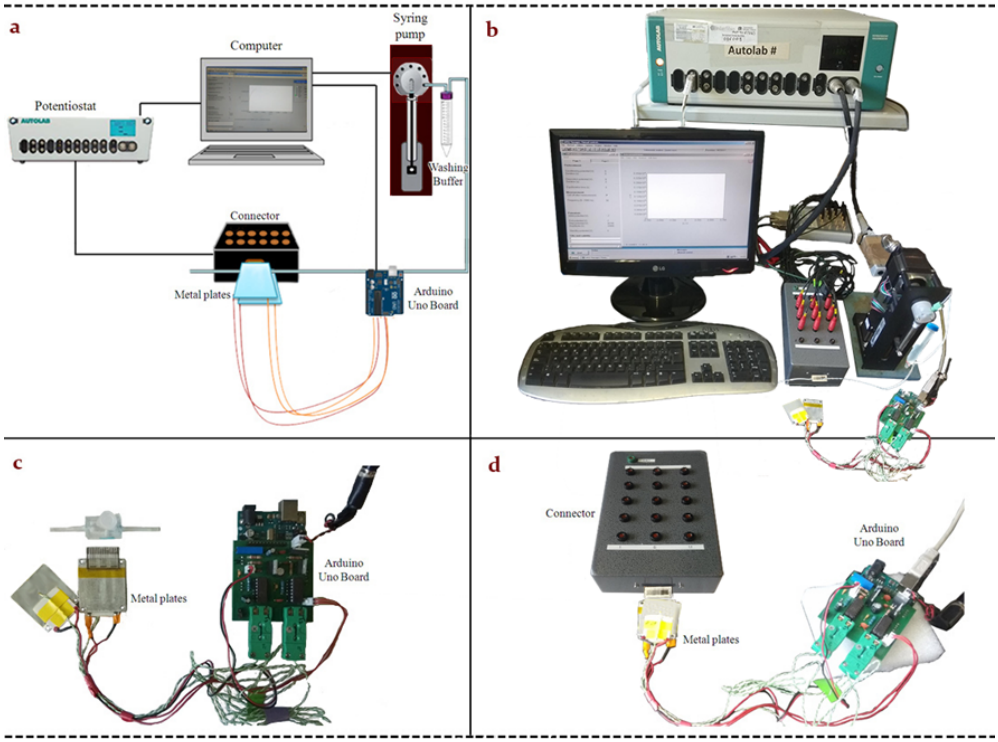

Figure 3.2. Set-up of the integrated system for SNPs detection using éMCA; (a) A schematic of the system showing how the heating plates of a homemade Peltier surround the gold electrode array connected to the potentiostat, and the connection of the syringe pump propulsed washing buffer to the reaction chamber, where electrochemical measurements and temperature control take place. (b) A real picture of the whole setup of the éMCA system. (c) and (d) homemade Peltier device consists of an Arduino uno board and two heating metal plates.

3.3. Methodology

3.3.1 Heating system characterization

Transfer function A type-k thermocouple and a BI BPC10 680 J resistor were attached using conductive tape to each of the heating blocks. To determine the step response of each system, a 0.48 mV step was applied to each resistor. All the temperature readings were recorded with the Arduino and with the Matlab 2013a software, the system behaviour was modelled. An inspection of each response revealed that both corresponded to a type I system. Using Matlab, the process gain Kp, the t1 and t2, which correspond to the time when the output attains the 63.2 and 28.3 percent of its final value, respectively, were defined. The theta (θ), tau (τ), and type I plus dead time-continuous transfer function can be calculated as follows.

$$\tau = \frac{3}{2} * (t_2 - t_1)$$

$$\theta = t_2 - \tau$$

$$G_p = \exp(-\theta * s) * \frac{K_p}{(1 + \tau * s)}$$

PI tuning The Matlab tool Simulink was used to model the closed-loop response of each PI controller in series with a heating plate. The correct model of the system behaviour required the transfer function of each plate. We were able to tune and observe the closed-loop response and reference tracking of each system as well as the error, the controller effort, the open-loop response, plus many other options using the Simulink tool PID tuner. For the PI control system the following equation was used:

$$C_{out} = K_c * e(t) + K_i * \int e(t)dt$$

Where e(*t*) represents the error or what is the same, the setpoint – input, C_{out} is the controller output, K_c is the proportional gain and K_i represents the integral gain.

To validate the functionality of the system, a glass slide was used and covered by a microfluidic PMMA filled with buffer to simulate an electrode array. A thermocouple was glued inside the microfluidic to monitor the temperature. This setup was placed between the metal blocks (and a plastic case surrounded the plate to isolate it from environment). The temperature was ramped and recorded by Arduino and compared with the one measured by the thermocouple. One end of the BI BPC power resistors was connected to a 24 V DC adapter and the other end to the drain of an IRF520 power transistor. These transistors are responsible for delivering a controlled current to each of the resistors. The power delivered by each IRF was modulated through the duty cycle variation of a 10 bit pulse width modulation (PWM) system implemented on the Arduino UNO. The PWM worked at a frequency of ~4 KHz at 5 V. Finally, the glass slide and reference readings were recorded using the Hi 93531.

3.3.2. Electrode fabrication

The gold electrode array (Figure 3.3) was designed with nine circular working electrodes (1 mm^2) and a rectangular counter electrode (4 mm^2). It was fabricated in a clean room using 75x25 mm

soda-lime glass slides substrate (Sigma-Aldrich, Spain). The sputtering processes consists of the following steps; after cleaning the glass slides were subjected to an oxygen plasma etching using AC O_2/Ar (5 cm^3/s^{-1} of Ar, 5 cm^3/s^{-1} of O_2, 50 W) for 5 minutes. A positive photoresist AZ 1505 (Micro Chemicals GmbH, Germany) was deposited by spin coating at (4000 rpm for 30s) on a pre-cleaned and dried glass slide. The glass slide was then exposed to UV light for 4 sec using a chromium mask in contact mode (LED Paffrath GmbH, Rose Foto Masken, Germany) and then immersed for one minute in a commercial developer AZ 726. Following development, the glass slide was introduced into the sputtering chamber (ATC Orion 8-HV, AJA International Inc, USA) and was subjected to an oxygen plasma etching using AC O_2/Ar (5 $cm^3 \cdot s^{-1}$ of Ar, 5 $cm^3 \cdot s^{-1}$ of O_2, 50 W) for 5 minutes. Subsequently, a layer of 30 nm of Ti/TiO_2 was sputtered (oxygen flow rate: 5 cm^3/s^{-1} of O_2 for the first 10 nm, then increased to 20 cm^3/s^{-1} for the last 5 nm. (Ar flow rate: constant 5 cm^3/s^{-1}). The next step is the deposition of 100 nm of Au by AC sputtering (5 cm^3/s^{-1} of Ar, 5 cm^3/s^{-1} of O_2, 50W). Finally, the arrays were sonicated in acetone for 5 minutes, sonicated in isopropanol for 5 minutes and then rinsed with Milli-Q water.

Custom-made microfluidics, which were fabricated using double adhesive gasket (Adhesive Research, Ireland) with 6 mm thick PMMA cover plates patterned using a CO_2 laser marker (Fenix, Synrad, USA). Following electrode array functionalisation, a double adhesive gasket and PMMA were aligned and bonded to produce a 672µL microfluidic chamber where DNA hybridization and electrochemical measurements were carried out. The washing buffer was flowed into the gold array through a tube embedded to the microfluidic chamber that was washed with 300 µL of (PBS pH 7.4) using a syringe pump (Cavro XL3000, Tecan Systems). Washing was driven by constant air pressure during melting curve analysis (Figure 3.3).

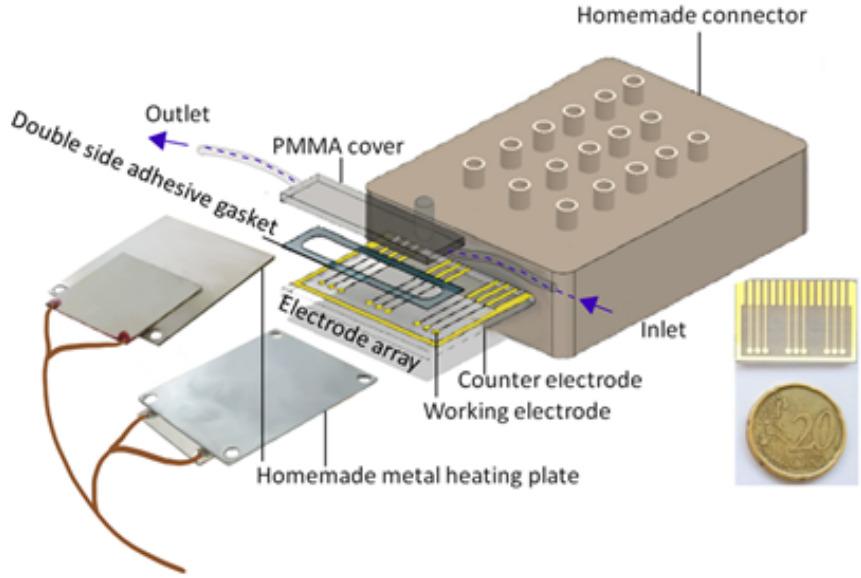

Figure 3.3 Schematic of the system set-up where the electrode array is placed between two metal plates and covered by a microfluidic cell. The electrode array, double adhesive gasket and PMMA cover are bound together to create 672 µL cells where hybridization and electrochemical measurements are carried out. The electrode array is heated by the aluminium heating plates from room temperature to 95ºc and is connected to the potentiostat through a homemade connector box.

3.3.3. Electrode functionalisation The electrode arrays were electrochemically cleaned by sweeping 10 times the potential from 0 to - 1.2 V vs Ag/AgCl in 0.1 M deoxygenated aqueous KOH solution. After washing with Milli-Q water, the electrode surface was cleaned again by cycling the potential 10 times between 0.2 and 1.5 V in 0.5 M H_2SO_4. The gold electrode array were washed with Milli-Q water, dried with nitrogen, and used immediately for surface functionalization. Thiolated probe was self-assembled, via spotting of 1 µL of (1 µM probe solution), and DT1 as back filler (ratio 1:100, thiolated probe:DT1) both freshly prepared in 1 M KH_2PO_4, onto each electrode surface of an array of 9 working electrodes and then left to self-assemble for 3 h in a humidity chamber to prevent evaporation, followed by thorough washing with buffer containing 10 mM Tris-HCl (pH 7.4) for 10 min at room temperature (25°C).

3.3.4. éMCA measurements and hybridization Target hybridization was carried out via 2 hour incubation by spotting 1 µL of 1 µM 21-mer target (Fully complementary (wild type)-Fc, SNP_B-Fc (SNP positioned at bottom), SNP_T-Fc (SNP positioned at top) ,SNP_M-Fc (SNP positioned at the middle) in 10 mM Tris buffer (pH 7.4) containing 0.5 M NaCl, onto the functionalised electrode

surface. Following hybridization, the sensor was extensively washed with the hybridization buffer. The array was then covered with the microfluidics using the double adhesive gasket and was placed between two aluminum plates of the heating device and the temperature ramped. All electrochemical measurements were carried out using an Autolab model PGSTAT 12 potentiostat/galvanostat controlled with the General Purpose Electrochemical System (GPES) software (Eco Chemie B.V., The Netherlands) 64-channel potentiostat, which was connected to the multi-electrode array through an in-house fabricated connector box. A classical reference electrode Ag/AgCl was used. All the potentials are recorded with respect to the reference electrode. Parallelised multiple SWV measurements were recorded throughout temperature ramping. The parameters employed in the SWV experiments were: potential window between 0 and 0.8 V (vs. Ag/AgCl), step potential 7 mV, modulation amplitude 50 mV, modulation time 0.05 s and interval time 0.15 s.

3.3.5. Asymmetric Polymerase Chain Reaction and Amplicon Detection

Asymmetric PCR was carried out in two stages – firstly 35 cycles of PCR with both primers, followed by 15 cycles with just forward primer. The first PCR was carried out using Fc-labelled-forward primers and phosphate labelled reverse primers. using a T100 thermal cycler (Biorad) using the following protocol: 95ºC for 2 minutes, followed by 35 cycles at 95ºC for 30 seconds, 58ºC for 30 seconds, and 72ºC for 30 seconds], followed by a final elongation step at 72ºC for 5 minutes. Each 25µL of PCR reaction mixture contained 0.05 units of DreamTaq and DreamTaq buffer 10X, both forward and reverse primers (Fc-FwP and phosphate RvP) at 0.2 µM, dNTPs at 200 µM as final concentration. In the second step, amplification was carried out using 2.5 µL of PCR product from the first step as template DNA and applying 95ºC for 2 minutes, followed by 15 cycles of 95ºC for 30 seconds, 58ºC for 30 seconds, and 72ºC for 30 seconds, followed by a final elongation step at 72ºC for 5 minutes. Each 25µL of asymmetric PCR mixture contained the same as PCR reaction mixture but with 0.4 µM of Fc-FwP. The PCR product was then incubated with lambda exonuclease to digest the strand elongated with the phosphate labelled primer in any remaining duplex DNA. The lambda exonuclease digestion via the addition of 10 units (10 unit/µL) of lambda exonuclease enzyme and 10 µL of exonuclease buffer followed by incubation at 37°C for 2 h and a final denaturation of the enzyme at 80°C for 10 minutes.

Amplification products were checked using agarose gel electrophoresis. The gel was made with ultralow pure agarose (3% w/v) in 1× Tris-Borate- EDTA buffer (TBE) and stained with GelRed™ nucleic acid stain. A mixture of 1µL of PCR product with 4µL of 2x loading buffer was loaded per gel well, electrophoresis was performed at 110 V for 30 min and gels were visualized in a UV transilluminator at λ = 254 nm.

éMCA with the single stranded PCR amplicons were carried out in two ways. In the first approach ferrocene labelled amplicon was hybridized to four different probes. Eight electrodes of an array were modified with diverse thiolated probes (four probes in duplicate), one of which is fully complementary to the wild type (i.e. the amplicon) and each of the other three contained a single mismatch at the top, bottom or middle of the probe. In the second format, one common thiolated probe was immobilized on all the electrodes, and four different PCR amplicons were used, where the part of the amplicon that hybridizes to the immobilized probe is fully complementary, or contains a mismatch at the top, bottom or middle of the hybridized duplex.

In both approaches, measurements were carried out in duplicate, and two electrodes were incubated with each asymmetric PCR generated product for three hours. After washing the electrode for 5 minutes, the electrode array was placed between the heating plates, covered by the microfluidics and the Peltier applied to start the temperature ramp and the ferrocene signal measured throughout the ramp.

For all electrochemical melting curve analyses, 8 parallel melting curves on a single electrode array were carried out simultaneously.

3.3.6. Fluorescence melting curve analysis

Melting curve analysis was carried out using a fluorescence spectrophotometer (CARY Eclipse, Varian), housed with a peltier thermostatted multicell holder. This peltier accessory contains chambers for four cuvettes. Ten microlitres of the DNA duplex to be analysed was added to a cuvette containing 100 µL of Tris-HCl (pH 7.4) and 0.2 µL of 20X Eva Greeen intercalating fluorescent dye. Each test was carried out by increasing the temperature from 25°C to 95°C at a fixed ramping rate, and the fluorescence continually measured at λ = 530nm and the first derivatives of the melting curve used to accurately determine the melting temperature.

3.4. Results and discussion

Transfer function

The resulting transfer functions are:

Heating plate 1:

$$G_{p1} = e^{(-6.08*s)} \frac{0.449}{252.3 * s + 1}$$

Heating plate 2:

$$G_{p1} = e^{(-7.18*s)} \frac{0.553}{272.3 * s + 1}$$

From the step response and simulated response obtained with Matlab. It shows that the step response of the transfer function is in concordance with the system behavior, allowing to use of this transfer function to model and study the closed-loop response of the PI controller in series with the system.

PID tuning The most common PID controllers was chosen to control the resolution of each of the heating blocks, because the proportional part improves the rising and settling time of the response, where the integrative part reduces the steady-state error, the derivative part is used to reduce both the overshoot and the change rate of the error. To control the step resolution, the correspondent Kp and Ki values were tuned to produce a system response with a fast-rising and settling time, and with the minimum or no overshoot (details in Figure. SI 3.1c, Figure. SI 3.2 for heating plate 2).

The best Kp and Ki parameters that produced the best response on both heating plates were 55.85 and 1.33, respectively. These variables allowed to have a rise time of 15.6 seconds, a settling time of 1 minute and 50 seconds, and a 10.4 % overshoot. The overshoot value in principle is unacceptable because, with each change on the set point, the temperature would overpass this set point. However, when the heating experiments were carried out on the real system, the output never exceeded the set point. One possible explanation for this is that the simulation was made with a step response of 1 V, although, the highest voltage change made by the PWM in order to increase the block temperature by 1 °C is 24.41 mV. This means that the input shift might not be that strong to produce such a response on the controller.

Heating test The heating system is composed of two (3.6 x 4.3 x 0.1 cm) aluminium sheets that have a BI BPC 680J resistor attached to each of them two type k thermocouples. The first thermocouple, together with HANNA Hi 93531, works as a temperature reference for the second thermocouple, and it was used temporarily to make the corrections for the corresponding temperature of the second thermocouple. Furthermore, the second thermocouple is connected to an

AD595 (Analog devices) that works both as a cold junction compensation system and as a thermocouple amplifier. The system output is 10 mV/°C. This second subsystem controls the reading of the heating block temperature. This signal is also used as the input for the PI controller (Figure. SI 3.1b, Figure. SI 3.2 for heating plate 2). Some heating tests were performed to observe the plate's behaviour and to determine if the PWM was able to produce and to read 0.2°C temperature changes. These tests were done on each of the heating blocks individually and enclosed in a plastic case for room temperature isolation, and from the results obtained, a significant difference between the reference and each reading system was observed.

This reason is related to the Hi 93531 device, which is a commercial thermometer that can be assumed to have an integrated correction circuit or makes a digital temperature correction. This suggests that some correction is required to increase the reading fidelity. After analyzing the heating tests data of each block, the difference between the reference and the temperature reading system output showed a linear behaviour. There are two possible options to make the temperature correction. EitIn the first option, a system capable of taking the block temperature as an input, to compare and correct each reading point by point and to give this signal as a feedback parameter to the PI controller, could be implemented. This would require a change in the design and the iincorporation of a specialized and complicated circuit, which would have had increased the production costs and the system complexity. The other option was to incorporate a digital correction. By making a linear regression, a correcting equation was obtained and the Arduino controlled the point by point correction. After the corresponding digital temperature corrections were made, the stability and functionality for each of the resolutions were tested by making a heating test on each plate working in parallel. Figure SI 3.4d shows the system's behaviour for a heating test starting at 25°C and finishing at 90°C. Both heating systems are capable of producing a stable and correct output with a 0.2, 0.5 and 1 °C/step.

To validate the entire system functionality, a complete heating test was performed using a glass slide with a microfluidic section made out of PMMA glued on top of it. A thermocouple was attached to the glass and the complete setup was placed between heating plates. All data was recorded with the Arduino and the Hi 93531. Figure SI 3.4e shows the system behaviour and the glass slide temperature evolution throughout the entire test. It is important to recall that there is still some small difference between the reference and the thermocouples that needs to be corrected. Heating plate 1 has a temperature error of 3.37% while the heating plate 2 has a lower error of 1.78%. It is important to highlight is that the highest temperature difference between the glass slide temperature and the set point is 1.4°C. One possible explanation for this, is that the heat transference from the plates to

the glass is not completely efficient due to the difference from the thermal conductivity coefficients of the aluminum (205 W/mK) with the PMMA (0.17 W/mK) and the glass slide (1.05 W/mK).

Electrochemical Melting Curve Analysis (éMCA) measurements Dithiolated probes were selected to strengthen the bond with the gold surface to avoid desorption of the capture probe from surface during the melting analysis. An alkyl-dithiol[29] was used as a spacer to provide a more organised self-assembled monolayer, avoiding steric hindrance and facilitating accessibility of the target for efficient hybridization with the ferrocene labelled target. By monitoring the decrease of the oxidation peak of the ferrocene in the consecutive square wave voltammograms (SWV), the melting curve can be constructed and melting temperature (Tm) calculated by applying the first derivative.
As a control to ensure that the changes in the electrochemical signal was solely attributed to the thermal induced denaturation of the surface-tethered duplex, the stability of the ferrocene signal with increasing temperature was evaluated. A thiolated oligo functionalised with ferrocene was chemisorbed onto the surface of the gold electrode array and subjected to the temperature ramp employed in the melting curve analysis, and as can be seen in Figure SI3.3, the observed voltametric signal was stable, thus demonstrating that any decrease in the signal was not due probe desorption or instability of the ferrocene label at elevated temperatures.
The optimum temperature ramp was elucidated by comparing different rates (0.2, 0.5 and 1°C/step). Three different electrode arrays were modified with the thiolated capture probe, and hybridized with 4 different targets, one of which was fully complementary (wild type), whilst the others contained a mismatch that was positioned at the top, bottom or middle of the labelled oligo. Duplicate measurements were carried out and after washing the electrode array for 5 minutes, each array was heated at different ramping temperature, the first array heated using 0.2°C/step, the second using 0.5 °C/step and the third heated using 1 °C/step. As can be observed in Table 1, the 0.2°C/step did not provide a significant discrimination between wild type and the single mismatch containing sequences. For 0.5 and 1°C/step a clear differentiation between sequences was observed and 1ºC/step was used in all subsequent experiments.

Table 3.1. Melting temperatures obtained applying different rates for ramping temperature.

SNP positions	Melting temperature (Tm / ºC) calculated for three different ramping temperature		
	0.2 °C	**0.5** °C	**1** °C
Fully Complementary	31.3 ± 0.2	35.7 ± 0.2	37.0 ± 0.9
Mismatch in middle	30.1 ± 0.1	30.4 ± 0.5	32.7 ± 0.2
Mismatch at top	30.0 ± 0.4	29.4 ± 1.5	34.2 ± 0.1
Mismatch at bottom	29.4 ± 0.1	31.3 ± 0.3	36.2 ±1.5

Using the 1ºC/step temperature ramp, the melting temperatures of the duplexes formed between a common probe with four different ferrocene labelled 21-mer targets, one of which was fully complementary (wild type), whilst the other contained a mismatch that was positioned at the top, bottom or middle of the labelled oligo. Square wave voltammetry measured the peak attributed to ferrocene throughout the temperature ramp and the measured signal was normalised to the signal obtained prior to initiation of the melt, and for a clear determination of the melting temperature first-derivative plots were used (Figure 3.4) As can be seen in Figure 3.4., where the melting curves and first derivatives of the melting curves obtained using the 1ºC/step, the highest melting temperature, as expected, is for the fully complementary duplex. The largest difference in the melting temperature is achieved when the single mismatch is positioned in the centre of the probe, but in all cases a clear difference in melting temperature can be observed.

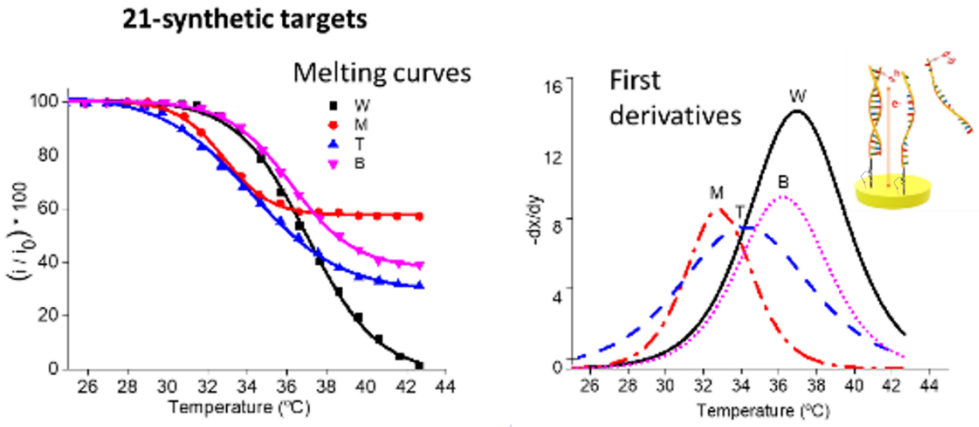

Figure 3.4. Melting curves and the corresponding first derivatives obtained for four different 21-mer synthetic targets hybridized to a common surface tethered capture probe, with each of the targets being the fully complementary wild type (W) or containing a single mismatch at the top (T), bottom (B) or middle (M) of the sequence.

Once the proof-of-concept of electrochemical melting curve analysis had been demonstrated with the short 21-mer fully complementary target, the methodology was applied to a full-length PCR amplicon. Two different formats were evaluated, one using one common PCR amplicon and four different immobilized probes and the second using a common surface-tethered probe and four different single stranded PCR amplicons (differing by one mismatch and position of mismatch). Both approaches were used to evaluate the effect of the position of the SNP site to be interrogated in the hybridized duplex and to elucidate if a better discrimination between fully complementary (wild type) and single mismatch (presence of non-wild type SNP), can be achieved by optimisation of this

position. In both cases, single stranded DNA was generated by a combination of asymmetric PCR and exonuclease digestion was checked using gel electrophoresis (the example for the second approach is given in Figure 3.6a), where the DNA after the first step of the PCR (DNA) and after the second step and exonuclease digestion (ssDNA).

The melting curves and first derivatives for the first approach can be seen in Figure 3.5, and it is clear that the highest melting temperature is obtained with the fully complementary wild type, and again similar to the 21-mer, the biggest difference between the wild type and single mismatch is obtained when this mismatch is positioned in the centre of the probe.

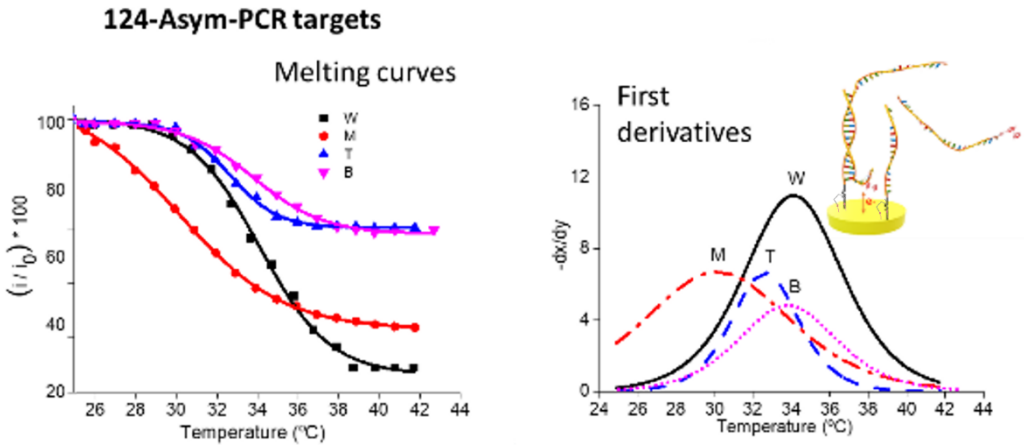

Figure 3.5 Melting curves and the corresponding first derivatives obtained for a common 124-mer amplicon hybridized to four different surface tethered capture probes, with each of the probes being the fully complementary wild type (W) or containing a single mismatch at the top (T), bottom (B) or middle (M) of the sequence.

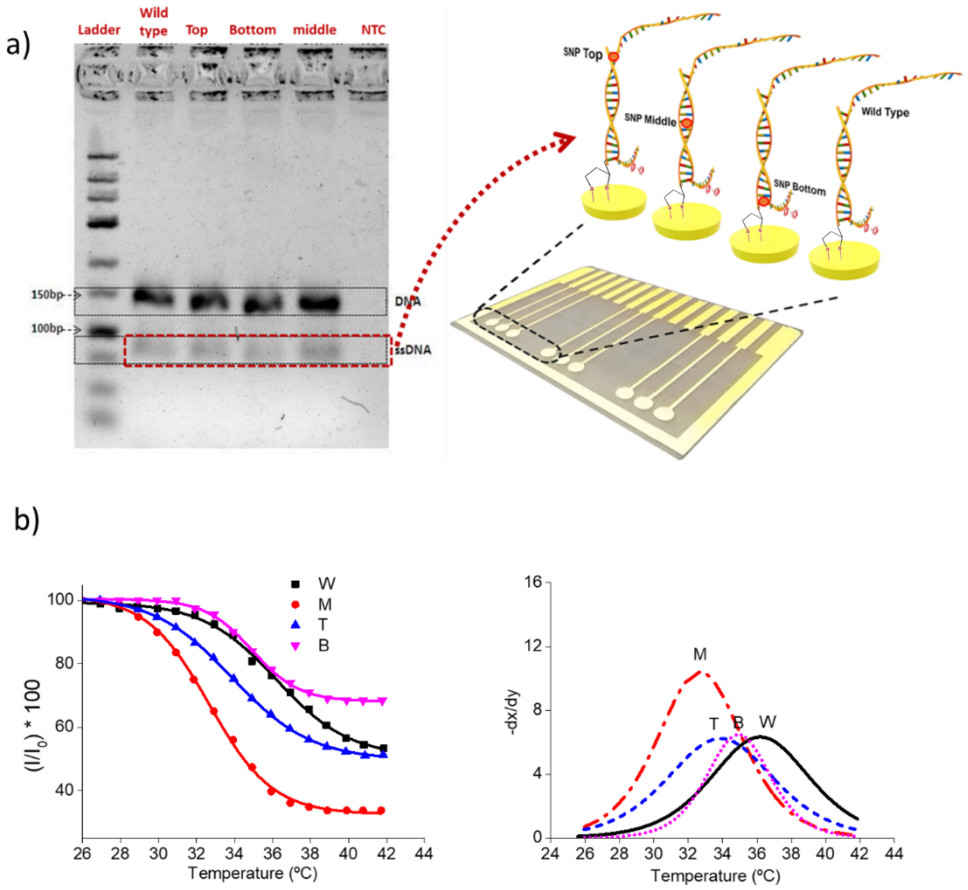

Figure 3.6. (a) Agarose gel electrophoresis analysis of each of the ssDNA 124-mer amplicons obtained after asymmetric PCR amplification, with the amplicons designed to be fully complementary (wild type) or to contain a single mismatch designed to be at the top, bottom or middle of the hybridized duplex; (b) Melting curves obtained for the four different- asymmetric PCR targets and the corresponding first derivatives.

The results obtained using electrochemical melting analysis were then compared with those determined using fluorescent melting curve analysis to see if similar trends were obtained. It should be noted that similar melting temperatures are not expected as it is known that the melting temperature of surface tethered DNA duplexes are ca. 10 ºC lower than that obtained in solution (Zhou *et al.*, 2015).[24] As can be seen in Table 3.2, very similar trends were observed, with the biggest difference in melting temperature between fully complementary and single mismatch containing is achieved when the mismatch is in the middle of the hybridized duplex.

Table 3.2. Tm calculated from melting curves

	Melting temperature (Tm / ºC) mean value Tm ± Standard deviation (n=3)				
SNP position	**21-mer target**		**124-mer target Asym-PCR product**		
	éMCA	Fluorescence MCA	éMCA 4 Fc-targets/ 1 capture probe	éMCA 1 Fc-target/ 4 capture probes	Fluorescence MCA
Wild type	37.0 ± 0.9	46.6 ± 3.3	36.3 ± 1.2	34.1 ± 0.5	46.5 ± 1.2
SNP in Middle	32.7 ± 0.6	24.6 ± 1.7	32.7 ± 1.1	30.0 ± 0.7	31.4 ± 1.6
SNP at Top	34.9 ± 0.1	30.6 ± 1.9	34.0 ± 0.7	32.6 ± 1.2	34.2 ± 0.1
SNP at Bottom	36.2± 1.5	32.4 ± 1.3	35.1 ± 0.5	33.8± 0.9	34.5 ± 0.5

The results obtained are in agreement with multiple previous studies, where terminal mismatches in short duplexes are known to have less effect than internal mismatches.[25] Mismatches near the centre of the probe have been reported to have a stronger destabilising effect than mismatches close to either end, both for hybridizations in solution[26] and for microarray hybridizations;[27, 28] and this difference in destabilisation has been observed frequently, and used in applications such as SNP detection.[29,30]

(Letowski *et al*. 2004) evaluated the effect of probe size, mismatch position as well as the number of mismatches and concluded that mismatches at the ends of a duplex have markedly lower effects as compared to a middle mismatch.[31] Lievens *et al*. used chemiluminescence to explore the influence of mismatch positions at regular intervals of positions (i.e. 1, 5, 10, 15 and 20) in different 20-mer sequences and varying types of mismatch at these positions and reported that mismatches at extreme positions are least distinguishable and are independent of the type of sequence.[32] In agreement with these studies, Naiser *et al*. 2008, found that thermodynamically a middle mismatch was found to be less stable in a 16-mer sequence [33], Rennie *et al*., 2008 carried out a large-scale investigation of microarray hybridizations to murine probes with known sequence mismatches, demonstrating that the effect of mismatches is strongly position-dependent, being stronger for mismatches near the centre of the probe than for those at the ends.[34] El-Yazbi *et al*., 2017, used a terbium (III) luminescent probe to studiy the effect of mismatch position and found that when comparing strands with only one mismatch, the oligonucleotide with a mismatch located at the center of the oligomer exhibited the most $Tb^{3þ}$ luminescence enhancement due to duplex instability. [35]

In summary, we have developed a semi-automated device for the detection of single base mismatches using electrochemical melting curve analysis, where an in-house Peltier device was

used to apply a controlled heating ramp to an electrode array. The optimum position of the SNP site to be interrogated in relation to the immobilized probe has been elucidated. Whilst multiplexed detection of SNPs was not demonstrated, multiple different duplexes were simultaneously subjected to melting curve analysis (in each array, 8 electrodes with duplicates for each allele and one control electrode) and future work will focus on multiplexed detection of SNPs, firstly using low density electrode arrays and then moving to arrays with a high number of individual electrodes.

3.5. Conclusions

We detailed an in-house fabricated device for multiplexed electrochemical melting curve analysis. The system consists of temperature controller (homemade Peltier) integrated with an electrode array housed within a microfluidic device, with multiplexed electrochemical detection. The platform was primarily demonstrated with a short DNA duplex, and the effect of the position of the mismatch interrogated. The platform was then extended to duplexes with a short surface-tethered DNA probe and a 124-mer single stranded asymmetric PCR amplicon. Again with the aim of elucidating the best position for mismatch discrimination, two different approaches were evaluated – one where four different probes mismatches at different positions and a single amplicon, and the other with a single probe and four different amplicons. In all cases, the optimum position for maximum destabilisation of the surface tethered DNA duplex and consequent optimal discrimination between fully complementary and single mismatch containing was observed with the mismatch site at the centre of the hybridized DNA duplex. The developed device is semi-automated, capable of multiplexed detection, relatively rapid, cost-effective and easy-to-use and future work will focus on detection of disease-associated SNPs in blood samples, and moving from PCR to isothermal amplification.

Acknowledgement

This project has received partial funding from the European Union's Horizon 2020 research and innovation program under grant agreement No 767325.

References

1. Cooper R. A., Jones D. C. N. and Parrott S., J. Gen. (1985). Isolation and mapping of Escherichia coli. K-12 mutants defective in phenylacetate degradation. Microbiol, 131, 2753–2757.
2. Brookes A. J. (1999). Identification of structurally and functionally significant deleterious nsSNPs of GSS gene: in silico analysis. Gene, 234, 177–186.
3. Budowle, B., & van Daal, A. (2008). Forensically relevant SNP classes. BioTechniques, 44(5), 603–610.
4. Schumm J. W., Knowlton R. G., Braman J. C., Barker D. F., Botstein D., Akots G., Brown V. A., Gravius T. C., Helms C., Hsiao K., Rediker K., Thurston J. G. and Donis-Keller H., Am. J. Hum. (1988). Identification of more than 500 RFLPs by screening random genomic clones. Genet , 42, 143–159.
5. Salimullah M., Hamano K., Tachibana M., Inoue K. and Nishigaki K. (2005). Efficient SNP analysis enabled by joint application of the μTGGE and heteroduplex methods. Cell. Mol. Biol. Lett, 10, 237–245.
6. Deulvot C., Charrel H., Marty A., Jacquin F., Donnadieu C., Lejeune-Hénaut I., Burstin J. and Aubert G. (2010). Highly-multiplexed SNP genotyping for genetic mapping and germplasm diversity studies in pea. BMC. Genomics, 11, 468.
7. Sobin Kim S., Misra A. (2007). SNP genotyping: technologies and biomedical applications. Annu. Rev. Biomed. Eng, 9, 289-320.
8. Reed G .H., Kent J.O., Wittwer CT. (2007). High-resolution DNA melting analysis for simple and efficient molecular diagnostics. Pharmacogenomics, 8(6), 597–608.
9. Hassibi A., Manickam A., Singh R., Bolouki S., Sinha R., Jirage K. B., Schoolnik G. (2018). Multiplexed identification, quantification and genotyping of infectious agents using a semiconductor biochip. Nature Biotechnology, 36 (8), 738-745.
10. Clutter D. S., Mazarei G., Sinha R., Manasa J., Nouhin J., LaPrade E., Shafer R. W. (2019). Multiplex Solid-Phase Melt Curve Analysis for the Point-of-Care Detection of HIV-1 Drug Resistance. The Journal of Molecular Diagnostics, 21 (4), 580-592.
11. Erdem A., Kerman K., Meric B., Akarca U. S. and Ozsoz M. (1999). Electrochemical biosensor for the detection of short DNA sequences related to the hepatitis B virus. Electroanalysis, 11, 586–7.

12. Erdem A., Meric B., Kerman K., Dalbasti T. and Ozsoz M. (1999). Detection of interaction between metal complex indicator and DNA by using electrochemical biosensor. Electroanalysis, 11, 1372–6.
13. Millan K. M., Saraullo S. and Mikkelsen S. R. (1994). Voltammetric DNA biosensor for cyctic fibrosis based on a modified carbon paste electrode Anal. Chem, 66, 2943–8.
14. Millan K. M., Mikkelsen S. R. (1993). Sequence-selective biosensor for DNA based on electroactive hybridization indicators. Anal. Chem, 65, 2317–23.
15. Napier M. E., Loomis C. R., Sistare M. F., Kim J., Eckhardt A. E. and Thorp H. H. (1997). Probing biomolecule recognition with electron transfer: electrochemical sensors for DNA hybridization. Chem, 8, 906–13.
16. Hason S., Dvorak J., Jelen F. and Vetterl V. (2002). Electrochemical impedance spectroscopy of polynucleotide adsorption. Talanta, 56, 905–13.
17. Jelen F., Erdem A. and Palecek E. (2002). Cyclic voltammetry of echinomycin and its interaction with double-stranded and single-stranded DNA adsorbed at the electrode. Bioelectrochemistry. Bioelectrochemistry, 55, 165–7.
18. Erdem A. and Ozsoz M. (2002). Interaction of the anticancer drug epirubicin with DANN. Anal. Chim. Acta, 437, 107–14.
19. Meunier-Prest R. (2003). Direct measurement of the melting temperature of supported DNA by electrochemical method. Nucleic Acids Research, 31 (23), 150e–150.
20. Deféver T., Druet M., Evrard D., Marchal D. and Limoges B. (2011). Real-time electrochemical PCR with a DNA intercalating redox probe. Anal Chem, 83 (5), 1815–1821.
21. Shen Z., Sintim H. O., Semancik S. (2015). Rapid nucleic acid melting analyses using a microfabricated electrochemical platform. Anal Chim Acta, 853 (1), 265–270.
22. Luo X., Hsing I. M. (2009). Real time electrochemical monitoring of DNA/PNA dissociation by melting curve analysis. Electroanalysis. Electroanalysis, 21(14), 1557–1561.
23. Nasef H., Beni V., O'Sullivan C.K. (2010). Electrochemical melting-curve analysis. Electrochem commun. Electrochem Commun, 12 (8), 1030–1033.
24. Zhou J. C., Feller B., Hinsberg B., Sethi G., Feldstein P., Hihath J., Miller, R. (2015). Immobilization-mediated reduction in melting temperatures of DNA–DNA and DNA–RNA hybrids: Immobilized DNA probe hybridization studied by SPR. Colloids and Surfaces A: Physicochemical and Engineering Aspects, 481, 72–79.
25. Fotin A. V., Drobyshev A. L., Proudnikov D. Y., Perov A. N., Mirzabekov A. D. (1998). Parallel thermodynamic analysis of duplexes on oligodeoxyribonucleotide microchips. Nucl Acids Res, 26, 1515-1521

26. Southern E., Mir K., Shchepinov M. (1999). Molecular interactions on microarrays. Nat Genet, 21, 5-9.
27. Zhang L., Miles M. F., Aldape K. D. (2003). A model of molecular interactions on short oligonucleotide microarrays. Nat Biotech, 21, 818-821.
28. Wick L. M., Rouillard J. M., Whittam T. S., Gulari E., Tiedje J. M., Hashsham S. A. (2006). On-chip non-equilibrium dissociation curves and dissociation rate constants as methods to assess specificity of oligo- nucleotide probes. Nucl Acids Res, 34, e26.
29. Gresham D., Ruderfer D. M., Pratt S. C., Schacherer J., Dunham M. J., Bot- stein D., Kruglyak L. (2006). Genome-Wide Detection of Polymor- phisms at Nucleotide Resolution with a Single DNA Microarray. Science, 311, 1932-1936.
30. Fish D. J., Horne M. T., Searles R. P., Brewood G. P., Benight AS. (2007). Multiplex SNP discrimination. Biophys J, 92, L89-91.
31. Letowski J., Brousseau R., Masson L. (2004). Microbiol. Methods, 57, 269–278.
32. Lievens B., Claes L., Vanachter A. C. R. C., Cammue B. P. A., Thomma B. P. H. J. (2006). FEMS Microbiol. Lett, 255, 129–139.
33. Naiser T., Kayser J., Mai T., Michel W., Ott A. (2008). BMC Bioinf, 9, 509–521.
34. Catriona Rennie C., Noyes H. A., Kemp S. J., Hulme H., Brass .A, Hoyle D. C. (2008). Strong position-dependent effects of sequence mismatches on signal ratios measured using long oligonucleotide microarrays, 9, 317.
35. El-Yazbi A. F., Wong A., Loppnow G. R. (2017). A luminescent probe of mismatched DNA hybridization: Location and number of mismatches. Analytica Chimica Acta, 994, 92–99.

3.6. Supporting information

Table SI 3.1. Oligonucleotides used for the melting curve analysis in this study: capture probes, 21-mer targets, 124-mer targets, and the primers used to generate the ferrocene-targets by asymmetric-PCR.(The regions of the target sequences complementary to the capture probes are underlined)

Oligonucleotides	Sequences (5 to 3)
	21-mer targets
Wild type (Full complementary)	Fc-5´-CGAAGTGTGAACTAGTCCCAC-3´
SNP at the top	Fc-5´- GAAGTGTGAACTAGTCCCAC-3´
SNP at the middle	Fc-5´-CGAAGTGTGAA**A**TAGTCCCAC-3´
SNP at the bottom	Fc-5´-CGAAGTGTGAACTAGTCCCA**A**-3´
	124-mer targets for Asymmetric PCR
No SNP (Full complementary)	5`AGCTCCAGAAGATAAATTACAGGCGAAGTGTGAACTAGTCCCACCACCTTAATTTCAC TGTGTGTTAACACTTGTAAAGAACCTGCATAATGTGTGTATCTTACAACTAGGATACTAT GACCCC-3 `
SNP at the top	5`AGCTCCAGAAGATAAATTACAGGCGAAGTGTGAACTAGTCCCA**A**CACCTTAATTTCAC TGTGTGTTAACACTTGTAAAGAACCTGCATAATGTGTGTATCTTACAACTAGGATACTAT GACCCC-3`
SNP at the middle	5´AGCTCCAGAAGATAAATTACAGGCGAAGTGTGAA**A**TAGTCCCACCACCTTAATTTCAC TGTGTGTTAACACTTGTAAAGAACCTGCATAATGTGTGTATCTTACAACTAGGATACTAT GACCCC-3`
SNP at the bottom	5´AGCTCCAGAAGATAAATTACAGG**A**GAAGTGTGAACTAGTCCCACCACCTTAATTTCAC TGTGTGTTAACACTTGTAAAGAACCTGCATAATGTGTGTATCTTACAACTAGGATACTAT GACCCC-3`
	Primers for Asymmetric-PCR
Fc-Forward primer	Fc-5´-AGCTCCAGAAGATAAATTACAGG-3`
Reverse primer	5´-GGGGTCATAGTATCCTAGTTG-3
	Capture probes
Full complementary to the target (thiol 5´-)	Thiocticacid-5´-TTTGTGGGACTAGTTCACACTTCG-3´
Full complementary to the target (thiol 3´-)	5´-GTGGGACTAGTTCACACTTCGTTT-3´-Thiocticacid
SNP at the top	5´-**A**TGGGACTAGTTCACACTTCGTTT-3´-Thiocticacid
SNP at the middle	5´-GTGGGACTA**A**TTCACACTTCGTTT-3´-Thiocticacid
SNP at the bottom	5´-GTGGGACTAGTTCACACTTC**A**TTT-3´-Thiocticacid
	Fc-DNA-thiol
	5´Fc -GTGGGACTAGTTCACACTTCGTTT-3´-Thiol

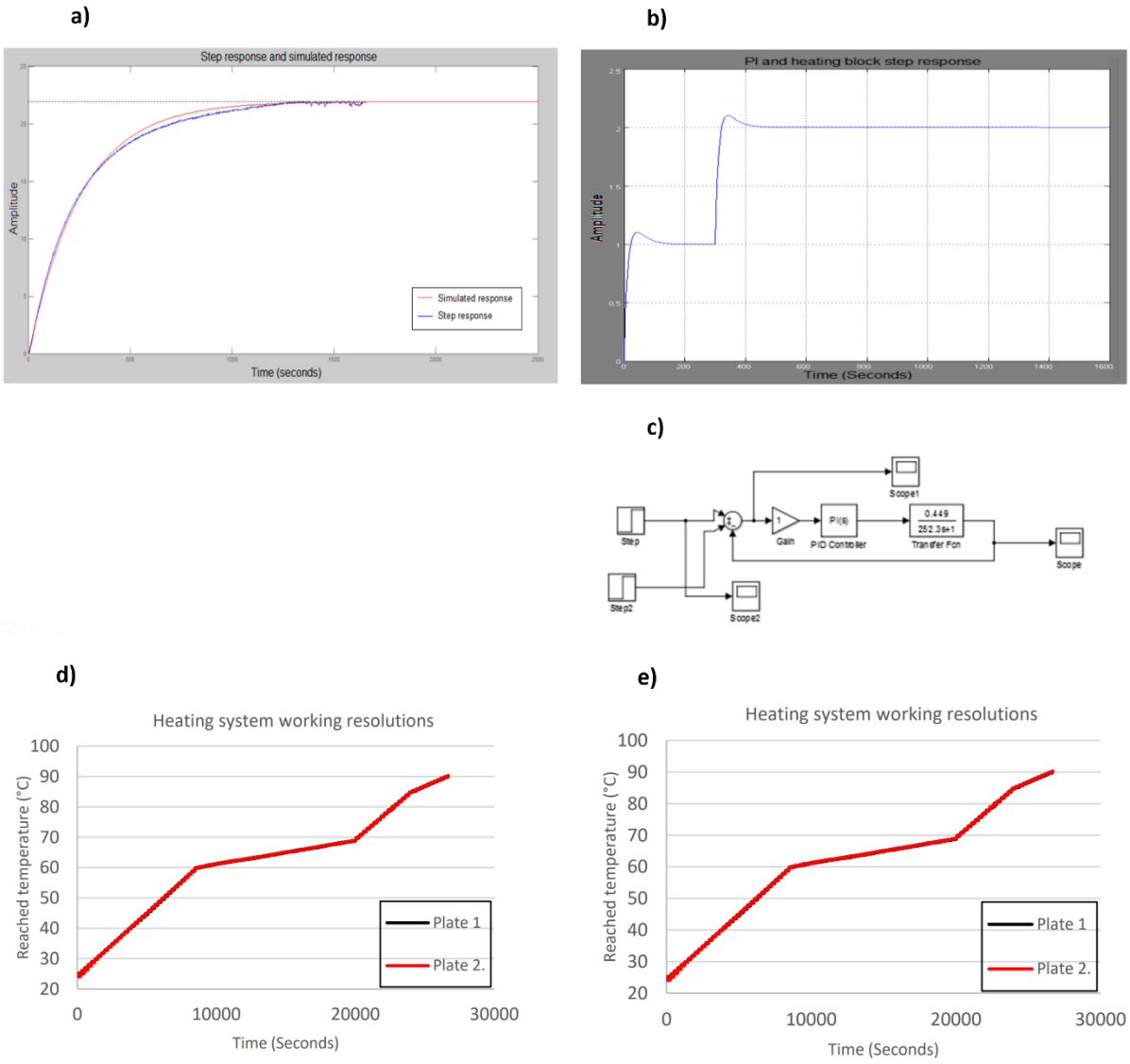

Figure. SI 3.1 (a) Step response and simulated transfer function of the heating plate 1 obtained with Matlab; (b) Modelled closed loop response of the PI controller in series with the heating block; (c) Modelled system of the PI controller in series with the transfer function plate that simulates the behaviour of the heating plate 1; (d) Example of the system's behaviour for a heating test starting at 25°C and finishing at 90°C. Both heating plates produced a stable output for 0.2, 0.5 and 1°C/step; (e) The heating ramp of the complete system with a glass slide – PMMA template in the middle of the heating plates.

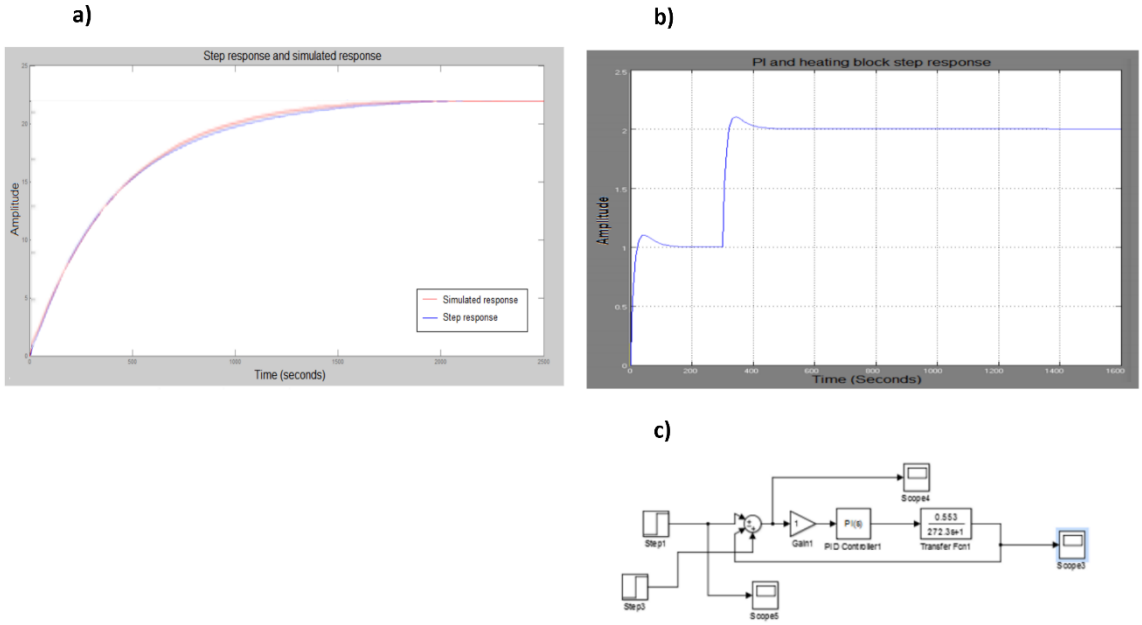

Figure. SI 3.2. (a) Step response and simulated transfer function of the heating plate 2 obtained with Matlab; (b) Modelled closed loop response of the PI controller in series with the heating block; (c) Modelled system of the PI controller in series with the transfer function plate that simulates the behaviour of the heating plate 2.

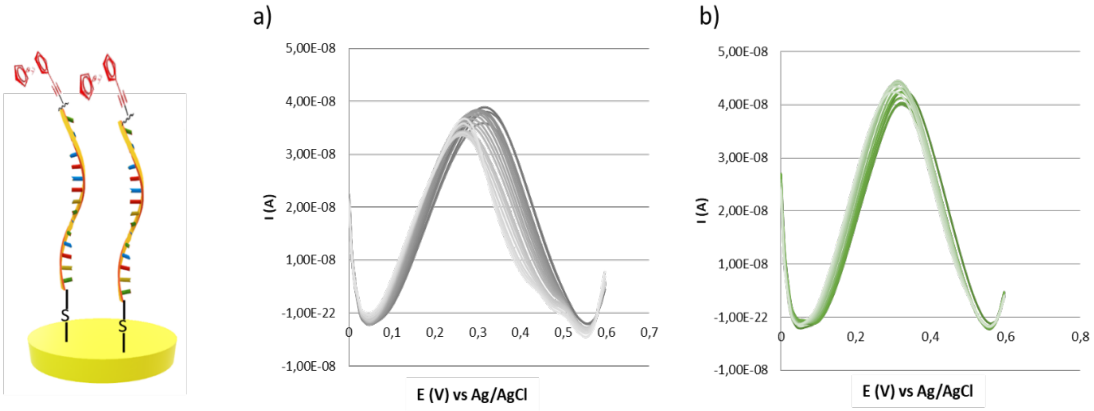

Figure. SI 3.3. (a) Repetitive SWVs of double functionalised Fc-DNA-SH on gold surface with temperature ramping; (b) Repetitive SWVs of double functionalised Fc-DNA-SH on gold surface during 1 h at 25ºC.

Chapter 4

Chapter 4

Semi-automated electrochemical melting curve analysis device for the detection of an osteoporosis associated single nucleotide polymorphisms in a fingerprick blood sample

Semi-automated electrochemical melting curve analysis device for the detection of an osteoporosis associated single nucleotide polymorphism in a fingerprick blood sample

Nassif Chahin[a], Miriam Jauset-Rubio[a], Mayreli Ortiz[a]*, Ciara K. O'Sullivan[a,b]*

[a] Department d'Enginyeria Química, Universitat Rovira i Virgili, Avinguda Països Catalans 26, 43007 Tarragona, Spain
[b]ICREA, Passeig Lluis Companys 23, 08010 Barcelona, Spain
mayreli.ortiz@urv.cat, ciara.osullivan@urv.cat, ckosulli@gmail.com

Abstract

The multiplexed detection of single nucleotide polymorphisms (SNPs) is of increasing importance in many areas including clinical diagnostics, patient stratification for pharmacogenomics and advanced forensic analysis. In the work reported, we describe a system for electrochemical melting curve analysis for the identification of the allele present at a specific SNP site associated with increased risk of bone fracture and predisposition to osteoporosis. Previously, we developed a semi-automated device for multiplexed electrochemical melting curve analysis, where a multielectrode array is coupled with microfluidics and housed between two aluminium plates of a Peltier device, with liquid introduction into the microfluidic channel controlled by a syringe pump. Individual electrodes of the array are functionalised with four different oligonucleotide probes, each probe equivalent in design with the exception of the base located in the centre of the probe. An optimised forward to primer ratio and amplification time in asymmetric isothermal recombinase polymerase amplification using ferrocene labelled forward primers was employed to generate single stranded redox labelled amplicons, which were allowed to hybridize to the different surface-tethered probes. The surface-tethered duplexes were subjected to electrochemical melting curve analysis and a clear difference between fully complementary and single mismatch was observed. Using the optimised conditions, the system was applied to the identification of the allele present at an osteoporosis associated Rs2741856 in a real fingerprick blood sample, and again a clear difference between fully complementary and single mismatch was observed, with the SNP present in the real sample corresponding to the wild type.

Keywords: Single nucleotide polymorphisms; Osteoporosis; Melting curve analysis; Isothermal recombinase polymerase amplification; Ferrocene labelled primer

4.1. Introduction

Single nucleotide polymorphisms (SNPs) are the most common type of genetic variation among people and occurs in at least 1% of the total population. [1] They can be defined by the presence of two alternative bases at a particular position in a DNA sequence and occur at about one per 100-300 bp in the human genome. [2] The identification of SNPs is of considerable importance for association studies of complex diseases, pharmacogenetics population genetics and advanced forensics and many genetic diseases are associated with specific SNPs including the inherited forms of cardiomyopathy, cystic fibrosis [3] , thalassemia [4] , sickle cell anaemia [5] , retinitis pigmentosa [6] and osteoporosis [7] .

A plethora of genotyping technologies for the identification of SNPs via allele-discrimination have been developed, including ligation, primer extension [8, 9] , allele-specific hybridization [10] or enzymatic cleavage [11] . However, these techniques are can be costly and complex, often requiring considerable infrastructure and instrumentation, experienced personnel, with considerable hands-on time due to the multiple steps involved in the analysis.

Hybridization approaches for the identification of SNPs exploit the differences in the thermal stability of double stranded DNA between perfectly matched and mismatched target-probe pairs to achieve allelic discrimination (Kim & Misra, 2007).[12] This methodology is referred to as melting curve analysis a PCR amplified duplex is placed in a cuvette and the melting temperature is determined by measuring the UV-Vis absorbance at 260nm as the temperature is ramped using a peltier. To improve the sensitivity of the technique, fluorescent intercalating dyes such as SBYR Green or Eva Green were employed and the decrease in fluorescence with increasing temperature was measured. High resolution melting curve analysis using highly controlled heating ramps and fluorescence detection facilitated single base mismatch differentiation. However, the technique is limited as it cannot achieve high levels of multiplexing due to limited availability of fluorescent intercalating with non-overlapping emission spectra.[13] Recently, a platform capable of multiplexed melting curve analysis was developed, where >1000 parallelised melts can be detected on a CMOS array. The platform, termed the Hydra 1K, uses cyanine labelled primers and asymmetric PCR to generate single stranded labelled amplicons, which are captured vis hybridization to probes immobilized on the CMOS array, which is then exposed to a controlled temperature ramp. The platform has been applied to the multiplexed fluorescence detection of 54 drug-resistance-associated mutations that are present in six genes of Mycobacterium tuberculosis.[14,15]

Electrochemistry is an attractive alternative to fluorescence due to its ease-of-use, high sensitivity, low cost, facile and cost-effective fabrication of electrode arrays and compatibility with multiplexed detection with multi-channel potentiostats. Indeed, different approaches of electrochemical melting

curve analysis have been reported, using a variety of labels such as methylene blue (MB), cobalt phenanthroline[16,17], cobalt bipyridine,[18,19] ruthenium bipyridine,[20] echinomycin[21,22] and epirubicin.[23]

Prest *et al.*, developed a method using methylene blue as an intercalating redox molecule, and measuring the change in the square wave voltammetry response to calculate the melting temperature.[24] Defever *et al*. reported a real-time PCR and melting curve analysis method based on the use of a osmium bipyridyl complex ($[Os(bpy)_2dppz]^{2+}$) intercalating redox molecule, again measuring the change in the square wave voltammetry response as the temperature was increased, and then generating the positive first-derivative analyses (*di/dT*) of the melt.[25] A microfluidic device integrating thermal control and a multi-electrode array was designed by Shento *et al.* who performed a rapid electrochemical melting curve analyses on small-volume samples of 10 µL. In this case an immobilized probe was hybridized to target labelled with methylene blue and the dissociation of the labelled target measured using square wave voltammetry.[26] In a similar approach, dsDNA denaturation between a ferrocene-labelled-PNA and a fully-complementary or single-base-mismatched DNA on the negatively charged electrode surface of indium tin oxide (ITO) was monitored electrochemically.[27]

Nasef *et al*, described a method based on labelless electrochemical melting curve analysis for the detection of the cystic fibrosis associated DF508 mutant, which a 3-base deletion mutation. A 21-base thiolated probe was immobilized on a gold electrode and hybridized to a ssDNA PCR amplicon of mutant target (85 bases) or wild type target of 82 bases. Methylene blue was used as an electrochemical indicator of hybridization, and differential pulse voltammograms were recorded during a discontinuous ramping of the temperature, and a clear discrimination between the melting temperature of the mutant and wild-type target was observed. Nasef *et al.* went on to report an alterntive approach, using ferrocene labelled target, and in this approach two different electrodes of an array were functionalised with probe complementary to the mutant and and probe complementary to the wild type, and both were hybridized with the ferrocene modified mutant sequence. The entire sensor array was subjected to discontinuous temperature ramping and the dissociation of the ferrocene labelled DNA from immobilized probes was monitored using DPV. The T_m recorded for the fully complementary and for the mismatched duplex was 38°C and 30°C, respectively which provided a clear discrimination between match and mismatch targets.[28]

Recently, we developed a semi-automated device capable of multiplexed electrochemical melting curve analysis (éMCA) for the detection of a single nucleotide polymorphism (As described in chapters 3, the melting temperature profiles were generated by following the decrease in the oxidation peak of the ferrocene labelled target when the surface anchored DNA was denatured by increasing temperature), using a SNP associated with cardiomyopathy as a model system. In the

previous work, we demonstrated the system using 21-mer immobilized probes with 21-mer oligos that were either fully complementary, or contained mismatches at the top, bottom or middle of the hybridized duplex. Having demonstrated that the device could be successfully employed for single mismatch discrimination using éMCA, asymmetric PCR combined with exonuclease digestion was employed to generate 124-mer single stranded DNA amplicons, which were also subjected to éMCA, and again single mismatch discrimination was achieved. Furthermore, in this previous work, we also demonstrated that in order to achieve a maximum differentiation in melting temperature between full complementarity and single mismatch, the SNP site to be interrogated for allele identification should be located in the middle of the hybridized duplex.

In the work reported herein, we wanted to extend on our previous work, to move closer towards a true point-of-care (POC) device that could be used to identify the allele present at a specific SNP site via multiplexed melting curve analysis. To meet the requirements of a POC device, PCR thermal cycling amplification was replaced with isothermal recombinant polymerase amplification, and the system was applied to the identification of the allele present at an osteoporosis associated Rs2741856 SNP in a real fingerprick blood sample.

Osteoporosis is known as a bone disease that affects around 200 million people globally. [29] It is characterised by low bone mass and microarchitecture deterioration, making the bones fragile and thus increasing the probability of fracture. [30, 31] It is more common in women than men, and bone loss is significantly increased following menopause due to lower levels of oestrogen. [32] Diagnosis of osteoporosis is typically achieved by measuring the bone density by dual-energy X-ray absorptiometry and monitoring bone density at periodic intervals over a 2-3 year timeframe. [33] Recently, specific protein biomarkers of bone turnover have been identified that can be used to replace absorptiometry, which can be measured using ELISA, representing a very cost-effective alternative, and currently disposable electrochemical biosensors are being developed to allow POC analysis of these biomarkers in fingerprick blood samples.[34,35] Recent reports have identified SNPs that are associated with an increased risk of bone fracture and can be used as markers of an increased risk of bone-fracture and as markers of a predisposition to osteoporosis (Trajanoska & Rivadeneira, 2019; Hidalgo *et al*., 2020). [36,37]

We thus applied our émCA to the identification of the allele present at the Rs2741856 SNP site using multiplexed melting curve analysis. In this approach, four different thiolated probes were immobilized on two individual electrodes of an array. Each of these probes were specifically designed to hybridize to a single stranded amplicon containing this SNP site, with the specific SNP site being designed to hybridize to the middle of the immobilized probe. At this specific site, each probe contained a different nucleotide (A, G, T, C). Single stranded 139-mer amplicons were either synthesised or isothermally

generated using asymmetric recombinase polymerase amplification with a ferrocene labelled forward primer and an unlabelled reverse primer and following hybridization, simultaneous multiplexed melting curve analysis of all 8 duplexes was carried out, with the temperature was ramped at 1 ^{o}C / step. The DPV voltammetric response of the ferrocene label was measured throughout the temperature ramp, and melting curves were generated and the melting temperatures were determined using first derivate analysis. The system was applied to the identification of the SNP in a real fingerprick blood sample and the result verified using sequencing analysis.

4.2. Materials

4.2.1 Reagents All chemicals and reagents were of analytical grade and used without further purification. All solutions were prepared in ultra-pure water (18 MΩ cm) obtained using a Simplicity Water Purification System. Synthetic oligonucleotides were purchased from Biomers (Ulm, Germany), KOD XL polymerase was purchased from Merck (Madrid, Spain), GelRed™ Nucleic Acid Gel Stain from Biotium (Barcelona, Spain) and the certified molecular biology agarose gel powder were obtained from Bio-Rad Laboratories S.A. (Barcelona, Spain). Three-millimetre thick polymethylmethacrylate (PMMA) was purchased from La Indústria de la Goma (Tarragona, Spain) and double-sided medical grade adhesive foil ARSeal 90880 from Adhesive Research (Ireland). RPA kits were purchased from TwistDx (www.twistdx.co.uk). Potassium dihydrogen phosphate (KH_2PO_4), sodium chloride (NaCl), potassium chloride (KCl), were purchased from Fluka. Sodium hydroxide, sulphuric acid (95–97%), Tris-HCl and boric acid were purchased from Scharlau, Barcelona, Spain and hydrochloric acid (35% v/ v) from Panreac. Phosphate-buffered saline (PBS), trisodium citrate, Aceton, where all purchased from sigma Aldrich, spain. The 10-(3,5-bis((6mercaptohexyl)oxy)phenyl)-3,6,9-trioxadecanol (DT_1) was purchased from SensoPath Technologies (Bozeman, MT). Oligo Clean & Concentrator Kit was purchased from Zymo Research, USA. A synthetic target of osteoporosis sequence with SNP Rs2741856 was designed to mimic the SNP site found in genomic DNA. This 139-mer was also generated using asymmetric recombinase polymerase amplification. The sequences were selected using specific oligonucleotide selection and design programs (http://bioinfo.ebc.ee/apex2/). Four probe sequences were designed in such a way to capture the SNP in the target at the middle. The sequences used (from 5`to 3`) are listed in Table 4.1.

Table. 4.1. Oligonucleotides used for the melting curve analysis: capture probes, 21-mer targets, 139-mer target and primers used to generate the ferrocene-targets by asymmetric-RPA (the regions of the target sequences complementary to the capture probes are underlined and also the fully complementary capture probe: Probe-C).

Oligonucleotide sequences:	
Rs2741856 Osteoporosis Target:	5′- CACACACACACCCCTCTTCACTATAATTATAATTACTATG**TTGGCTTCCAGA** **TCAGGGGTT**AGAGCCTTGGCATGGAGACGCCTGAAAGGCACCCAAGGCAA TTAGTGGTGTCCCTTCTCCACCCCCTACATACCTTCA - 3′
Forward primer	5′- Fc-CACACACACACCCCTCTTCACTATAAT- 3′
Reverse primer:	5′- GAAGGTATGTAGGGGGTGGAGAAG- 3′
Four sequence specific probes each one has a SNP at the middle	
(probe-A):	5’- AACCCCTGATATGGAAGCCAA-thioctic acid -3′
(probe-T):	5’- AACCCCTGATTTGGAAGCCAA-thioctic acid-3′
(probe-C):	5’- AACCCCTGATCTGGAAGCCAA-thioctic acid -3′
(probe-G):	5’- AACCCCTGATGTGGAAGCCAA-thioctic acid-3′

4.2.2 Homemade Peltier device

The Peltier device consists of an Arduino Uno board connected with two heating aluminum plates controlled by Arduino software for data visualization. The Peltier device provides a robust control and ramping of temperature in three different resolutions (0.2, 0.5, or 1^{o}C/step). The gold electrode array functionalised with DNA probes was placed between the heating plates and covered by a poly(methyl methacrylate) (PMMA) microfluidic cell that allows liquid buffer to wash the gold surface while heating as detailed previously (as described in Chapter 3). Arduino UNO, IRF520, the resistances, condensers, type K thermocouples, connectors, BI BPC10 resistors, AD595, breadboard, and the 2.5 W/mK thermally conductive tapes were all purchased from Farnell (Madrid, Spain). For the temperature reference system, a type K thermocouple connected to the precision thermometer Hi 93531 (Hanna instruments, Bilbao, Spain) was used. The variable DC power supply PeakTech 6006D (Telonic instruments LTD, Berkshire, UK) was used to supply the temperature reading system at 5.1 V

4.3. Methodology

4.3.1 Electrode fabrication

The electrode array was designed with a set of nine circular working electrodes (1 mm^2) and a rectangular counter electrode (4 mm^2). It was fabricated by sputtering on a 75x25 mm soda-lime glass slides substrate (Sigma-Aldrich, Spain) as described previously with minor modifications. Briefly, a positive photoresist AZ1505 (MicroChemicals GmbH, Germany) was deposited by spin coating at 4000 rpm for 30 s on a pre-cleaned and dried glass slide. The photoresist was then exposed to UV light for 4 s using a chromium mask in contact mode (LED Paffrath GmbH, Rose FotoMasken, Germany) and the transferred pattern was developed using the commercial developer AZ726. Following development, the glass slide was introduced into the sputtering chamber (ATC Orion 8-HV, AJA International Inc., USA) and was subjected to an oxygen plasma etching using AC O_2/Ar (5 $cm^3 \cdot s^{-1}$ of Ar, 5 $cm^3 \cdot s^{-1}$ of O_2, 50 W) for 5 minutes. A layer of 30 nm of Ti/TiO_2 was then sputtered (oxygen flow rate: 5 $cm^3 \cdot s^{-1}$ of O_2 for the first 10 nm, then increase up to 20 $cm^3 \cdot s^{-1}$ for the last 5 nm. Ar flow rate: constant 5 $cm^3 \cdot s^{-1}$). This was followed by the deposition of 100 nm of Au by AC sputtering (5 $cm^3 \cdot s^{-1}$ of Ar, 5 $cm^3 \cdot s^{-1}$ of O_2, 50 W). Lift-off was achieved using sonication in acetone for 5 minutes, then 5 minutes in isopropanol and finally rinsing with Milli-Q water.

4.3.2 Electrochemical cleaning of electrode array and probe immobilization

A classical reference electrode Ag/AgCl electrode was used , and an array of 9 working gold electrodes prepared as previously described. Working electrodes were cleaned by sequential sonication in isopropanol, acetone and water for 5 minutes each, followed by electrochemical cleaning by cycling 10 times, firstly in 0.5 M KOH between 0.0 and -1.2 V vs Ag/AgCl, and secondly in 0.5 M sulphuric acid between 0.0 and 1.6 V vs Ag/AgCl at a scan rate of 100 $mV.s^{-1}$. Washing steps in Milli-Q water were included in between both cleaning procedures and again at the end. After drying with nitrogen, the electrodes were immediately used for surface functionalisation. Thiolated capture probes (SNP-A-probe, SNP-T-probe, SNP-C-probe, SNP-G-probe) were self-assembled on each of the individual electrodes, by spotting 1 µL of 1 µM thiolated capture probe solution + DT_1 as backfiller with a 1:100 Probe:DT_1 molar ratio freshly prepared in 1 M KH_2PO_4. This functionalisation solution was left to assemble at room temperature (22 °C) for 3 h in humidity chamber to avoid evaporation, followed by a thorough wash with MilliQ water and dried with nitrogen.

4.3.3. Electrochemical Detection

Electrochemical measurements were carried out using an Autolab model potentiostat/galvanostat 12 controlled with GPES software. The working electrode array was housed iwithinthe microfluidics and placed between the heating aluminum plates of the homemade Peltier and the temperature increased at a rate of 1 °C/step. Differential pulse voltammetry (DPV) measurements were recorded after the sensor had been exposed to each temperature starting from 25 until 40°C. The parameters employed in the DPV experiments were: potential window between 0 and 0.6 V (vs. Ag/AgCl), step potential 10 mV, modulation amplitude 10 mV, modulation time 0.015 s and interval time 0.1 s. Every melting profile was carried out in duplicate, leaving the remaining 9th electrode modified with the back filler to evaluate the non-specific binding.

4.3.4 Asymmetric isothermal recombinase polymerase amplification and hybridization

Single stranded ferrocene labelled DNA amplicons containing the osteoporosis associated SNP-site were generated using asymmetric recombinase polymerase amplification, where the forward primer was labelled with ferrocene at the 5´- end and was used at a higher concentration than the reverse primer, used without any modification. The target was added at 0.8 nM to the RPA mixture and then, using a T100 thermal cycler (Biorad), the temperature was kept constant at 37 ºC and then increased to 95 °C for 15 min to stop the reaction by enzyme denaturation. An oligo Clean & Concentrator™ kit was used to purify the products from the reaction mixture and the amplification products were visualised using agarose gel electrophoresis.

Different Fc-Fw:Rev primer molar ratios were evaluated to find the optimum conditions for amplification and electrochemical detection, by maintaining the reverse primer concentration at 200 nM and increasing the Fc-forward primer concentrations, resulting in Fc-Fw:Rev Primer molar ratios of 2:1, 5:1, 10:1, 25:1, 50:1, using a 20 min reaction time. Once the primer concentration had been optimised, different amplification times (5, 10, 15, 20, 25 and 30 min) were tested using 1000 nM of forward primer and 200 nM of reverse primer and 0.8 nM target DNA. The optimum parameters were selected from the comparison of the band intensities of the products from positive reaction and from non-templated controls.

Additionally, the primer ratios and amplification time were also evaluated via hybridization of with electrode-immobilized probes and detection of the hybridized duplex using differential pulse voltammetry of the oxidation peak of ferrocene moiety. In these studies, thiolated probes fully complementary to the asymmetric RPA amplicon generated from a 139-mer synthetic DNA sequence mimicking the wild type were used to functionalise all the electrodes in an array. Hybridization was carried out by injecting 5 µL of asymmetric-RPA product (positive control) + 10

µL uL of 10 mM Tris buffer (pH 7.4 at 25 °C) containing 0.5 M NaCl into the 15 µL channel of the array containing the functionalised electrodes. Following 1 h incubation at 22ºC, the sensor was washed 3 times and the DPV signal measured. Non-template controls, where template DNA was replaced with nuclease free water was used as a negative control.

For gel electrophoresis analysis, a gel was made with ultralow pure agarose (3% w/v) in 1× Tris-Borate- EDTA buffer (TBE) and stained with GelRed™ nucleic acid stain. A mixture of 5 µL of asymmetric-RPA product with 4 µL of loading buffer 2x was loaded per gel well and the electrophoresis was performed at 100 V, 400 mAh for 40 min and gels were visualized in a UV transilluminator at λ = 254 nm. Finally, the amplified single stranded DNA samples were used immediately or stored at -20 °C until use.

4.3.5. Extraction of DNA from fingerprick blood sample and asymmetric-RPA amplification

A fingerprick blood sample was obtained by piercing the finger with a lancet and 5 µL was added to 19 µL of DNase free water + 1 µL of 5 mM EDTA, then heated at 95 °C for 30 seconds and finally left to cool to room temperature (ca. 22 ºC). The treated blood sample was added to 50 µL of asymmetric-RPA master mix to generate ssDNA-Fc osteoporosis target. Recombinase asymmetric PCR was carried out using the optimised conditions of 15 minutes at 37 °C using a master mix consisting of 25 µL containing 2X Reaction buffer, 10X Basic Mix buffer enhancer, 20X Core Reaction Mix buffer, 2 mM regular dNTPs, 1000 nM ferrocene labelled forward primer, and 200 nM reverse primer. Two microlitres of 10 nM DNA target (final concentration of 0.8 nM) was used. A non-template control (without target) was also produced to evaluate the approach. Following asymmetric-RPA, an Oligo Clean & Concentrator™ kit was used to purify the products and gel electrophoresis was then performed in 3 % w/v agarose gel Tris-Borate-EDTA buffer, to confirm the generation of single stranded DNA.

4.4. Results and Discussion

4.4.1 Optimisation of RPA parameters

The ratio of forward:reverse primers for asymmetric RPA was optimised for the amplification of the 139-mer target sequence, 250 µL of master mix containing 2 X Reaction buffer, 10 X Basic Mix buffer enhancer, 20 X Core Reaction Mix buffer, 2 mM dNTPs, different concentrations of ferrocene labelled forward primer and reverse primer shown in Table 4.2 below. This master mix was divided into 10 portions - 5 using 0.8 nM of a synthetic 139-mer target as a positive sample and 5 without target as non-template controls (NTC), and each using different ratios of forward:reverse primer.

Table 4.2. Ratio between forward and reverse primers used for optimization of the asymmetric-RPA

Primers (nM) used	**Samples**				
	1	**2**	**3**	**4**	**5**
Final concentration of Fc-forward Primer (**Fc-Fw-P**) (nM)	500	1000	2000	5000	10000
Final concentration of Reverse Primer (**Rev-P**) (nM)	200	200	200	200	200
(**Fc-Fw-P**: **Rev-P**) **Ratio**	2.5	5	10	25	50

After amplification at 37°C, the samples were heated at 95°C for 10 min for enzyme denaturation and finally kept at 4°C until use. An Oligo Clean & Concentrator™ kit was used to purify the products and gel electrophoresis was then performed using 3 % w/v agarose gel in Tris-Borate-EDTA buffer (pH 8), to confirm the generation of single stranded DNA. This enzyme denaturation step and purification was required to avoid smearing on the gel and to allow a correct visualization of sharp bands.

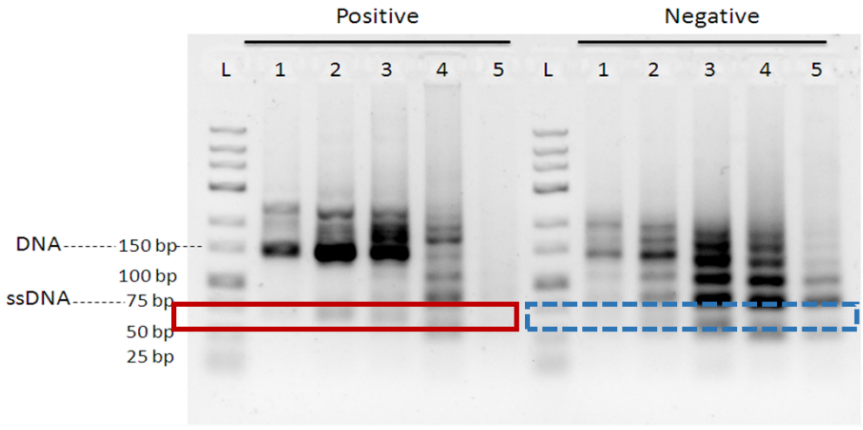

Figure 4.1. 3 % w/v agarose gel after electrophoresis of asymmetric-RPA products obtained using different primer concentrations, Ratio of Fc-Fw-P:Rev-P in nM is 1=500:200, 2=1000:200, 3=2000:200, 4=5000:200, 5=1000:200. Right: negative samples with no target. L= ladder

As can be seen in Figure 4.1, the optimum ratio to obtain a maximum amount of ferrocene labelled DNA was 1000nM Fc-forward primer: 200 nm Reverse primer. It should be noted that we also tested the use of phosphate labelled reverse primers and lambda exonuclease digestion following asymmetric RPA, but no further improvement in band intensity was obtained (data nit shown) and thus for further experiments this exonuclease digestion step was omitted and a 5:1 ratio of forward to reverse primer employed.

These results were also confirmed electrochemically. Two electrode arrays were prepared by functionalising all 18 electrodes with the thiolated capture probe containing C at the SNP site, which is full complementary to the ferrocene labelled target amplicon generated by asymmetric-RPA using the synthetic 139-mer as target. Positive and negative controls generated from asymmetric-RPA amplified for 15 minutes at 37 °C, using different Fw-Fc/Rev primer concentration ratios of 500:200, 1000:200, 2000:200, 5000:200, 1000:200nM, respectively were added to the array and allowed to hybridize for 1 hour at room temperature (ca. 22 °C). The level of labelled ssDNA generated was evaluated via the DPV signal obtained following hybridization with the immobilized probes. As can be seen in Figure 4.2, the optimum ratio of 5:1 Fc-labelled forward primer: reverse primer is confirmed to be the correct ration, with a considerably higher signal obtained following hybridization with amplicons generated using this primer ratio.

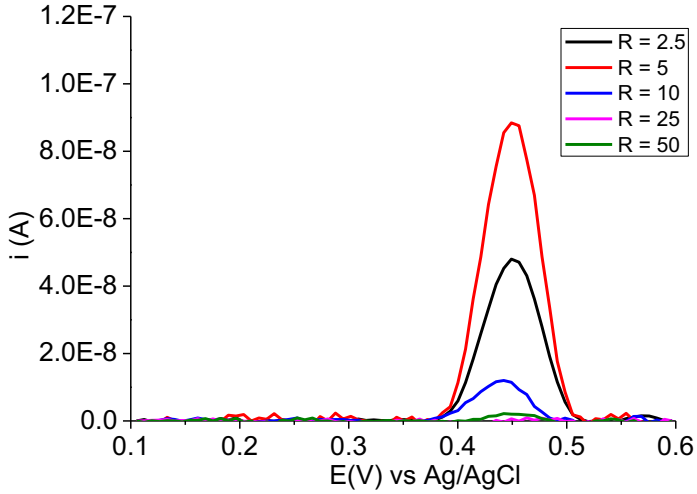

Figure 4.2. DPV responses after hybridization of positive samples with target labelled ferrocene of asymmetric-RPA using different molar ratios of Fw-Fc:Rev primers, R of 2.5=500:200nM, R of 5 =1000:200nM, R of 10 =2000:200nM, R of 25 =5000:200nM, R of 50 =1000:200nM.

The optimum amplification time was then studied, and in this case for amplification of the 139-mer synthetic target sequence, two master mixes of 150 µL each containing 2 X Reaction buffer, 10 X Basic Mix buffer enhancer, 20 X Core Reaction Mix buffer, 2 mM regular dNTPs, 1000 nM ferrocene labelled forward primer and 200 nM reverse primer were used. Each master mix was divided into 12 portions - 6 with 0.8 nM 139-mer target DNA as positive samples and 6 without target as negative samples, and each positive and negative sample was amplified 5, 10, 15, 20, 25 and 30 min, at 37°C. Again, to avoid smearing on the gel and a clear visualization of the bands, the amplicons were heated to 95°C for 10 min and an Oligo Clean & Concentrator™ kit was used to purify the products. Gel electrophoresis was then performed in 3 % w/v agarose gel in Tris-Borate-EDTA buffer (pH 8). As can be seen in Figure 4.3, 15 minutes amplification time was adequate and no increased band intensity was observed with longer amplification times.

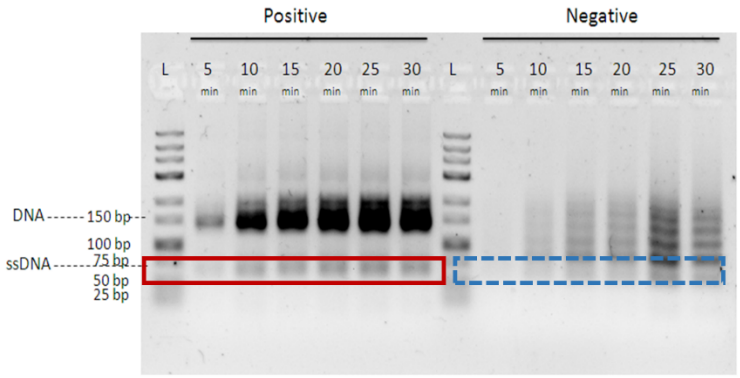

Figure 4.3. 3 % w/v agarose gel after electrophoresis of asymmetric-RPA products obtained using different amplification times (5, 10, 15, 20, 25 and 30 min), Left: Positive samples with target. Right: negative samples with no target.

As with the optimization of the primer ratio, the results were also confirmed electrochemically. Again, two electrode arrays were prepared by functionalising all 18 electrodes with the thiolated capture probe containing C at the SNP site and hybridized for 1 h at room temperature (ca. 22 ^{o}C) with positive and negative controls generated from asymmetric-RPA using the 5:1 forward:reverse primer ratio and amplified for 5, 10, 15, 20, 25 or 30 minutes at 37 °C. Figure 4.4 shows the intensity of the DPV signals following hybridization of the asymmetric-RPA amplicons using these diverse amplification times. In agreement to with the bands observed using gel electrophoresis, the signals obtained with both positive and negative controls increased with amplification time. The highest DPV signal obtained following hybridization was obtained with the amplicon generated following 15 minutes of isothermal amplification, with longer amplification times resulting in false positives (inset), which may be attributable to non-specific amplification.

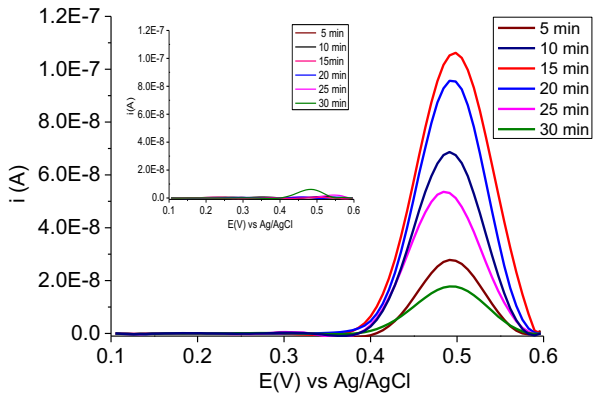

Figure 4.4. DPV responses after hybridization of positive and negative controls generated using asymmetric-RPA with a 5:1 forward to reverse primer ratio using different amplification times (5, 10, 15,

20, 25 and 30 min). Amplification with non-template control (NTC, DNA template replaced by nuclease free water) displayed in the inset.

Using these optimised conditions, the device was then applied to the identification of a specific SNP associated with osteoporosis, using a single stranded DNA product generated using asymmetric RPA using the 139-mer synthetic DNA template and then with DNA amplified directly from a fingerprick blood sample. Building on the work carried out previously (unpublished work, as described in Chapter 3), where the optimum position on the immobilized probe for hybridization to the SNP site under interrogation was demonstrated to be in the middle, four probes were designed with each containing a different base (A, G, T or C) at this position, which are defined as Probe A, Probe G, Probe T and Probe C, respectively, with Probe C being fully complementary to the wild type found in the majority of the population. Electrode arrays were functionalised with each of these probes (in duplicate) with the ninth electrode of the array serving as a control electrode to evaluate any non-specific binding events. These functionalised electrode arrays were housed within microfluidics and then placed between the two aluminium blocks of the in-house Peltier heating device. The RPA amplicons were injected into the microfluidics and hybridization with the immobilized probes allowed to take place for 1 hour at room temperature (ca. 22 ^{o}C). Following hybridization, the microfluidics were connected via tubing to a container with wash buffer, and this washing buffer was propulsed through the microfluidics via syringe pump actuation. Following hybridization and thorough washing, the baseline DPV for each of the electrodes was measured. It should be noted that whilst SWV was used in our previous work (Chapter 3) in order to reduce analysis time, in this work DPV was employed in order to increase sensitivity. The electrode array was then subjected to multiplexed melting curve analysis using the previously optimised (Chapter 3) temperature ramp of 1 ^{o}C / step for all 9 electrodes, with washing buffer flowed over the electrode array to continuously remove the denatured and liberated Fc-labelled DNA, with the DPV signal was measured throughout the melt.

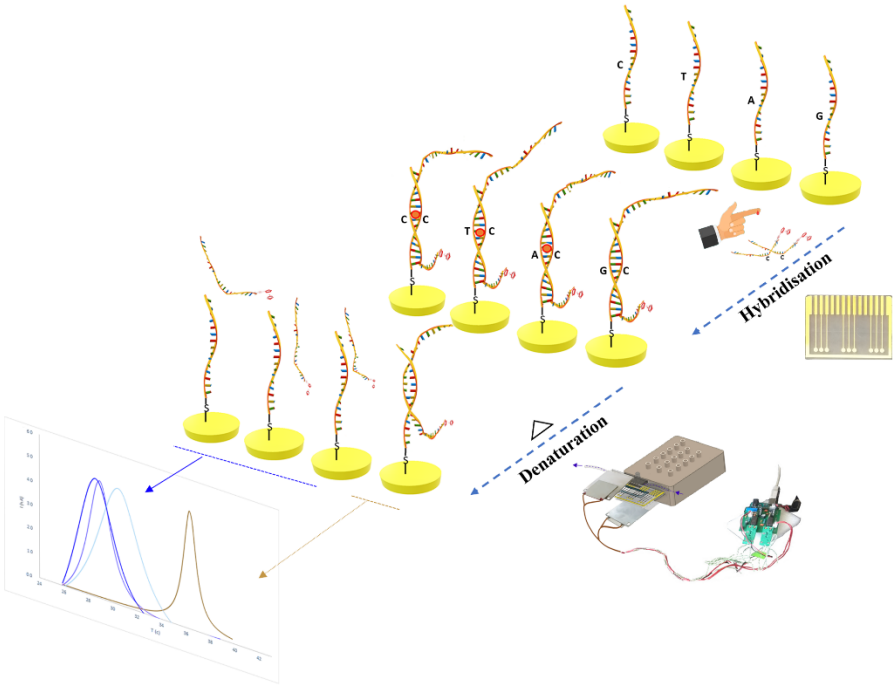

Figure 4.5. Schematic representation of the proposed approach for electrochemical melting-curve analysis, hybridization, denaturation and measurement of the DPV responses with the 4 different probes, three with different bases at the SNP site positioned at the middle (different shades of blue melting curve first derivatives) and one fully complementary to the target (brown melting curve first derivative).

The gel electrophoresis visualising the ferrocene labelled single stranded DNA generated using asymmetric RPA can be seen in Figure 4.6a where the band for ths ssDNA can be clearly observed. The melting curves obtained using the four different probes with the same RPA generated amplicon and their first derivative curves are shown in Figure 4.6b, and the melting temperatures calculated for the capture probe Probe-C, which was fully complementary to the target carrying SNP G, was 33.8 °C, whilst considerably lower melting temperatures of 31.9 °C, 28.5°C and 27.6 °C were obtained for each of Probe-A, Probe-T and Probe-G, respectively. This multiplexed melting curve analysis approach could thus clearly identify the allele present at the SNP site, and quite interestingly exposed different melting temperatures for each of the Capture probes G, T and A, despite the different bases in the probe being located at the same position.

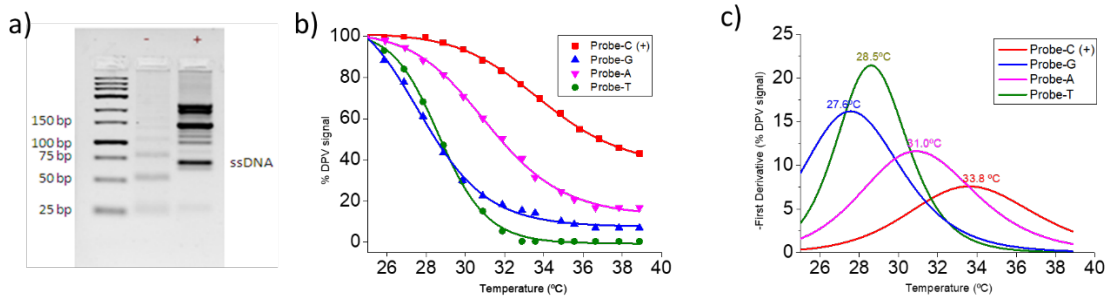

Figure 4.6. (a) Gel electrophoresis image of Fc-ssDNA generated using asymmetric-RPA; (b) éMCA profiles generated recording DPV signals of ferrocene label at each with ramping (1°C /step) and c) The corresponding first derivatives.

Having demonstrated the proof-of-concept of using multiplexed melting curve analysis using diverse probes on individual electrodes to identify the allele found at a specific SNP site, the device was then applied to real sample analysis using a fingerprick blood sample. Five microlitres of blood procured via lancet piercing of the index finger was diluted in 19 µL of DNase free water + 1 µL of 5 mM EDTA, then heated at 95 °C for 30 seconds and finally left to cool to room temperature (ca. 22 ºC). The heat-treated blood sample was added to 50 µL of asymmetric-RPA master mix to generate ssDNA-Fc labelled target, which was then added to the functionalised electrode array and multiplexed melting curve analysis carried out as described above. In this case, a similar trend was observed with the fully complementary duplex with the probe containing the C base in the middle having a melting temperature of 36.1 ºC, whilst the probe containing the A base had a melting temperature of 30.6 ºC and the C and T containing probes having very similar melting temperatures of 28.9 and 28.5 ºC, respectively.

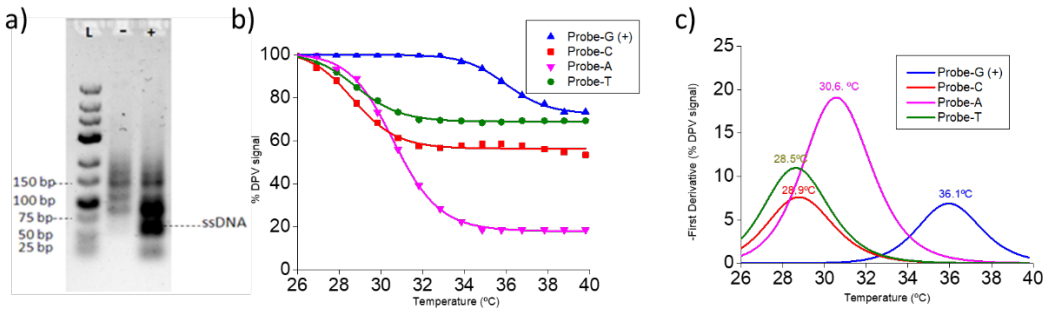

Figure 4.7. (a) Gel electrophoresis image after Fc-ssDNA generation from real sample using asymmetric-RPA; (b) éMCA profiles by recording DPV with T ramping (1°C /step); (c) Corresponding first derivatives

4.5. Conclusions

In the described experiments, we have demonstrated the proof of concept of our platform to detect SNPs based on éMCA method. We exploited a combination of ferrocene labelled forward primer with a reverse primer in asymmetric RPA, to produce a single strand labelled amplicon for hybridization to a surface tethered DNA probes. The amplification times and primers concentrations for the ssDNA Target associated osteoporosis Rs2741856 were optimised to be 15 minutes and (1:5 ratio, Rev: Fw primers), respectively. The results confirmed perfectly capable of distinguishing between the full complementary and the single mismatched ones, identifying the SNP exists in synthetic target and even more in the real fingerpick sample. The future work represented in developing our setup assay to accept more samples (up to 64) in one single test to enhance the multiplex SNPs detection especially the targets of Tb related drug resistance mutations.

Acknowledgement This project has received partial funding from the European Union's Horizon 2020 research and innovation program under grant agreement No 767325. We want to thank Phil Biggs from Labman Autimation (uk) for the fabrication of the connection box.

References

1. Winkelstein J. A., Colten H. R., Scriver C. R., Beaudet A. L., Sly W. S., and Valle D. (1989). Genetically determined disorders of the complement system. Clin. Immun, 6, 2711–2737.

2. Pryor R. J., and Wittwer C. T. (2006). Real-time polymerase chain reaction and melting curve analysis. Methods Mol. Biol, 336, 19–32.
3. Lay M. J., and Wittwer C. T. (1997). Real-time fluorescence genotyping of factor V Leiden during rapid-cycle PCR. Clin. Chem, 43,12, 2262–2267
4. Bernard P. S., Ajioka R. S., Kushner J. P., and Wittwer C. T. (1998). Homogeneous multiplex genotyping of hemochromatosis mutations with fluorescent hybridization probes. Am. J. Pathol., 153, 4, 1055–1061.
5. Crockett A. O. and Wittwer C. T. (2000). Fluorescein-labeled oligonucleotides for real-time pcr: using the inherent quenching of deoxyguanosine nucleotides. Anal. Biochem, 290,1, 89–97.
6. Zhou L., Myers A. N., Vandersteen J. G., Wang L., and Wittwer C. T. (2004). Closed-Tube Genotyping with Unlabeled Oligonucleotide Probes and a Saturating DNA Dye. Clin. Chem, 50,8, 1328–1335.
7. Huang Q. Y. and A. Kung W. C. (2006). Genetics of osteoporosis. Mol. Genet. Metab, 88,4, 295–306.
8. Wittwer CT., Kusukawa N. (2004). Real-Time PCR, in Molecular Microbiology. ASM Press; Washington DC, 71–84
9. Lyon E. and Wittwer C. T. (2009). LightCycler technology in molecular diagnostics. J. Mol. Diagnostics, 11, 2, 93–101.
10. Ririe K. M., Rasmussen R. P., and Wittwer C. T. (1997). Product Differentiation by Analysis of DNA Melting Curves during the Polymerase Chain Reaction. Anal. Biochem, 245, 2, 154–160.
11. Livak K. J., Flood S. J. A., Marmaro J., Giusti W., and Deetz K. (1995). Oligonucleotides with fluorescent dyes at opposite ends provide a quenched probe system useful for detecting PCR product and nucleic acid hybridization. Genome Res, 4, 6, 357–362.
12. Sobin Kim S., Misra A. (2007). SNP genotyping: technologies and biomedical applications. Annu. Rev. Biomed. Eng, 9, 289-320.
13. Reed G .H., Kent J.O., Wittwer CT. (2007). High-resolution DNA melting analysis for simple and efficient molecular diagnostics. Pharmacogenomics, 8(6), 597–608.
14. Hassibi A., Manickam A., Singh R., Bolouki S., Sinha R., Jirage K. B., Schoolnik G. (2018). Multiplexed identification, quantification and genotyping of infectious agents using a semiconductor biochip. Nature Biotechnology, 36 (8), 738-745.

15. Clutter D. S., Mazarei G., Sinha R., Manasa J., Nouhin J., LaPrade E., Shafer R. W. (2019). Multiplex Solid-Phase Melt Curve Analysis for the Point-of-Care Detection of HIV-1 Drug Resistance. The Journal of Molecular Diagnostics, 21 (4), 580-592.
16. Erdem A., Kerman K., Meric B., Akarca U. S. and Ozsoz M. (1999). Electrochemical biosensor for the detection of short DNA sequences related to the hepatitis B virus. Electroanalysis, 11, 586–7.
17. Erdem A., Meric B., Kerman K., Dalbasti T. and Ozsoz M. (1999). Detection of interaction between metal complex indicator and DNA by using electrochemical biosensor. Electroanalysis, 11, 1372–6.
18. Millan K. M., Saraullo S. and Mikkelsen S. R. (1994). Voltammetric DNA biosensor for cyctic fibrosis based on a modified carbon paste electrode Anal. Chem, 66, 2943–8.
19. Millan K. M., Mikkelsen S. R. (1993). Sequence-selective biosensor for DNA based on electroactive hybridization indicators. Anal. Chem, 65, 2317–23.
20. Napier M. E., Loomis C. R., Sistare M. F., Kim J., Eckhardt A. E. and Thorp H. H. (1997). Probing biomolecule recognition with electron transfer: electrochemical sensors for DNA hybridization. Chem, 8, 906–13.
21. Hason S., Dvorak J., Jelen F. and Vetterl V. (2002). Electrochemical impedance spectroscopy of polynucleotide adsorption. Talanta, 56, 905–13.
22. Jelen F., Erdem A. and Palecek E. (2002). Cyclic voltammetry of echinomycin and its interaction with double-stranded and single-stranded DNA adsorbed at the electrode. Bioelectrochemistry. Bioelectrochemistry, 55, 165–7.
23. Erdem A. and Ozsoz M. (2002). Interaction of the anticancer drug epirubicin with DANN. Anal. Chim. Acta, 437, 107–14.
24. Meunier-Prest R. (2003). Direct measurement of the melting temperature of supported DNA by electrochemical method. Nucleic Acids Research, 31 (23), 150e–150.
25. Deféver T., Druet M., Evrard D., Marchal D. and Limoges B. (2011). Real-time electrochemical PCR with a DNA intercalating redox probe. Anal Chem, 83 (5), 1815–1821.
26. Shen Z., Sintim H. O., Semancik S. (2015). Rapid nucleic acid melting analyses using a microfabricated electrochemical platform. Anal Chim Acta, 853 (1), 265–270.
27. Luo X., Hsing I. M. (2009). Real time electrochemical monitoring of DNA/PNA dissociation by melting curve analysis. Electroanalysis. Electroanalysis, 21(14), 1557–1561.
28. Nasef H., Beni V., O'Sullivan C.K. (2010). Electrochemical melting-curve analysis. Electrochem commun. Electrochem Commun, 12 (8), 1030–1033.

29. Khashayar P., Aghaei Meybodi H. R., Homami M. R., Heshmat R., & Larijani B. (2010). The Prevalence of Osteoporosis in an Iranian Population. Journal of Clinical Densitometry, 13(1), 112.
30. Kanis J. A., & Kanis J. A. (1994). Assessment of fracture risk and its application to screening for postmenopausal osteoporosis: Synopsis of a WHO report. Osteoporosis International, 4(6), 368–381.
31. Lee S. W., Jo H. H., Kim M. R., Kim J. H., & You Y. O. (2015). Association between osteocalcin and metabolic syndrome in postmenopausal women. Archives of Gynecology and Obstetrics, 292(3), 673–681.
32. Odén A., McCloskey EV., Kanis JA., Harvey NC., Johansson H. (2015). Burden of high fracture probability worldwide: secular in- creases 2010-2040. Osteoporos Int 26, 2243–2248
33. Liu L., & Webster T. J. (2016). In Situ Sensor Advancements for Osteoporosis Prevention, Diagnosis, and Treatment. Current Osteoporosis Reports, 14(6), 386–395.
34. Parmar B. J., Longsine W., Sabonghy E. P., Han A., Tasciotti E., Weiner B. K., Righetti R. (2010). Characterization of controlled bone defects using 2D and 3D ultrasound imaging techniques. Physics in Medicine and Biology, 55(16), 4839–4859.
35. Universiteit Gent. (2017). PoC in-office device for identifying individuals at high risk of osteoporosis and osteoporotic fracture, Retrieved from https://cordis.europa.eu/project/id/767325.
36. Koromani F., Trajanoska K., Rivadeneira F., & Oei L. (2019). Recent Advances in the Genetics of Fractures in Osteoporosis. Frontiers in Endocrinology, 10, 337.
37. Hidalgo A., Hernández C., Sevilla R., Rivera B., Ramirez E. G., Flores J., Velázquez R. (2020). Single-nucleotide polymorphism rs10036727 in the SLIT3 gene is associated with osteoporosis at the femoral neck in older Mexican postmenopausal women. Gynecological Endocrinology, 36, 12, 1096-1100.

Chapter 5

Semi-automated electrochemical melting curve analysis platform for multiplexed detection of SNPs

Semi-automated electrochemical melting curve analysis platform for multiplexed detection of SNPs

Nassif Chahin[a,1], Mayreli Ortiz[a,*], Philip Biggs, Matthew Hall, Ciara K. O'Sullivan[a,c,*]

a Interfibio Research Group, Department of Chemical Engineering, Universitat Rovira i Virgili, Avinguda Països Catalans 26, 43007 Tarragona
b Labman Automation
c ICREA, Passeig Lluís Companys 23, 08010 Barcelona, Spain

Abstract

In previous work we reported the development and use of an in-house set-up for the semi-automated detection and identification of the allele present at an individual single nucleotide polymorphism site in a fingerprick blood sample, using multiplexed electrochemical melting curve analysis. In the work reported here, we extend on the previous work using a more advanced and more automated system for performing the melting curve analysis and apply it the multiplexed detection of SNPs, using two SNPs associated with osteoporosis as a model system. This final part of my work is a step towards achieving true multiplexed

5.1. Introduction

The human genome project, completed in 2003, not only identified the number and role of the >30,000 genes found in the human genome, but also revealed the existence of single nucleotide polymorphisms.[1] A single nucleotide polymorphism (SNP) is a single allele variation that occurs at a frequency of 1 in 100 to 300 bases throughout the genome.[2.] Following the human genome project and pushing the advances in next generation sequencing, several projects including the HapMap, 1000 genome and 10,0000 genome projects, the occurrence of SNPs in both the coding and non-coding parts of the genome was established. [3] SNPs have the potential for an improved understanding of personalized disease pathogenesis, advanced forensics, as well as for patient stratification in pharmacogenomics.[4] Some examples include the rs2596538 SNP found in the MICA promoter region, which is associated with an increase in the risk of liver cancer due to the hepatitis C virus,[5] as well as the rs2279744 SNP found in the promoter region of MDM2, which increases

transcriptional activity raising tumorigenesis by overexpression MDM2 mediated by cyclin D1.[6] There is a global trend in an increasing resistance to antibiotics, such as the resistance to the first-line medication for tuberculosis (TB) treatment, and the existence of SNPs in different genes including the rpoB, aphC, inhA, katG, gyrA and gyrB genes, have been identified to be associated with rifampicin and isoniazid resistance,[7,8] and SNPs have alse been identified to be linked to HIV-1 drug resistance. [9] Furthermore, and with specific relevance to the work reported here, many SNPs have been linked to an increased risk of bone fragility and bone structure, that often leads to osteoporosis, including the PLS3, SNP7 and LRP5 SNPs. [10,11,12] The development of rapid, cost-effective and reliable diagnostic tools as part of companion tests in the emerging paradigm of personalized medicine is thus of increasing importance.[13,14]

Hassibi et al., (2018) described multiplex mutation detection using a HYDRA-1K biosensor array, which is composed of a CMOS-integrated sensor of 32x32 pixels, each integrated with thermo-cycler and photo-sensor, with each sensor of an array functionalized with individual probes, with each probe designed to detect different SNPs. Using the developed platform, 54 SNPs associated with antibiotic resistance in *Mycobacterium tuberculosis* were detected, where the melting profiles for the fluorophore-labelled surface-tethered probes hybridized to wild or quencher-labelled targets containing single-mismatches, showed a clear differentiation between the WT and all SNPs. [7] Using the same generic platform, SNPS associated with drug-resistance were detected in the HIV-1 rt gene. Melting curve analysis was performed in just 20 minutes, ramping the temperature from 45 to 90 ºC and taking images every 10 s to plot the melting curves from fluorescent signal intensity versus the temperature for each probe. The calculated melting temperatures confirmed the distinction between each of the six codons at the HIV-1 DRM (drug-resistance mutation) reverse transcriptase position 103 in both synthetic and plasma samples.[15]

We previously reported a simple, cost-effective and semi-automated platform capable of carrying out meultiplexed solid-phase melting curve analysis, that detected a SNP associated with cardiomyopathy as a proof-of-concept and was then applied to detection of the osteoporosis associated SNP Rs2741856 [16] in a fingerprick blood sample. These assays were carried out using a simple and relatively crude in-house Peltier device that was used to house an electrode array integrated with microfluidics, which was then exposed to a controlled ramping of temperature and the melting temperatures of targets that were fully complementary or containing a single mismatch were determined.

In this study, we extended our previous work and developed a more automated prototype system for the simultaneous detection of multiple SNPs, using solid-phase electrochemical melting curve analysis. The developed strategy is based on generating the melting profiles of multiple nucleic acid

targets conjugated with redox labels and hybridized with capture probes surface-tethered on a 64-eñectrode array, which is exposed to a continuous temperature ramp with concomitant recording of the differential pulse voltametric signal. This prototype is a compact device that is composed of a heating system accompanied by a washing module run by a small pump, and the overall device is controlled by a single Arduino Uno board. Moreover, a new program with an easy GUI windows interface was developed to connect this new device with the GPES software on the Autolab potentiostat, and used to control both devices in parallel facilitating an almost fully automated solid-phase éMCA process. To demonstrate the performance of this platform for the multiplexed detection of SNPs, two SNPs (Rs2741856 and rs1107946[17]) recently identified to be associated with an increased risk of bone fracture and development of osteoporosis were detected.

5.2. Materials

5.2.1 Reagents

All chemicals and reagents were of analytical grade and used without further purification. All solutions were prepared in ultra-pure water (18 MΩ cm) obtained using a Simplicity Water Purification System. Synthetic oligonucleotides were purchased from Biomers (Ulm, Germany), GelRed™ Nucleic Acid Gel Stain from Biotium (Barcelona, Spain) and the certified molecular biology agarose gel powder from Bio-Rad Laboratories S.A. (Barcelona, Spain). Potassium dihydrogen phosphate (KH_2PO_4), sodium chloride (NaCl), potassium chloride (KCl), were purchased from Fluka. Tris-HCl and boric acid were purchased from Scharlau, Barcelona, Spain. phosphate-buffered saline (PBS) was purchased from Sigma Aldrich, Spain. The 10-(3,5-bis((6mercaptohexyl)oxy)phenyl)$^{-3}$,6,9-trioxadecanol (DT_1) was purchased from SensoPath Technologies (Bozeman, MT). Double-sided medical-grade adhesive foil ARSeal 95880 was acquired from Adhesive Research (Ireland).
The RPA TwistAmp® Liquid Basic kit was purchased from TwistDx (www.twistdx.co.uk). DNA Clean & Concentrator and Oligo Clean & Concentrator Kits were purchased from Zymo Research, USA. A model target of osteoporosis sequence with SNP Rs2741856 and Rs1107946 was designed to mimic the SNP site found in genomic DNA, and in our model system we have the SNP sites located in a 139-mer amplicon and 130-mer amplicon respectively that are amplified individually in different amplification tubes. The sequences were selected using specific oligonucleotide selection and design programs (http://bioinfo.ebc.ee/apex2/). Four thiolated capture probes were designed per target, positioning the SNP site at the middle of the capture probe. The sequences used (from 5`to 3`) are listed in Table 5.1.

Table. 5.1. Oligonucleotides used for the melting curve analysis: capture probes, 21-mer, 139-mer target-SNP-27 and 130-mer target-SNP-11 and the primers used to generate the ferrocene-labelled targets using asymmetric-RPA (the regions of the target sequences complementary to the capture probes are underlined and also the fully complementary capture probe: Probe-C for target-SNP27 and Probe-A for target-SNP-11).

Oligonucleotide sequences:	
Rs2741856 Osteoporosis Target: (SNP 27)	5'- CACACACACACCCCTCTTCACTATAATTATAATTACTATG**TTGGCTTCC AGATCAGGGGTT**AGAGCCTTGGCATGGAGACGCCTGAAAGGCACCC AAGGCAATTAGTGGTGTCCCTTCTCCACCCCCTACATACCTTCA - 3'
Forward primer:	5'- Fc-CACACACACACCCCTCTTCACTATAAT- 3'
Reverse primer:	5'- GAAGGTATGTAGGGGGTGGAGAAG- 3'
Four sequence specific probes each one has the SNP position allocated at the middle of the sequence	
Probe-A	5'- AACCCCTGAT**A**TGGAAGCCAA-thioctic acid -3'
Probe-T	5'- AACCCCTGAT**T**TGGAAGCCAA-thioctic acid-3'
Probe-C fully complementary	5'- AACCCCTGAT**C**TGGAAGCCAA-thioctic acid -3'
Probe-G	5'- AACCCCTGAT**G**TGGAAGCCAA-thioctic acid-3'
Oligonucleotide sequences:	
Rs1107946 Osteoporosis Target: (SNP 11)	5'-agc ttt tcc tgt att gac tcc tta gat cat caa aca acc tat gag gta aat att att tgt ata tat tgc aga tag gga aat tga aga gca cag aga agt tgc ata ata tac ttg aga cca tat aac tgg t-3'
Forward primer:	5'- Fc-agc ttt tcc tgt att gac tc- 3'
Reverse primer:	5'- acc agt tat atg gtc tca ag- 3'
Four sequence specific probes each one has the SNP position allocated at the middle of the sequence	
Probe-A fully complementary	5'-tac aaa taa tat tta cct cat-thioctic acid -3'
Probe-T	5'-tac aaa taa ttt tta cct cat-thioctic acid -3'
Probe-C	5'-tac aaa taa tct tta cct ca-thioctic acid t -3'
Probe-G	5'-tac aaa taa tgt tta cct cat-thioctic acid -3'

5.2.2. Electronic components

Arduino UNO, IRF520, the resistances, condensers, type K thermocouples, connectors, BI BPC10 resistors, AD595, breadboard and the 2.5 W/mK thermally conductive tapes were all purchased from Farnell (Madrid, Spain), while 5v DC small pump Code:702-6894 washing was purchased from RS PRO. The variable DC power supply PeakTech 6006D (Telonic instruments LTD, Berkshire, UK) was used to supply the temperature reading system at 5.1 V. A new software programmed using Microsoft visual studio with a GUI interface that controls the whole éMCA process besides the GPS software for a fully automated process (Figure SI-5.3, SI-5.4 more details). Two aluminum blocks were manufactured at Labman, the top block has modified with two holes sealed with a small aluminum top stuck to a piece of Perspex. Thermocouples type K, the temperature sensing elements and heaters were purchased from Farnell (Madrid, Spain), the Arduino Uno original script was modified to integrate Arduino heater and syringe pump.

The electrode array (Figure 5.2) was designed at URV and fabricated using screen printing technology by C-MAC (Belgium). The electrodes and electrical contacts were printed with gold ink while the tracks were printed using silver ink on one side of a 635 µm think ceramic substrate. The final dimensions of each panel were 54.93 x 55.89 mm. The 64 gold working electrodes (1.0 mm diameter and 8 - 10 µm gold thickness) were integrated with microflduics to produce 4 individual channels (16 electrodes/channel) having common counter and reference electrodes, and the conductive tracks of the electrode array were insulated with a solder mask.

5.3. Methodology

5.3.1. RPA Amplification

Both the ssDNA (139-mer and 130-mer) osteoporosis targets labelled with ferrocene were generated using asymmetric Recombinase Polymerase Amplification (RPA), where the forward primer was labelled with ferrocene at the 5´-end to incorporate the ferrocene moiety in the amplified product and was added at higher concentration than the reverse primer (Fc-Fw:Rev primer molar ratio = 5:1 (c(Fc-Fw Primer) = 1000 nM: c(Rev Primer) = 200 nM)). The target was added at a concentration of 0.8 nM to the RPA mixture and the temperature was kept constant using a T100 thermal cycler (Biorad) at 37 °C for 15 min and then increased to 95 °C for 15 min to stop the reaction by enzyme denaturation. An Oligo Clean & Concentrator™ kit was used to purify the products from the reaction mixture. The amplification products were observed using agarose gel electrophoresis. The gel was prepared using ultralow pure agarose (3% w/v) in 1× Tris-Borate- EDTA buffer (TBE) and stained with GelRed™ nucleic acid stain. A mixture of 5 µL of asymmetric-RPA product with 4 µL of 2X

loading buffer was loaded per well and electrophoresis was performed at 100 V, 400 mAh for 40 min and the gels were visualized in a UV transilluminator at λ = 254 nm. Finally, the samples were immediately used or stored at -20 °C until use.

5.3.2. Electrochemical detection for the functionality test of the device

Electrochemical measurements were carried out using an Autolab model potentiostat/galvanostat 12 controlled with GPES software integrated to the developed device using a breakout box (Figure 5.1) specifically fabricated for this array at Labman Automation (Stokeley, UK) using a FSI-140-03-G-D-AD connector (Samtec, UK). The SPE array was cleaned by sequential immersion in isopropanol and water for 5 minutes, followed by drying with nitrogen and the electrodes were then immediately functionalised.

Thiolated capture probes (SNP-A-probe, SNP-T-probe, SNP-C-probe, SNP-G-probe) were self-assembled on each of the individual electrodes, by spotting of 1 µL of 1 µM thiolated capture probe + DT1 as backfiller with a 1:100 Probe:DT1 molar ratio freshly prepared in 1 M KH_2PO_4. This functionalization solution was incubated at room temperature (22 °C) for 3 h in a humidity chamber to avoid evaporation, followed by thorough washing with MilliQ water and finally drying with nitrogen. The functionalized electrode array was linked to the connector box and placed between two aluminum blocks of the heating device (Figure 5.2), and the upper part of the array was glued directly to the top heating aluminum block. In detail, 24 electrodes of the array were divided into two sets of 12 electrodes, each set consisting of a row of 4 electrodes (each one with a different probe) and a column of 3 electrodes (each immobilized with same probe) and at the bottom another 8 electrodes immobilized with different probes as negative controls. In Set 1, each row was immobilized with one capture probe with the SNP located to be at the middle of the DNA duplex following hybridization with the Rs2741856 (SNP-27) target and in Set 2 each row was immobilized with one capture probe with the SNP located to be at the middle of the DNA duplex following hybridization with the the target Rs1107946 (SNP-11). The ferrocene labelled asymmetric-RPA product was added in volume ratio 1:2 with Tris buffer (pH 7.4 at 25 °C) containing 0.5 M NaCl were added to the electrode array. Following 1 h incubation, the sensor was washed with Tris-HCl buffer (pH 7.4), and following baseline measurement the temperature was increased at intervals of 1 °C/step and the differential pulse voltammograms (DPV) recorded throughout the temperature ramp from 25°C to 40°C . The parameters employed in the DPV were a potential window between -0.1 and 0.3 V (vs. gold reference), a step potential of 10 mV, a modulation amplitude of 10 mV, a modulation time of 0.015 s and an interval time of 0.1 s. Each melting profile was carried out in triplicate.

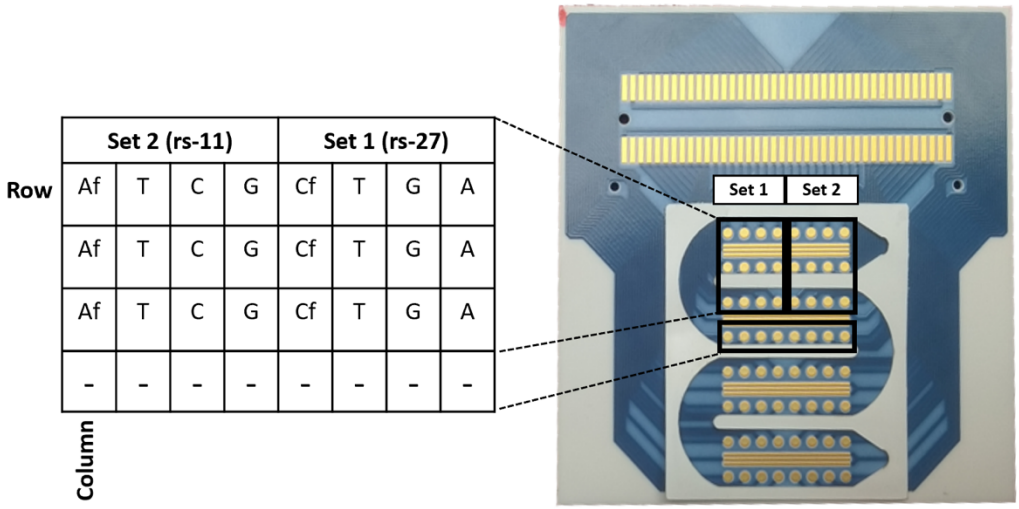

Figure 5.1. The multielectrode array was functionalised with two sets of probes, **Set-1** was immobilized with probes complementary to the SNP-27 target (Af= SNP-A full match, T=SNP-T, C=SNP-C, G=SNP-G) and **Set-2** Immobilized with probes complementary to SNP-11 target (Cf= SNP-C full match, T=SNP-T, A=SNP-A, G=SNP-G) and the bottom 8 electrodes were negative controls.

5.4. Results and Discussion

A compact set-up for éMCA was fabricated as shown in Figure 5.2. This new setup is composed of two parts (Figure 5.3), the heating-device box which contains the Arduino board, a small pump, and the breakout box where the 64-electrode array is connected to the multichannel potentiostat. The ceramic array is placed between the top and bottom heating blocks, where the top block is glued to the array surface using a double sided adhesive gasket to cover all the electrodes, with the top block containing two holes at the corners for introduction of the liquid from the pump to the electrode array. This new prototype has several advantages over the previously used in-house produced set-up. The first one is the avoidance of the use of an additional XL-Cavro syringe pump for washing the array as well as removing the requirement of an additional laptop to control the Arduino heating board. Additionally the actuation of the washing syringe is completely automated and the data automatically stored throughout the entire temperature ramping process. Finally, the use of a 64-electrode array (the maximum number of electrodes defined by the maximum number of channels in the Autolab multichannel potentiostat) increases the number of SNPs that can be detected simultaneously (4 electrodes per SNP).

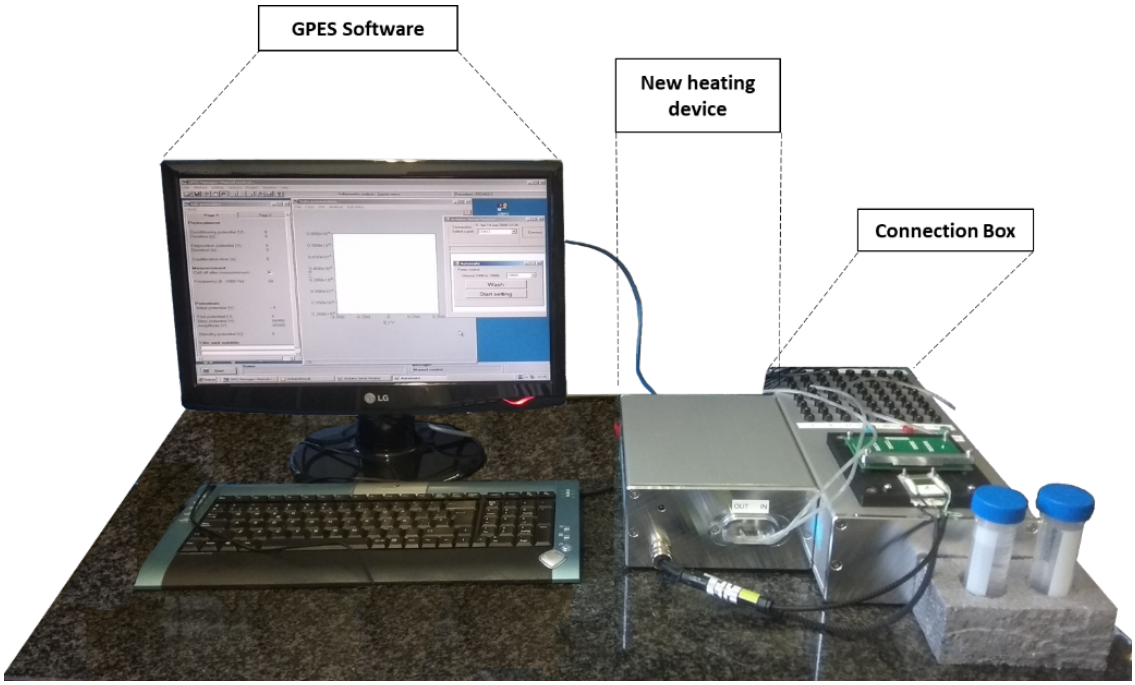

Figure 5.2. Set-up of the new device for multiplex SNP detection using éMCA

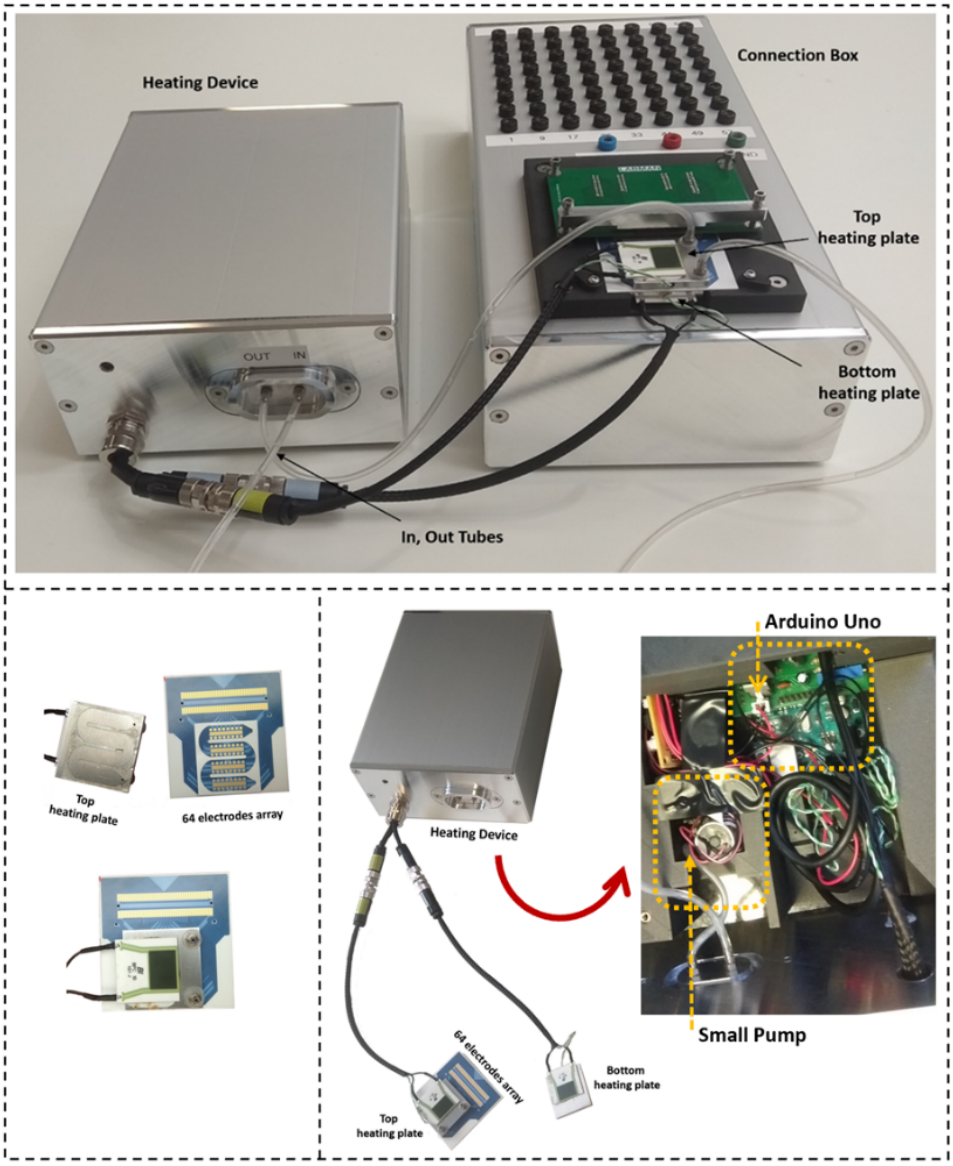

Figure 5.3 (a) Image of the new prototype device with the connection box for multiplexed SNP detection using éMCA; (b) The heating device and its internal components of an Arduino Uno board and a small pump; (c) 64 electrode array on ceramic substrate with double sided adhesive gasket microfluidics temporarily stuck to the top heating plate.

5.4.1 Functionality test

The simultaneous detection of two osteoporosis-associated SNPs contained in the 130- mer Rs1107946 (SNP 11) and 139-mer Rs2741856 (SNP 27) amplicons was carried out using the developed device. As described in chapters 3 and 4, the melting temperature profiles were generated by following the decrease in the oxidation peak of the ferrocene labelled target when the surface anchored duplex was thermally denatured by increasing the temperature. Asymmetric RPA using ferrocene labelled forward primers was used to generate the desired electroactive targets in single stranded form (Figure 5.4).

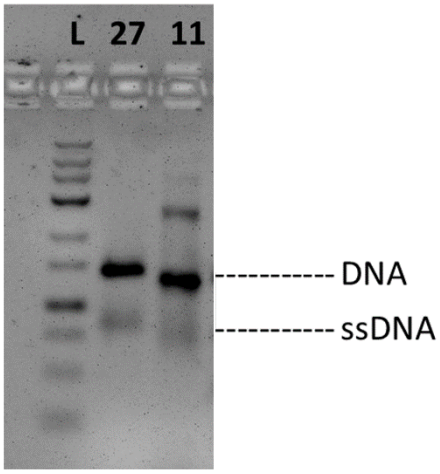

Figure 5.4. 3 % w/v agarose gel after electrophoresis of asymmetric RPA products, showing the DNA band following the first step of amplification and and the single stranded amplicons of targets SNP-27 and SNP-11 following the asymmetric second step pf amplification.

To demonstrate the proof-of-concept of multiplexed detection of SNPs, the ferrocene -labelled single stranded RPA amplicons were added to the electrode array and allowed to hybridize, where one of the four probes for each target would have fully complementarity and the other three would have a single base mismatch, with the SNP site designed to be located in the middle of the hybridized duplex, and each probed was repeated on three electrodes of the array. The temperature was increased by 1ºC/ step and the ferrocene DPV signal recorded. An image of the software controlling the melting curve analysis can be seen in Figure 5.5.

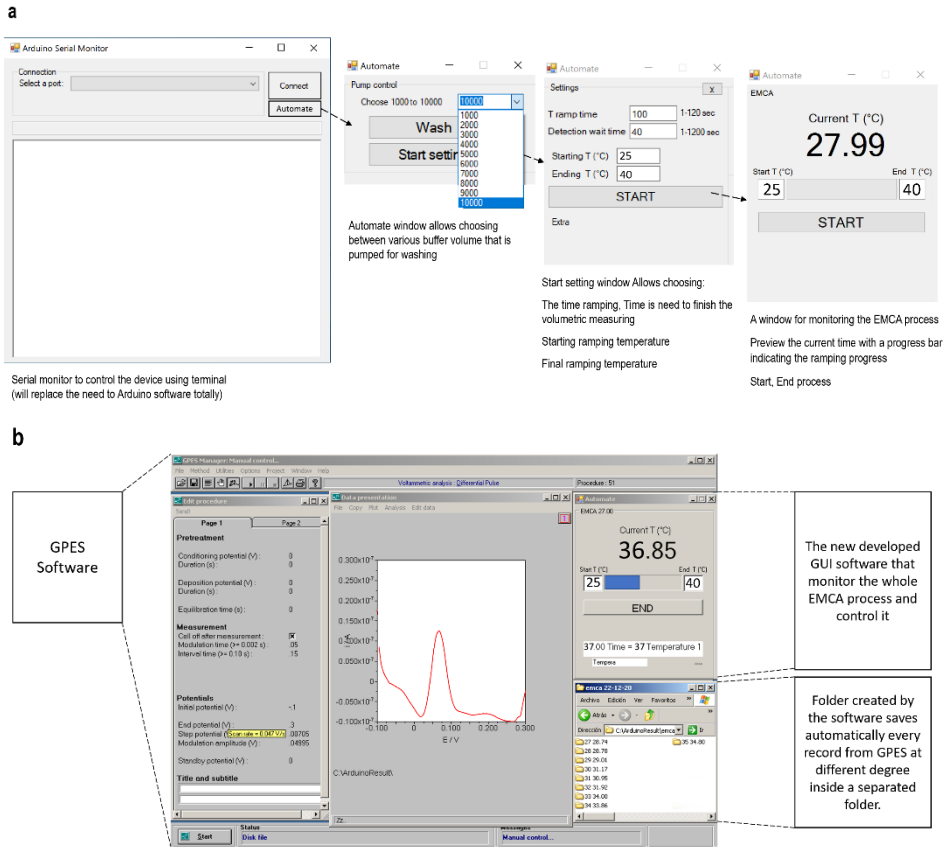

Figure 5.5. (a) Screen shot of the software specifically developed to run the electrochemical melting curve analysis prototype showing how the flow-rate of the washing buffer and the rate of the temperature ramp are controlled, and the temperature continuously measured throughout; (b) Screen shot of the continuous DPV measurement throughout the temperature ramp.

Figure 5.6 shows the trend of the DPV responses as a function of increasing temperature and the corresponding first derivative curves, where the melting temperatyres were determined to be 29.7 °C for SNP 11 with capture probe-A (fully complementary to the SNP-11-target carrying SNP T), whilst for the probes T, C and G duplexes, the melting temperatures were calculated to be 27.0 °C, 27.2°C and 26.6 °C, respectively. In the case of the the SNP 27 SNP the melting temperature for capture probe-C (fully complementary to the SNP-27-target carrying SNP G) was observed to be 34.1 °C, whilst for the probes A, G and T duplexes, the melting temperatures were determined to be 29.5 °C, 27.2°C and 30.3 °C, respectively. The results showed a clear discrimination between the melting points of the different capture probes and correctly the SNP that present in each target based on the higher melting temperatures observed, demonstrating the use of the platform for the multiplexed detection of SNPs.

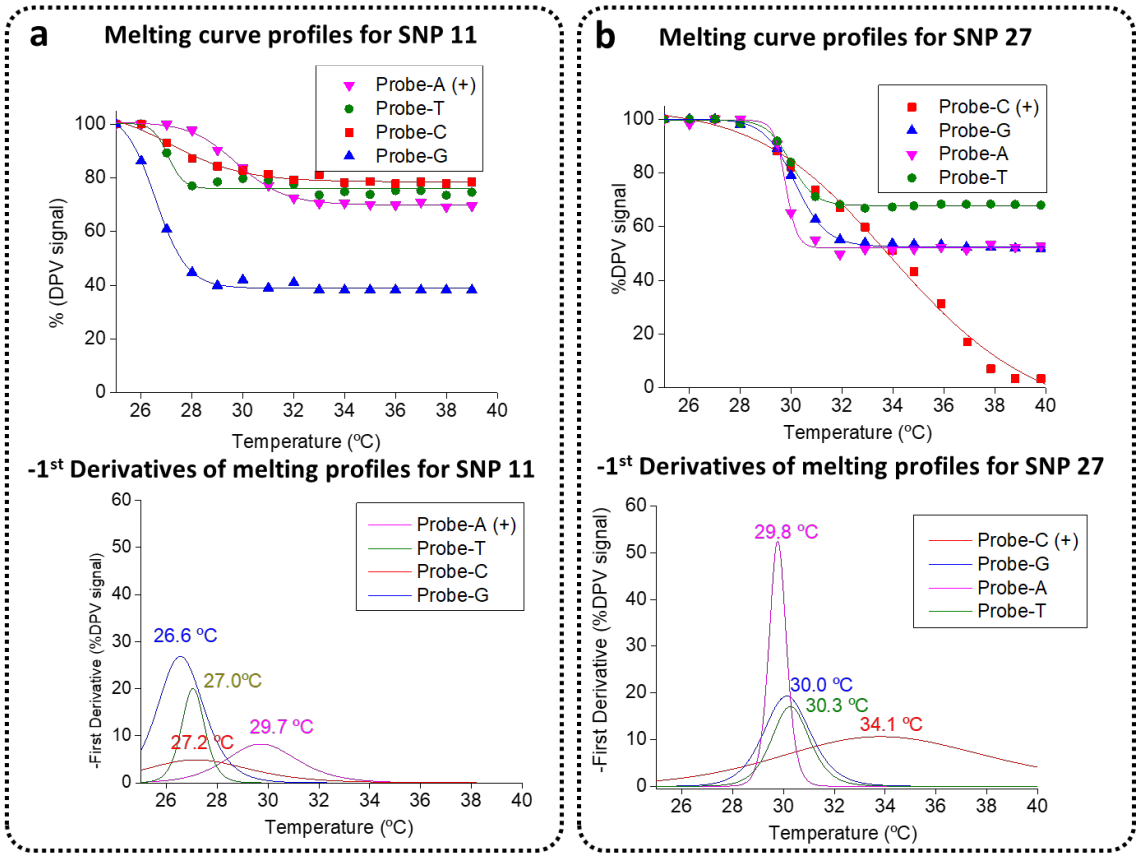

Figure 5.6. Melting curves for each of the SNPs under interrogation for each of the immobilized probes with the associated first derivative curves, where the identity of the allele at the SNP site can easily be determined by the higher melting temperature observed.

5.5. Conclusion

In the preliminary work reported here, in collaboration with Labman Automation (UK), we developed an elegant and almost fully-automated system for the multiplexed detection of single nucleotide polymorphisms. A 64-electrode array was produced via screen-printing in a ceramic substrate and was integrated with a patterned double adhesive gasket to create microfluidic channels over the array. This new prototype device housed both the pump for propulsion of fluids via the microfluidic channels over the electrode array as well as the Arduino board for control of the temperature ramp. Software was developed to allow facile control of both the flow rate and the rate of the temperature ramp and this software was also linked with the multichannel Autolab potentiostat and controlled the procurement of the differential pulse voltammetry throughout the temperature ramp. Using this sophisticated set-up, the possibility of achieving multiplexed detection of single nucleotide polymorphisms was demonstrated using two SNPs associated with an increased risk of bone fracture and development of osteoporosis. This work will be continued to integrate the isothermal asymmetric amplification within the microfluidic chip and will be applied to the detection of 11 mutations found in the rpoB gene and known to be associated with resistance to the rifampicin antibiotic used for the treatment of tuberculosis.

Acknowledgement

This project has received partial funding from the European Union's Horizon 2020 research and innovation program under grant agreement No 767325.

References

1. Gonzaga-Jauregui C., Lupski J. R., Gibbs R. A. (2012). Human Genome Sequencing in Health and Disease. Annual Review of Medicine, 63(1), 35–61.
2. Pastinen T., Kurg A., Metspalu A., Peltonen L., Syvanen A. (1997). Minisequencing: a specific tool for DNA analysis and diagnostics on oligonucleotide arrays. Genome Res, 7, 606–614.
3. Sachidanandam R., Weissman D., Schmidt S.C. (2001). A map of human genome sequence variation containing 1.42 million single nucleotide polymorphisms. Nature, 409, 928–933
4. Durbin R. (2001). A map of human genome variation from population-scale sequencing. Nature, 467, 1061-1073.
5. Lo P. H., Urabe Y., Kumar V., Tanikawa C., Koike K., Kato N., Miki D., Chayama K., Kubo M., Nakamura Y., Matsuda K. (2013). Identification of a functional variant in the MICA promoter which regulates MICA expression and increases HCV-related hepatocellular carcinoma risk. PLoS One. 8, e61279.
6. Yang Z. H., Zhou C. L., Zhu H., Li J. H., He C. D. (2014). A Functional SNP in the MDM2 Promoter Mediates E2F1 Affinity to Modulate Cyclin D1 Expression in Tumor Cell Proliferation. Asian Pac J Cancer Prev, 15, 3817–3823
7. Hassibi A., Manickam A., Singh R., Bolouki S., Sinha R., Jirage, K. B. Schoolnik G. (2018). Multiplexed identification, quantification and genotyping of infectious agents using a semiconductor biochip. Nature Biotechnology.
8. Michael C. A., Dominey-Howes D., Labbate M. (2014). The antimicrobial resistance crisis: causes, consequences, and management. Front. Public Health 2, 145
9. Phillips A. N., Stover J., Cambiano V., Nakagawa F., Jordan M. R., Pillay D., Doherty M., Revill P., Bertagnolio S. (2017). Impact of HIV drug resistance on HIV/AIDS-associated mortality, new infections, and antiretroviral therapy program costs in Sub-Saharan Africa. J Infect Dis, 215, 1362,1365
10. Van Dijk F. S., Byers P. H., Dalgleish R., Malfait F., Maugeri A., Rohrbach M., Pals, G. (2011). EMQN best practice guidelines for the laboratory diagnosis of osteogenesis imperfecta. European Journal of Human Genetics, 20(1), 11–19.
11. Van Dijk F. S., Zillikens M. C., Micha D., Riessland M., Marcelis C. L. M., de Die-Smulders, C. E., Pals, G. (2013). PLS3 Mutations in X-Linked Osteoporosis with Fractures. New England Journal of Medicine, 369(16), 1529–1536.

12. Gong Y., Slee R. B., Fukai N., Rawadi G., Roman-Roman S., Reginato A. M. (2001). LDL receptor-related protein 5 (LRP5) affects bone accrual and eye development. Cell, 107:513–23.
13. Bartlett J. G., Gilbert D. N., Spellberg B. (2013).Seven ways to preserve the miracle of antibiotics. Clin. Infect. Dis. 56, 1445–1450
14. Caliendo A. M. (2013).Better tests, better care: improved diagnostics for infectious diseases. Clin. Infect. Dis. 57 (Suppl. 3), S139–S170
15. Clutter D. S., Mazarei G., Sinha R., Manasa J., Nouhin J., LaPrade E., Shafer R. W. (2019). Multiplex Solid-Phase Melt Curve Analysis for the Point-of-Care Detection of HIV-1 Drug Resistance. The Journal of Molecular Diagnostics.
16. Song G. G., Lee Y. H. (2019). Causal Association between Bone Mineral Density and Osteoarthritis: A Mendelian Randomization Study, 26(2),104-110
17. Maylyan E. A. (2019). Association of COL1A1 gene -1997 C>A (rs1107946) polymorphism with bone mineral density in postmenopausal women. Medical Herald of the South of Russia, 8(2), 23-29.

Chapter 6

Conclusions

6. Conclusions

My doctoral project overall had the main goal of developing a simple and cost-effective platform for the electrochemical detection of SNPs using multiplexed melting curve analysis.

In Chapter 2, we explored a simple approach to perform solid-phase primer extension éPEX, hybridization, and electrochemical detection using ddNTPs labelled with redox (POMs). Specifically, we demonstrated that the Therminator® enzyme is able to incorporate ddNTP labelled with SiW11Sn-Keggin and P2W17Sn-Dawson POMs in the éPEX reaction for electrochemical detection of SNPs. To increase the electrochemical signal of the incorporated POMs to the DNA on the electrode surface, a post-incorporation step of dulplex dernaturation via addition of glycine pH 3 was incorporated, which also resulted in a decrease of the background signal via removal of the non-incorporated ddNTPs.

In Chapter 3, we pursued an alternative approach for the detection of single nucleotide polymorphisms based in the electrochemical detection of melting curve analysis, where either a ferrocene labelled 21-mer or a full length single stranded ferrocene labelled PCR amplicon were hybridized with a surface-tethered DNA probe and exposed to increasing temperatures. In order to achieve this goal, we developed an “in-house” fabricated device where we housed an electrode array consisting of 9 gold electrodes fabricated using sputtering with double adhesive gasket microfluidics, which created the microchannels for introduction and removal of reagents. This set-up was placed between two alumunium plates and exposed to a controlled rampong of temperature, with concomitant and continuous washing of the electrode array and measurement of the ferrocene oxidation peak. The optimum position of the SNP to be interrogated within the hybridized duplex was elucidated to be in the centre of the immobilized probe. The melting curve was analysed and using the first derivative of this curve, the melting temperature was established, and the system was demonstrated sing a SNP associated with cardiomyopathy as a proof-of-concept.

Having demonstrated the proof-of-concept in Chapter 3, in Chater 4 we tried to move closer to a point-of-care application, where we replaced the thermal cycling PCR with isothermal recombinase polymerase amplification. Using four separate probes, each designed to have the SNP site in the middle of the probe, asymmetric RPA was used to generate single stranded, ferrocene-labelled amplicons and using multiplexed melting curve analysis allele discrimination and identification at the SNP site was achieved.

In the final chapter, we moved towards a more automated version of the melting curve analysis prototype, which integrated the fluidic pump for propulsion of the RPA amplicon and washing buffer to the 64-electrode array with the automated Peltier temperature ramp, together with the multichannel potentiostat, to facilitate simultaneous and continuous heating, washing and measurement of the voltammetric signal. This multiplexed platform has now been preliminarily demonstrated and future work will focus on the multiplexed detection of 11 SNPs in the rpoB gene associated with resistance to the antibiotic rifampicin used to treat tuberculosis..

Appendix:

Biosensors and Bioelectronics 117 (2018) 201–206

Contents lists available at ScienceDirect

Biosensors and Bioelectronics

journal homepage: www.elsevier.com/locate/bios

Electrochemical primer extension based on polyoxometalate electroactive labels for multiplexed detection of single nucleotide polymorphisms

Nassif Chahin[a,1], Laura A. Uribe[a,1], Ahmed M. Debela[b], Serge Thorimbert[b], Bernold Hasenknopf[b], Mayreli Ortiz[a,*], Ioannis Katakis[a], Ciara K. O'Sullivan[a,c,*]

[a] Departament d'Enginyeria Química, Universitat Rovira i Virgili, Avinguda Països Catalans 26, 43007 Tarragona, Spain
[b] Sorbonne Université, Institut Parisien de Chimie Moléculaire, UMR CNRS 8232, 4 place Jussieu, 75005 Paris, France
[c] ICREA, Passeig Lluis Companys 23, 08010 Barcelona, Spain

ARTICLE INFO

Keywords:
SNP detection
Polyoxometalate-labelled ddNTPs
Electrochemical primer extension reaction (ePEX)
Multiplexed electrochemical detection

ABSTRACT

Polyoxymetalates (POMs) ($[SiW_{11}O_{39}\{Sn(CH_2)_2CO)\}]^{4-}$ and $[P_2W_{17}O_{61}\{Sn(CH_2)_2CO)\}]^{6-}$) were used to modify dideoxynucleotides (ddNTPs) through amide bond formation, and applied to the multiplexed detection of single nucleotide polymorphisms (SNPs) in an electrochemical primer extension reaction. Each gold electrode of an array was functionalised with a short single stranded thiolated DNA probe, specifically designed to extend with the POM-ddNTP at the SNP site to be interrogated. The system was applied to the simultaneous detection of 4 SNPs within a single stranded 103-mer model target generated using asymmetric PCR, highlighting the potential of POM-ddNTPs for targeted, multiplexed SNP detection. The four DNA bases were successfully labelled with both ($[SiW_{11}O_{39}\{Sn(CH_2)_2CO)\}]^{4-}$ and $[P_2W_{17}O_{61}\{Sn(CH_2)_2CO)\}]^{6-}$), and $[SiW_{11}O_{39}\{Sn(CH_2)_2CO)\}]^{4-}$ demonstrated to be the more suitable due to its single oxidation peak, which provides an unequivocal signal. The POM-ddNTP enzymatically incorporated to the DNA anchored to the surface was visualised by AFM using gold coated mica. The developed assay has been demonstrated to be highly reproducible, simple to carry out and with very low non-specific background signals. Future work will focus on applying the developed platform to the detection of SNPs associated with rifampicin resistance in real samples from patients suffering from tuberculosis.

1. Introduction

Polyoxometalates (POMs) are anionic metal oxygen clusters with remarkable properties including tuneable redox properties, magnetism and biocompatibility (Boglio et al., 2008; Debela et al., 2014). POMs are formed from early transition metals (such as W, Mo or V), oxygen, and can also bear a heteroatom (Si, P, Ge, etc) (Boglio et al., 2008; Debela et al., 2014). Recently the successful bioconjugation of polyoxotungstates $[SiW_{11}O_{39}\{Sn(CH_2)_2CO)\}]^{4-}$ (SiW_{11}Sn-Keggin) and $[P_2W_{17}O_{61}\{Sn(CH_2)_2CO)\}]^{6-}$ (P_2W_{17}Sn-Dawson) with DNA primers (Debela et al., 2015), and deoxynucleotide triphosphates (Ortiz et al., 2017) and the incorporation of these POM-primers and POM-dNTPs in PCR has been described. In both cases, the electroactive properties of POM allowed rapid and sensitive electrochemical detection of a DNA target. In the work reported here, we wish to expand the extraordinary possibilities of POMs in electrochemical genotyping, by their application in SNP detection through an electrochemical primer extension (ePEX) reaction (Fig. 1).

A SNP is a DNA sequence variation occurring when a single nucleotide in the genome differs between members of a species or paired chromosomes and occur in at least 1% of the total population (Pastinen et al., 1997; Sachidanandam et al., 2001). By unravelling the human genome, and in subsequent international efforts such as the HapMap project, the presence of around 15 million SNPs has been identified to date (Durbin, 2001). SNP genotyping can be used to facilitate patient stratification, to detect predisposition to certain diseases (Durbin, 2001), to perform evolutionary studies (Hacia, 1999), as well as providing information on drug metabolism (Evans and Relling, 1999). Furthermore, SNP genotyping shows great promise for forensics, where SNPs can be used to obtain a genetic fingerprint even in degraded DNA samples, and can also be used for prediction of phenotypic characteristics. Whilst next generation sequencing has been extensively used for the identification and detection of SNPs, there is a defined need for the targeted detection of a specific subset of SNPs, rather than a genome wide SNP map.

The discrimination of a single point mismatch in DNA analysis is a

* Corresponding authors.
E-mail addresses: mayreli.ortiz@urv.cat (M. Ortiz), ciara.osullivan@urv.cat (C.K. O'Sullivan).
[1] N. Ch and L. A.U. contributed equally and both are first authors.

https://doi.org/10.1016/j.bios.2018.06.014
Received 9 April 2018; Received in revised form 4 June 2018; Accepted 6 June 2018
Available online 07 June 2018
0956-5663/

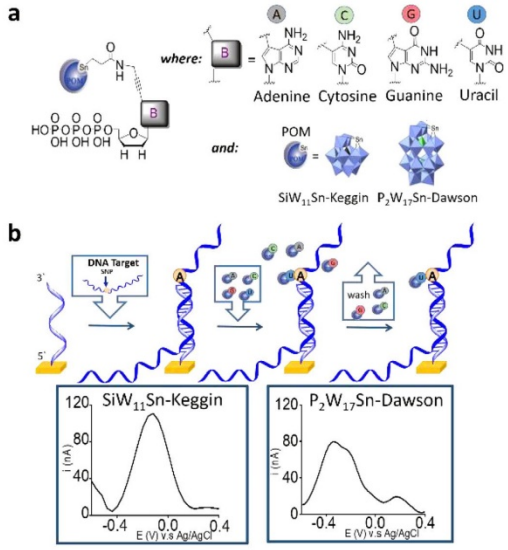

Fig. 1. Schematic representation of a) POM-modified-ddNTPs and b) the application of POM-modified-ddNTPs in éPEX (Insets: Differential Pulse Voltammograms (DPV) of $SiW_{11}Sn$-ddUTP and $P_2W_{17}Sn$-ddUTP incorporated at 3′-end of primers. DPV were recorded in 10 mM Tris + 0.5 NaCl, pH 7).

challenge that needs to be addressed, with multiplexed detection of SNPs finding increasing application in diagnostics, theranostics, as well as in advanced forensics. The combination of fluorescence and nanostructured composites have been demonstrated to be a highly promising strategy for the solution-based detection of SNPs (Tian et al., 2015a, 2015b; Yang et al., 2015; Duan et al., 2009). However, this approach suffers great difficulties in the simultaneous multiplexed detection of SNPs and to address this shortfall, array based primer extension (APEX) using fluorescent detection has been successfully employed. However, fluorescence APEX is inherently expensive and laboratory based due to the optics and instrumentation required. In the APEX reaction, an isothermal reaction that takes advantage of immobilised single stranded DNA (ssDNA) probes designed to hybridise to a single stranded PCR amplicon one base downstream from the SNP site being interrogated. Following hybridisation, labelled ddNTPs, modified nucleotides that lack the 2′ and 3′-hydroxyl groups, are added (Tonisson et al., 2010). Using either ligation or elongation with a ligase or polymerase enzyme, respectively, the immobilised probe is extended by a single labelled ddNTP, complementary to the SNP being addressed (Sanger et al., 1977) (Fig. 1b). Following incorporation of the ddNTP, no further phosphodiester bonds can be formed due to the lack of the 2′/3′-hydroxyl group, and thus further elongation cannot take place (Sanger et al., 1977).

Electrochemical techniques for screening of SNPs offer cost-effective and facile detection platforms as an alternative to colorietry (Zhang et al., 2018), fluorescence (Sanger et al., 1977) or radioactive detection (Krjutskov et al., 2008). A broad spectrum of electroactive markers such as intercalators (Wakai et al., 2004), ferrocene modified probes (Yu et al., 2001) and nanoparticle probes (Liu et al., 2007) and nanocrystal labelled nucleotides (Liu et al., 2005) have been reported for the electrochemical detection of SNPs. Solid phase éPEX is a variant of APEX using an electroactive label. In this context, we recently demonstrated the feasibility of performing éPEX reaction with ddNTPs labelled with different electroactive markers: ferrocene, anthraquinone, phenothiazine and methylene blue (Debela et al., 2016). Whilst the concept of éPEX was successfully demonstrated, a small level of non-specific background signal was observed due to the electrostatic interaction with methylene blue, and to this end, an alternative redox label was pursued. Consequently, we explored the possibility of using POMs to label ddNTPs for use in éPEX. POMs are robust molecules at neutral-acid pH, inexpensive and easy to prepare and functionalise, and offer a potential window compatible with biomolecules. Furthermore, we expanded on our previous proof-of-concept work, extending to simultaneous, multiplexed detection of SNPs using an electrode array housed within a microfluidic set-up.

2. Materials and methods

2.1. Reagents

All reagents were of analytical grade and used as received. Potassium dihydrogen phosphate (KH_2PO4), sodium chloride (NaCl), potassium chloride (KCl), were purchased from Fluka, while sodium perchlorate ($NaClO_4$) was received from Acros Organics. Sodium hydroxide, sulphuric acid (95–97%), Tris-HCl and boric acid were purchased from Scharlau, Barcelona, Spain and hydrochloric acid (35% v/v) from Panreac. Phosphate-buffered saline (PBS), trisodium citrate, acetone, dimethyl sulfoxide (DMSO), perchloric acid (70% v/v), triethylamine, glacial acetic acid, phenothiazine, anthraquinone carboxylic acid, ferrocene carboxylic acid, N-(3-dimethylaminopropyl N′-ethyl-carbodiimide hydrochloride and N-hydroxy succinimide were all purchased from Sigma Aldrich, Spain. The propargyl amino modified ddNTPs were purchased from Jena Bioscience and the 10-(3,5-bis((6-mercaptohexyl)oxy)phenyl)-3,6,9-trioxadecanol (DT1) was purchased from SensoPath Technologies (Bozeman, MT). Unless otherwise stated, all reactions were carried out under argon atmosphere with magnetic stirring. The organic solvents were redistilled before use.

Thermosequenase polymerase was purchased from GE Healthcare Life Technology (GE Healthcare Europe GmbH, Spain) and Therminator™ DNA Polymerase from New England BioLabs. Inc, UK. GelRed nucleic acid stain was acquired from Biotium, KAPA2G Robust polymerase from KAPABIOSYSTEMS (distributed by Sigma Aldrich, Spain) and Lambda exonuclease, agarose and DNA Gel Loading Dye (6 ×) from ThermoFisher Scientific, Spain. DNA Clean &Concentrator and Oligo Clean &Concentrator Kits were purchased from Zymo Research, USA.

A model target sequence was designed based on SNPs previously identified within the MYH7 gene present in a group of patients known to suffer from Laing cardiomyopathy (Muelas et al., 2012), where several SNP sites were included in a single PCR amplicon, thus mimicking the SNP sites found in genomic DNA. However, in human genomic DNA these SNP sites are located in different parts of the MYH7 gene and would require multiple amplifications, whereas in our "model" system we have four different SNP sites located in a 103-mer amplicon that is amplified in a single amplification. The sequences were selected using specific oligonucleotide selection and design programs (http://bioinfo.ebc.ee/apex2/). The sequences were designed in such a way to detect the SNPs using four different labels corresponding to the four bases. The HPLC purified oligonucleotides were purchased from Biomers.net, Germany and used as received. The sequences used (from 5`to 3`) are listed below:

Primers and ssDNA template used for PCR amplification:

Forward primer (FW-P)	5′-CGAAGTGTGAACTAGTCCCAC-3′
Phosphorylated Reverse primer (Rv-P)	5′-PO_3-GGGGACTAGGGGACTGAAGAA-3′

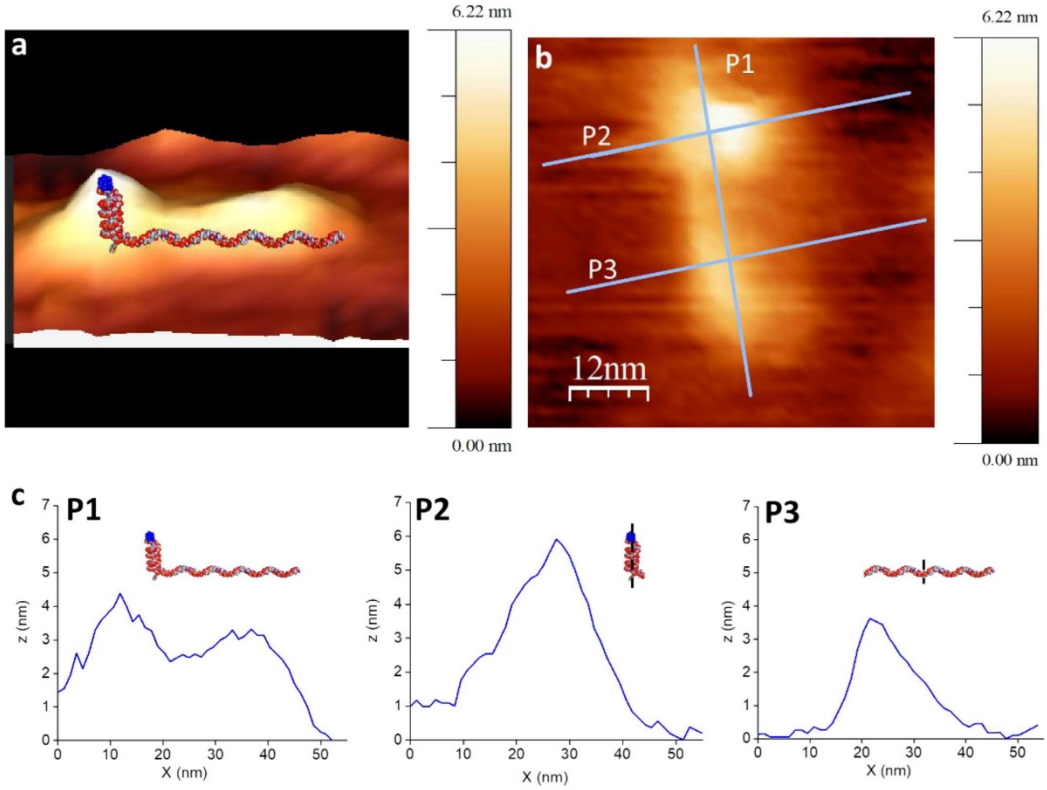

Fig. 2. Topographic AFM images in ambient conditions of the enzymatic incorporation of P_2W_{17}-ddCTP. The 21-mer thiotic acid capture probe was first self-assembled on a 10 nm thick gold coated mica surface followed by hybridisation of a 103-mer ssDNA target before POM incorporation. a) 3D image, b) 2D image including profile lines, c) x-z profiles obtained along the P1, P2 and P3 lines shown in b).

The 103-mer oligonucleotide DNA target/template (a synthetic sequence containing four "SNPs")	5`CGAA***G*** TGTGAACTAGTCCCACCACCTTAA***T*** TTCACTGTGTGTTAACACTTGTAAAG***A*** ACCTGCATAATGTGTGTATCTTAA***C*** TTCTTCAGTCCCCTAGTCCCC -3

The surface-tethered thiolated probes and the short ssDNA sequences containing SNPs used in the electrochemical detection of SNPs are detailed below:

SNP	Surface-tethered thiolated probes:	Short ssDNA sequences containing SNPs:
A	thioctic acid-C5-AGATACACACATTATGCAGGT	AAG***A*** ACCTGCATAATGTGTGTATCT
C	thioctic acid-C5-TACAAGTGTTAACACACAGTGAA	TAA***C*** TTCTTCAGTCCCCTAGTCCCC
G	thioctic acid-C5-AGGTGGTGGGACTAGTTCACA	CGAA***G*** TGTGAACTAGTCCCACCACCT
T	thioctic acid-C5-GGGGACTAGGGGACTGAAGAA	TAA***T*** TTCACTGTGTGTTAACACTTGTA

2.2. Electrochemical measurements

All electrochemical measurements were carried out using an Autolab model PGSTAT 12 potentiostat/galvanostat controlled with the General Purpose Electrochemical System (GPES) software (Eco Chemie B.V., The Netherlands).

All optimisation studies were carried out with individual 1.6 mm gold electrodes (BAS model MF-2014, 1.6 mm diameter), platinum counter electrode (BAS model MW-1032) and a pseudo-reference electrode of Ag/AgCl (CH Instruments., model CHI111) and the electrochemical measurements were performed in a 1 cm^3 cell. For the multiplexed detection of SNPs, electrode arrays of 36 individual 1 mm^2 square gold working electrodes (150 nm in thick) with a common gold counter electrode and Ag silver reference electrode were used. Fig. SI3). The electrodes were fabricated at Fraunhofer ICT-IMM, Germany using a photolithographic process as previously reported (Fragoso et al., 2011; Joda et al., 2014; Ortiz et al., 2015). (See SI for more details).

Differential Pulse Voltammetry (DPV) was used to detect the incorporation of the labelled ddNTPs. The measurements were performed at room temperature in 10 mM Tris buffer containing 0.5 M NaCl, pH 7. For the three electrodes configuration (optimisation studies), the measurements were recorded in a 1 mL electrochemical cell and for the electrode array (multiplexed studies) in 20 μL of volume. DPVs were recorded at various potential windows depending on the redox

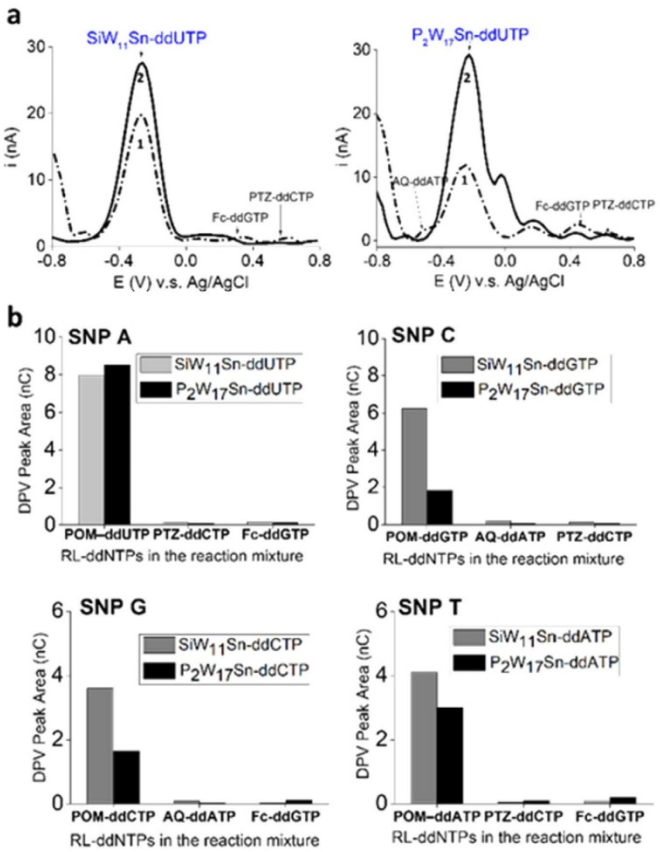

Fig. 3. a) Comparison of the DPV after the incorporation of SiW_{11}-ddUTP (left) and P_2W_{17}Sn-ddUTP (right) at the SNP A position before (1) and after (2) duplex denaturation. b) DPV peak area values of the redox-labelled bases (RL-ddNTPs) present in the reaction mixture for detecting each SNP in a synthetic 103-mer ssDNA. The residual signal coming from the non-specific bases (AQ-ddATP, PTZ-ddCTP and Fc-ddGTP) is also plotted (Average of three electrodes RSD less than 5%).

potential of the labels (vs Ag/AgCl), using a pulse amplitude of 0.1 V, a step potential of 10 mV, a pulse width of 100 ms and a pulse period of 5 ms. For specificity studies and multiplex detection of SNP, the potential window used was from – 0.8 to 0.8 V vs Ag/AgCl, including all the potentials corresponding to the redox labels used in the work reported.

2.3. Atomic force microscopy characterisation

The enzymatic incorporation of P_2W_{17}-ddCTP after 103-mer ssDNA hybridised on thiol surface tethered capture probe on 10 nm thick gold coated mica was studied by atomic force microscopy (AFM). Prior to measurement, the surface was incubated with a 25 mM water solution of $MgCl_2$ to extend the DNA from the surface by minimising the repulsion forces from the gold surface, DNA and polyoxometalate, (Hansma et al., 1993; Herrero-Moreno et al., 2005), and dried with nitrogen. The details of surface preparation and reaction are explained in detail in SI.

The AFM images were recorded in a 5420 at. Force Microscope (AFM) from Agilent Technologies (USA) and processed using WSxM 5.0 Develop 9.2 (Horcas et al., 2007). The surface was scanned in tapping mode at 0.25 ln/min using a SHR-150 kHz frequency tip from NanoAndMore GMBH, Germany. The SHR-150 probe has a single hydrophobic diamond-like carbon extra tip at the apex of a gold coated silicon etched probe. The tip diameter is ca. 1 nm.

3. Results and discussion

Activated polyoxotungstates $[SiW_{11}O_{39}\{Sn(CH_2)_2CO)\}]^{4-}$ (SiW_{11}Sn-Keggin) and $[P_2W_{17}O_{61}\{Sn(CH_2)_2CO)\}]^{6-}$ (P_2W_{17}Sn-Dawson) were coupled with propargyl amino derivatised dideoxynucleotides at position 7 of the purine and 5 of the pyrimidine bases through amide bond formation (Fig. 1) following our established protocol (Boglio et al., 2008; Debela et al., 2014; Debela et al., 2016, Debela et al., 2017) with small variations. A 1.6 mm gold electrode was functionalised with a mixture of thioctic acid ssDNA probe and a bipodal alkanethiol at a ratio of 1:100 (see SI for details).

The optimum buffer for the éPEX reaction and differential pulse voltammetry (DPV) detection was elucidated by evaluating assay performance in Tris-HCl, or phosphate buffered saline (PBS) at pH of 3, 7 and 8. The sharpest and highest DPV peaks was obtained using Tris-HCl at pH 7. Furthermore the use of the two polymerases, Therminator® and

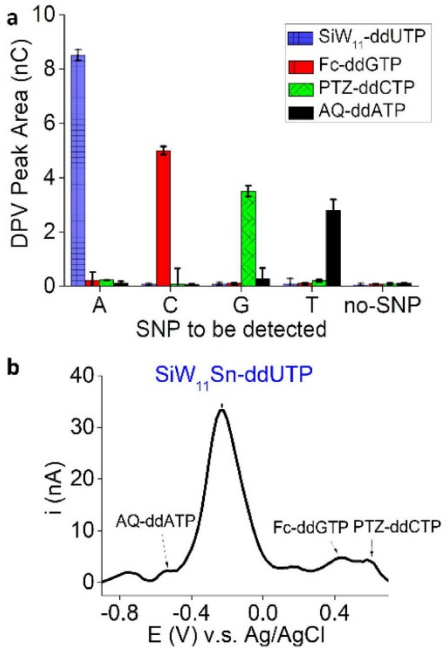

Fig. 4. a) Averaged integrated areas (nC) of the specific and non-specific DPV signals per per SNP interrogated (A for SNP A, C for SNP C, G for SNP G, T for SNP T. Each column represents the value of the DPV signal of each electrochemically active bases (SiW_{11}-ddUTP, PTZ-ddCTP, Fc-ddGTP and AQ-ddATP) measured on the same electrode (Average of six electrodes, RSD less than 5%). b) DPV registered for detecting SNP A by the incorporation of the complementary SiW_{11}Sn-dUTP in 10 mM Tris + 0.5 NaCl, pH 7 (after denaturation at pH 3).

Thermosequenase®, both known to be compatible with modified nucleotide incorporation, were compared. Higher DPV signals were obtained using the Therminator® enzyme, which is also relatively less expensive than the Thermosequenase®. Whilst the optimal temperature for Therminator activity is 75 °C, the use of milder temperatures (24, 42 and 50 °C) were also evaluated. Equivalent performance was observed at 42 and 50 °C, whilst a lower DPV signal intensity was observed at 75 °C, which can be attributed to the thermal cleavage of the thiol-Au bond, resulting in release of the immobilised probe from the electrode surface. No ddNTP incorporation was observed at 24 °C.

Fig. 1b shows the DPV of ddUTPs labelled with SiW_{11}Sn-Keggin and P_2W_{17}Sn-Dawson POMs at SNP A position, using a short (24–mer) synthetic ssDNA target. POMs have different oxidation states as indicated by oxidation peaks at different potentials. Following the éPEX reaction, the main signal is observed at − 0.3 V vs Ag/AgCl for both SiW_{11}Sn-Keggin and P_2W_{17}Sn-Dawson ddNTPs. Once the incorporation of the POM–ddNTP was demonstrated for a short oligonucleotide target sequence, the possibility of carrying out the éPEX reaction using a longer synthetic target sequence was then tested. To demonstrate multiplexing, a 103-mer DNA target containing 4 different "SNP sites" (5`CGA-A***G***T-GTG-AAC-TAG-TCC-CAC-CAC-CTT-AA***T***-TTC-ACT-GTG-TGT-TAA-CAC-TTG-TAA-AG***A***-ACC-TGC-ATA-ATG-TGT-GTA-TCT-TAA-***C***TT-CTT-CAG-TCC-CCT-AGT-CCC-C-3), was amplified using asymmetric PCR followed by exonuclease digestion to generate ssDNA for hybridisation to the surface immobilised probe (Figs. SI1 and 2).

The enzymatic incorporation of POM in the DNA system was visualised by Atomic Force Microscopy (AFM). As observed in Fig. 2, the topographic AFM images obtained using a 1 nm diameter ultrasharp tip show an elongated feature of about 50 nm long and 3–6 nm height, compatible with the size of a 103-mer target hybridised to an immobilised and in situ POM-modified 21-mer probe, in ambient conditions of humidity (Di Santo et al., 2009).

The multiplexed detection of SNPs was carried out using DPV. Following incorporation of the POM-labelled ddNTP, the duplex was chemically denatured using glycine-HCl (pH 3), facilitating increased flexibility and elasticity of the surface tethered POM-DNA, allowing the POM label to move closer to the electrode surface, thus enhancing electron transfer and addressing higher DPV signal (Fig. 3a and SI4). This denaturation step also served to wash away unincorporated labelled ddNTPs and the low pH used can also contribute to the stability of the POM cluster during washing steps.

As can be seen in Fig. 3b, the incorporation of either the Keggin or Dawson labelled ddNTPs e.g. SNP A only shows incorporation of POM-ddUTP and no signal is observed with either AQ-ddATP, PTZ-ddCTP or Fc-ddGTP. The difference in responses for different SNPs can be attributed to different degrees of elasticity of the POM-tethered surface bound DNA, and the dissimilar shapes of the Keggin and Dawson labels. As the signal for SiW_{11}Sn-Keggin was consistently higher than the P_2W_{17}Sn-Dawson for all ddNTPs, they were used as labels for the simultaneous and multiplexed detection of SNPs. Here, an array of 36 electrodes (Fragoso et al., 2011; Joda et al., 2014; Ortiz et al., 2015) was used (Fig. SI3), with each electrode functionalised with a mixture of 1:100 thioctic acid-DNA probe and a bipodal alkanethiol, with six electrodes per SNP, and the remaining twelve electrodes were used as negative controls. A patterned double-sided adhesive gasket was used to create microfluidic channels, and the fluidic housing was completed with PMMA creating a channel with an inlet and outlet for reagent addition (Fig. SI 3). Fig. 4a shows the electrochemical signals for the multiplexed detection of the four SNPs using a mixture of SiW_{11}Sn-dUTP (SNP A), Fc-ddGTP (SNP C), PTZ-ddCTP (SNP G) and AQ-ddATP (SNP T), (Schematic representation shown in Fig. SI 5) and, Fig. 4b shows the highly distinguishable specific signal of SiW_{11}Sn-dUTP (SNP A) from the other non-specific redox labelled ddNTPs.

Moreover, the possibility of also using SiW_{11}-Keggin-ddATP, SiW_{11}-Keggin-ddCTP and SiW_{11}-Keggin-ddGTP for multiplex detection of SNP in combination with other redox labelled bases was also successfully carried out and is reported in Fig. SI6.

4. Conclusions

In summary, we have demonstrated the exploitation of ddNTPs labelled with SiW_{11}Sn-Keggin and P_2W_{17}Sn-Dawson POMs for solid-phase primer extension, and the electrochemical detection of SNPs. The use of the relatively inexpensive Therminator® polymerase was demonstrated to successfully and accurately incorporate the POM-labelled ddNTPs. A post-incorporation denaturation step was observed to increase the DPV signal due to enhanced flexibility and elasticity of the POM-tethered surface bound ssDNA as compared to the rigid duplex. This denaturation step also assisted in the removal of any residual non-specific ddNTPs. SiW_{11}Sn-Keggin ddNTPs gave consistently higher signals as compared to the P_2W_{17}Sn-Dawson ddNTPs and were thus used for the simultaneous and multiplexed detection of SNPs using an electrode array housed within a microfluidic set-up. Four different "SNP sites" were successfully interrogated with negligible background signals. Following this proof-of-concept demonstration, current work is focusing on a higher level of multiplexing for detection of osteoporosis related SNPs (> 20), SNPs associated with rifampicin resistance (7) and SNPs for advanced forensics (> 150).

Acknowledgements

This project has received partial funding from the European Union's

Horizon 2020 research and innovation programme under grant agreement No 767325 and under the Marie Sklodowska-Curie grant agreement No. 659211. We want to thank to Fraunhofer ICT-IMM for provision of gold electrode arrays and the Microscopy and Nanometric Techniques Area of the SRCiT, Universitat Rovira I Virgili, especially to Dr. M. Stefanova Stankova and Dr. L. Vojkuvka for their valuable help in the AFM measurements and surface preparation.

Appendix A. Supporting information

Supplementary data associated with this article can be found in the online version at http://dx.doi.org/10.1016/j.bios.2018.06.014.

References

Boglio, C., Micoine, K., Derat, E., Thouvenot, R., Hasenknopf, B., Thorimbert, S., Lacôte, E., Malacria, M., 2008. J. Am. Chem. Soc. 130, 4553–4561.
Debela, A.M., Ortiz, M., O'Sullivan, C.K., Thorimbert, S., Hasenknopf, B., 2014. Polyhedron 68, 131–137.
Debela, A.M., Ortiz, M., Beni, V., Thorimbert, S., Lesage, D., Cole, R.B., O'Sullivan, C.K., Hasenknopf, B., 2015. Chem. Eur. J. 21, 17721–17727.
Debela, A.M., Thorimbert, S., Hasenknopf, B., O'Sullivan, C.K., Ortiz, M., 2016. Chem. Commun. 52, 757–759.
Di Santo, G., Tobenas, S., Adamcik, J., Dietler, G., 2009. Imaging Microsc. ⟨https://www.imaging-git.com⟩.
Duan, X., Liu, L., Wang, S., 2009. Biosens. Bioelectron. 24, 2095–2099.
Evans, W.E., Relling, M.W., 1999. Science 286, 487–491.
Fragoso, A., Latta, D., Laboria, N., Germar, F.V., Hansen-Hagge, T.E., Kemmner, W., Gartner, C., Klemm, R., Drese, K.S., O'Sullivan, C.K., 2011. Lab Chip 11, 625–631.
Hacia, J.G., Fan, J.B., Ryder, O., Jin, L., Edgemon, K., Ghandour, G., Mayer, R.A., Sun, B., Hsie, L., Robbins, C.M., Brody, L.C., Wang, D., Lander, E.S., Lipshutz, R., Fodor, S.P., Collins, F.S., 1999. Nat. Genet. 22, 164–167.
Hansma, H.G., Bezanilla, M., Zenhausern, F., Adrian, M., Sinsheimer, R.L., 1993. Nucleic Acids Res. 21, 505–512.
Horcas, I., Fernández, R., Gómez-Rodríguez, J.M., Colchero, J., Gómez-Herrero, J., Baro, A.M., 2007. Rev. Sci. Instrum. Nanotec Electron. WSxM Free. 78, 013705.
Joda, H., Beni, V., Alakulppi, N., Partanen, J., Lind, K., Strömbom, L., Latta, D., Höth, J., Katakis, I., O'Sullivan, C.K., 2014. Anal. Bioanal. Chem. 406, 2757–2769.
Krjutskov, K., Andreson, R., Magi, R., Nikopensius, T., Khrunin, A., Mihailov, E., Tammekivi, V., Sork, H., Remm, M., Metspalu, A., 2008. Nucleic Acids Res. 36, e75.
Liu, G., Lee, M.H., Wang, J., 2005. J. Am. Chem. Soc. 127, 38–39.
Muelas, M., Hackman, P., Luque, H., Suominen, T., Espinós, C., Garcés-Sánchez, M., Sevilla, T., Azorín, I., Millán, J.M., Udd, B., Vílchez, J.J., 2012. Clin. Genet. 81, 491–494.
Ortiz, M., Joda, H., Hoth, J., Beni, V., Katakis, I., Klemm, R., Lind, K., O'Sullivan, C.K., Fragoso, A., 2015. Electrophoresis 36, 1920–1926.
Ortiz, M., Debela, A.M., Svobodova, M., Thorimbert, S., Lesage, D., Cole, R.B., Hasenknopf, B., O'Sullivan, C.K., 2017. Chem. Eur. J. 23, 10597–10603.
Pastinen, T., Kurg, A., Metspalu, A., Peltonen, L., Syvanen, A.-Ch, 1997. Genome Res. 7, 606–614.
Sachidanandam, R., Weissman, D., Schmidt, S.C., et al., 2001. Nature 409, 928–933.
Sanger, F., Nicklen, S., Coulson, A.R., 1977. Proc. Natl. Acad. Sci. USA 74, 5463–5467.
Tian, J., Liu, Q., Shi, J., Huc, J., Asiri, A.M., Xuping Sun, X., Yuquan, H., 2015a. Biosens. Bioelectron. 71, 1–6.
Tian, J., Cheng, N., Liu, Q., Xing, W., Sun, X., 2015b. Angew. Chem. Int. Ed. 54, 5493–5497.
Tonisson, N., Oitmaa, E., Krjutskov, K., Pullat, J., Lind, I., Leego, M., Kurg, A., Metspalu, A., 2010. Molecular Diagnostics, Second edition. Elsevier Ltd, pp. 267–284.
Wakai, J., Takagi, A., Nakayama, M., Miya, T., Miyahara, T., Iwanaga, T., Takenaka, S., Ikeda, Y., Amano, M., 2004. Nucleic Acids Res. 32, e141.
Yang, L., Liu, D., Hao, Sh, Qu, F., Ge, R., Ma, Y., Du, G., Asiri, A.M., Chen, L., Sun, X., 2017. Anal. Chem. 89, 2191–2195.
Yu, C.J., Wan, Y.J., Yowanto, H., Li, J., Tao, C.L., James, M.D., Tan, C.L., Blackburn, G.F., Meade, T.J., 2001. J. Am. Chem. Soc. 123, 11155–11161.
Zhang, H., Liu, X., Liu, M., Gao, T., Huang, Y., Liu, Y., Zeng, W., 2018. Biosens. Bioelectron. 99, 625–636.

UNIVERSITAT
ROVIRA i VIRGILI